

Integrated spectrum of the planetary nebula NGC 7027*

Y. Zhang^{1,2}, X.-W. Liu¹, S.-G. Luo¹, D. Péquignot² and M. J. Barlow³

¹ Department of Astronomy, Peking University, Beijing 100871, P. R. China
e-mail: zhangy@stsci.edu

² LUTH, Laboratoire l'Univers et ses Théories, associé au CNRS (FRE 2462) et à l'Université Paris 7, Observatoire de Paris-Meudon, F-92195 Meudon Cédex, France

³ Department of Physics and Astronomy, University College London, Gower Street, London WC1E 6BT, UK

Received ; accepted

Abstract. We present deep optical spectra of the archetypal young planetary nebula (PN) NGC 7027, covering a wavelength range from 3310 to 9160 Å. The observations were carried out by uniformly scanning a long slit across the entire nebular surface, thus yielding average optical spectra for the whole nebula. A total of 937 emission features are detected. The extensive line list presented here should prove valuable for future spectroscopic analyses of emission line nebulae. The optical data, together with the archival *IUE* and *ISO* spectra, are used to probe the temperature and density structures and to determine the elemental abundances from lines produced by different excitation mechanisms. Electron temperatures have been derived from the hydrogen recombination Balmer jump (BJ), from ratios of He I optical recombination lines (ORLs) and from a variety of diagnostic ratios of collisionally excited lines (CELs). Electron densities have been determined from the intensities of high-order H I Balmer lines and of He II Pfund lines, as well as from a host of CEL diagnostic ratios. CEL and ORL diagnostics are found to yield compatible results. Adopting respectively electron temperatures of $T_e = 12\,600$ and $15\,500$ K for ions with ionization potentials lower or higher than 50 eV and a constant density of $N_e = 47\,000 \text{ cm}^{-3}$, elemental abundances have been determined from a large number of CELs and ORLs. The C^{2+}/H^+ , N^{2+}/H^+ , O^{2+}/H^+ and $\text{Ne}^{2+}/\text{H}^+$ ionic abundance ratios derived from ORLs are found to be only slightly higher than the corresponding CEL values. We conclude that whatever mechanism is causing the BJ/CEL temperature discrepancies and the ORL/CEL abundance discrepancies that have been observed in many PNe, it has an insignificant effect on this bright young compact PN. The properties of the central star are also discussed. Based on the integrated spectrum and using the energy-balance method, we have derived an effective temperature of 219 000 K for the ionizing star. Finally, we report the first detection in the spectrum of this bright young PN of Raman-scattered O VI features at 6830 and 7088 Å, pointing to the existence of abundant neutral hydrogen around the ionized regions.

Key words. line: identification — ISM: abundances — planetary nebulae: individual (NGC 7027)

1. Introduction

NGC 7027 (PNG 84.9–3.4° 1) is a high-excitation, young, dense planetary nebula (PN) ionized by a hot central star (CS). Due to its proximity ($\sim 880 \pm 150$ pc; Masson, 1989), its high surface brightness and exceedingly rich spectrum, NGC 7027 has been one of the most intensively

observed astronomical objects. It has long served as an ideal laboratory for studies of the physics of low density astrophysical plasmas and for testing the accuracy of current atomic data. Extensive spectroscopy has been carried out for this object. Early spectroscopic observations using photographic plates were presented by Bowen & Wyse (1939) and Wyse (1942). Combining photographic and spectrophotometric techniques, Kaler et al. (1976) measured intensities of lines between 3132–8665 Å. They suggested that the nebula may contain a dense central ionized region with electron density of $N_e \sim 10^7 \text{ cm}^{-3}$. Using an echelle spectrograph equipped with a CCD detector, Keyes et al. (1990) presented the spectrum of NGC 7027 over the wavelength range 3673–8750 Å and showed that the nebula has an average electron density $\sim 60\,000 \text{ cm}^{-3}$ and an electron temperature $\sim 14\,000$ K. Based on deep

Send offprint requests to: Y. Zhang

* Tables 2 and 4 are only available in electronic form at the CDS via anonymous ftp to cdsarc.u-strasbg.fr (130.79.126.5) or via <http://cdsweb.u-strasbg.fr/cgi-bin/qcat?J/A+A/>; Tables 1, 3, and Fig. 1 and the Appendices A and B with their tables are only available in electronic form at <http://www.edpsciences.org>

** Also Space Telescope Science Institute, 3700 San Martin Drive, Baltimore, MD 21218

medium resolution optical spectra, Péquignot & Baluteau (1994) detected forbidden lines from heavy elements with $Z > 30$ from this nebula, while deep CCD spectra encompassing the wavelength range of 6540–10460 Å have been published by Baluteau et al. (1995).

The infrared (IR) spectrum of NGC 7027 has also been extensively studied (e.g. Dyck & Simon, 1976; Telesco & Harper, 1977; Melnick et al., 1981; Condal et al., 1981; Gee et al., 1984; Nagata et al., 1988; Rudy et al., 1992). Owing to its status as a wavelength standard, IR observations were repeatedly taken by the Infrared Space Observatory (*ISO*) (see e.g. Liu et al., 1996; Bernard-Salas et al., 2001). One advantage of observing in the IR is the reduced effect of dust extinction. The IR spectrum also gives access to lines emitted by ionized species unobservable in other wavelength regions, thus reducing uncertainties in abundance determinations. The ISO observations yielded a large number of molecular features, which give information of the photodissociation regions and molecular envelope surrounding the ionized region (e.g. Liu et al., 1996; Justtanont et al., 2000). A large number of ultraviolet (UV) spectra of NGC 7027 are available from the International Ultraviolet Explorer (*IUE*) data archive (Bohlin et al., 1975; Keyes et al., 1990). The UV spectra are particularly useful for the investigation of the interstellar and circumstellar reddening, mass-loss rate and properties of the stellar winds. The UV spectra yield intensities of strong collisionally excited lines (CELs) from ionized carbon not available in other wavelength regions, such as C III] $\lambda\lambda 1906, 1909$ and C IV $\lambda\lambda 1548, 1550$, and are therefore crucial for the determination of carbon abundances.

NGC 7027 is known to contain a large amount of local dust. Seaton (1979) shows that the dust reddening varies across the nebula. He used a two-dust-component model to fit the radio and infrared observations. A wedge-shaped extinction model is presented by Middlemass (1990), assuming that dust extinction increases linearly across the surface of the nebula. Walton et al. (1988) deduced an extinction map of NGC 7027 and found an average extinction of $E_{B-V} = 1.02$. They also deduced that the CS lies at a position of low extinction, $E_{B-V} = 0.8$. The latter result is however not supported by the high-resolution imaging observations of Robberto et al. (1993) and Wolff et al. (2000) who find that $E_{B-V} = 1.07$ and 1.10 towards the CS, respectively.

The large number of CELs and optical recombination lines (ORLs) detected in the spectrum of NGC 7027 from a variety of ionic species provide a unique opportunity to study the chemical composition of the nebula at a level normally unachievable in other emission line nebulae. A long-standing problem in nebular abundance studies has been that heavy-element abundances derived from ORLs are systematically higher than those derived from CELs. In extreme cases, the discrepancies can exceed a factor of 10 (see Liu 2003 for a recent review). Related to the CEL versus ORL abundance determination dichotomy, electron temperatures determined from traditional CEL

diagnostic ratios, such as the [O III] $(\lambda 4959 + \lambda 5007)/\lambda 4363$ nebular to auroral line ratio, are found to be systematically higher than those determined from analyses of the recombination spectrum, such as the H I recombination continuum Balmer discontinuity and He I recombination lines. The two phenomena are found to be correlated, the larger the discrepancy between the CEL and ORL abundances, the larger the difference between the CEL and recombination line/continuum temperatures (Liu et al., 2001b; Liu, 2003). Liu et al. (2000) ascribed the CEL versus ORL temperature/abundance determination discrepancies to the existence of ultra cold H-deficient inclusions embedded in nebulae. In the case of NGC 7027, Bernard-Salas et al. (2001) compared C⁺⁺/H⁺, N⁺⁺/H⁺ and O⁺⁺/H⁺ ionic abundance ratios derived from CELs and from ORLs and found that the abundance discrepancies in this young, compact PN are insignificant.

Compared to the gaseous nebula, the CS of NGC 7027 is less well studied. Embedded in a bright nebula, it is a difficult task to measure its visual magnitude, which is necessary for the determination of the effective temperature of the CS using the Zanstra method. Analyses published so far have yielded discrepant results. Shaw & Kaler (1982) estimate that the CS has an effective temperature of 180 000 K, compared to a much higher value of 310 000 K obtained by Walton et al. (1988). More recently, based on near IR observations where the CS is better observed, Latter et al. (2000) derive a value of 198 000 K. All these estimates were based on the Zanstra method (Zanstra, 1927). Latter et al. (2000) also estimate that the CS has a mass of 0.7 solar masses. By comparing the observed nebular elemental abundances and the predictions of semi-analytical TP-AGB evolutionary models of Marigo et al. (1996), Bernard-Salas et al. (2001) suggest that the CS is probably descended from a C-rich progenitor star with a main sequence mass between 3–4 solar masses.

In this paper, we present new optical spectra of this archetypal young PN, obtained by uniformly scanning a long slit across the entire nebular surface. The spectra reveal a large number of emission lines. The comprehensive line list generated from the spectra is intended to facilitate future spectroscopic observations and line identifications of emission line nebulae. In order to have a comprehensive view of the thermal and density structures of the nebula and its chemical composition, we have also included in our analysis available *IUE* spectra in the UV and *ISO* spectra from the near- to far-IR. Section 2 describes our new optical observations and the procedures of data reduction and presents identifications and fluxes of detected emission lines. In Section 3, we report the first detection of Raman-scattered features from this nebula. Dust extinction towards NGC 7027 is briefly discussed in Section 4. In Section 5, we present plasma diagnostic results. Ionic and elemental abundances derived from ORLs and CELs are presented and compared in Section 6. Section 7 discusses the CS. A summary then follows in Section 8.

2. Observations

2.1. Optical spectroscopy

The observations were carried out in 1996 and 1997, using the ISIS long-slit double spectrograph mounted on the 4.2 m William Herschel Telescope (WHT) at La Palma. An observational journal listing the spectral wavelength coverage and FWHM resolution is presented in Table 1. For both the Blue and Red arms of the spectrograph, a Tek $1024 \times 1024 \text{ } 24\mu\text{m} \times 24\mu\text{m}$ chip was used, yielding a spatial sampling of $0.3576 \text{ arcsec per pixel}$ projected on the sky. In 1996, a 600 g mm^{-1} and a 316 g mm^{-1} grating were used for the Blue and Red Arm, respectively. In 1997, they were replaced respectively by a 1200 g mm^{-1} and a 600 g mm^{-1} grating. A dichroic with a cross-over wavelength near 5200 \AA was used to split the light beam. In order to avoid uncertainties caused by ionization stratification when comparing the ionic abundances derived from the optical spectrum with those deduced from UV and IR spectra obtained with space-borne facilities which use large apertures and thus yield total line fluxes for the whole nebula, the long slit of the ISIS spectrograph was used to uniformly scan across the entire nebular surface by differentially driving the telescope in Right Ascension. The mean optical spectrum thus obtained, when combined with the total $\text{H}\beta$ flux measured with a large aperture, $\log F(\text{H}\beta) = -10.12 \text{ (erg cm}^{-2} \text{ s}^{-1})$ (Shaw & Kaler, 1982), yields integrated fluxes for the whole nebula for all emission lines detected, which are therefore directly comparable to those measured with the space-borne facilities.

Four wavelength regions were observed in 1996. The $\lambda\lambda 3620\text{--}4400$ and $\lambda\lambda 4200\text{--}4980$ ranges were observed with the Blue Arm and the $\lambda\lambda 5200\text{--}6665$ and $\lambda\lambda 6460\text{--}7930$ regions with the Red Arm. In 1997, ten spectral regions covering the wavelength range from 3310 to 9160 \AA were observed (c.f. Table 1). Spectral lines falling in the overlapping wavelength region of two adjacent wavelength setups were used to scale the spectra and ensured that all spectra were on the same flux scale. Short exposures were taken in order to obtain intensities of the brightest emission lines, which were saturated on spectra with long exposure times.

All spectra were reduced using the LONG92 package in MIDAS¹ following the standard procedure. Spectra were bias-subtracted, flat-fielded and cosmic-rays removed, and then wavelength calibrated using exposures of copper-neon and copper-argon calibration lamps. Absolute flux calibration was obtained by observing the *HST* spectrophotometric standard stars, BD +28° 4211 and Hz 44 using a 6 arcsec wide slit.

All line fluxes, except those of the strongest, were measured using Gaussian line profile fitting. For the strongest and isolated lines, fluxes obtained by direct integration over the observed line profile were adopted. A total of 937 distinct emission features were measured, including 739 isolated lines, 198 blended fea-

tures of two or more lines and 18 unidentified features. Combining the single and blended features, a total of 1174 lines were identified. The main references used for line identifications and laboratory wavelengths are Keyes et al. (1990), Péquignot & Baluteau (1994), Baluteau et al. (1995), Hirata & Horaguchi (1995)², the NIST Spectroscopic Database³, the Atomic Line List Version 2.04 compiled by P. A. M. van Hoof⁴ and reference therein. The complete optical spectrum is plotted in Fig. 1 with identified lines marked. Several emission lines from ions of $Z > 30$ have been detected. In Appendix A, their observed fluxes are compared with those obtained by Péquignot & Baluteau (1994).

A full list of lines detected in our deep integrated optical spectrum and their measured fluxes are presented in Table 2. The first column gives the observed wavelengths after correcting for Doppler shifts determined from H I Balmer lines. The observed fluxes are given in column 2. Column 3 lists the fluxes after correcting for dust extinction (cf. Section 4). The remaining columns of the table give, in sequence, ionic identification, laboratory wavelength, multiplet number (with a prefix ‘V’ for permitted lines, ‘F’ for forbidden lines, and ‘H’ and ‘P’ for hydrogen Balmer and Paschen lines, respectively), lower and upper spectral terms of the transition, and statistical weights of the lower and upper levels, respectively. All fluxes are normalized such that $F(\text{H}\beta) = I(\text{H}\beta) = 100$.

2.2. IUE and ISO observations

NGC 7027 was observed by the *IUE* over the period from 1979 to 1983. Both high- and low-resolution spectra were obtained with the Short Wavelength Prime (SWP) and with the Long Wavelength Redundant (LWR) cameras, covering the wavelength ranges $1150\text{--}1975 \text{ \AA}$ and $1910\text{--}3300 \text{ \AA}$, respectively. Only observations obtained with the *IUE* large aperture are included in the current analysis. They are listed in Table 3. The *IUE* large aperture has an oval shape of dimensions $10'' \times 23''$, larger than the angular size of the ionized region of NGC 7027 as revealed by radio imaging (c.f. Roelfsema et al., 1991). All the *IUE* spectra were retrieved from the *IUE* Final Archive hosted by the ESA Data Centre in Vilspa, Spain. Short exposures were used for measuring the strongest lines, which were saturated in the spectra of long exposure time. The measured line fluxes are given in Table 4. Our measurements are in reasonable agreement with those reported by Keyes et al. (1990), who used fewer spectra (SWP17240L, SWP17242L, SWP19579L, SWP19877L, LWR05615L, LWR15105L, LWR15861L and LWR15862L). The fluxes were normalized to $F(\text{H}\beta) = 100$ using an $\text{H}\beta$ flux of $\log F(\text{H}\beta) = -10.12 \text{ (ergs cm}^{-2} \text{ s}^{-1})$ (Shaw & Kaler, 1982) and then dereddened using a reddening constant of $c(\text{H}\beta) = 1.37$ (c.f. Section 4). The nor-

¹ MIDAS is developed and distributed by the European Southern Observatory.

² <http://amods.kaeri.re.kr/spect/SPECT.html>.

³ http://www.physics.nist.gov/cgi-bin/AtData/main_asd.

⁴ <http://www.pa.uky.edu/~peter/atomic/>.

malized observed and dereddened line fluxes are listed in the last column of Table 4.

NGC 7027 has also been extensively observed with the Short Wavelength Spectrometer (SWS; de Graauw et al., 1996) and Long Wavelength Spectrometer (LWS; Clegg et al., 1996), on board *ISO* (Kessler et al., 1996), covering wavelength ranges from 2.38–45.2 μm and 40–197 μm , respectively. The smallest ISO-SWS aperture has a rectangular size of 14'' \times 20'', comparable to the large aperture of *IUE*. The LWS has an effective entrance aperture of approximately 70'' in diameter. Thus both the SWS and LWS apertures are big enough to contain the whole ionized region of NGC 7027. The LWS and SWS spectra of NGC 7027 have previously been analyzed by Liu et al. (1996) and Bernard-Salas et al. (2001). Emission line fluxes reported in these papers are included in the current analysis. We normalized the observed fluxes to $F(\text{H}\beta) = 100$ using the total H β flux given above and then dereddened assuming $c(\text{H}\beta) = 1.37$.

3. Raman scattering features

A broad feature at 4852 \AA detected in the optical spectrum of NGC 7027 has been proposed to be the Raman-scattered line of He II(2-8) by atomic hydrogen (Péquignot et al., 1997). This was the first detection of a Raman line from a PN. More recently, Péquignot et al. (2003) report the detection in this PN of another two Raman features, He II(2-10) and He II(2-6) at 4332 \AA and 6546 \AA , respectively. Except for the 6546 \AA feature, which is seriously blended with the strong [N II] line at 6548 \AA , the detection and identification of the other two He II Raman lines are confirmed by our new observations (c.f. Fig. 1). The detection of Raman lines suggests the abundant presence of neutral hydrogen around the ionized regions of this high excitation PN.

Our spectrum also reveals an abnormally broad feature redward of the [Kr III] $\lambda\lambda 6827$ line (Fig. 2). A two-Gaussian profile fit shows that the broad feature has a central wavelength of 6829.16 \AA and a $FWHM$ of 253 km s^{-1} , which is much broader than the [Kr III] $\lambda\lambda 6827$ line ($FWHM \sim 88 \text{ km s}^{-1}$). The feature was also detected by Péquignot & Baluteau (1994) and was identified by them as a Si II line. Given the narrow width of other Si II lines, we regard this as a mis-identification. Schmid (1989) suggested that Raman scattering of the O VI $\lambda\lambda 1032, 1038$ resonance doublet by neutral hydrogen gives rise to two velocity-broadened lines at 6830 and 7088 \AA that have been widely observed in the spectra of symbiotic stars. Therefore, based on its measured wavelength and the large $FWHM$, we identify the broad emission feature at 6829.16 \AA as the O VI Raman line at 6830 \AA . Our identification is strengthened by the detection of another feature, marginally above the detection limit, at 7088 \AA , i.e. at the expected position of the other O VI Raman line. The measurements yield a $\lambda\lambda 7088/\lambda\lambda 6830$ intensity ratio of approximately 1/7, smaller than the ratio of 1/4 typically found in symbiotic stars. While our mea-

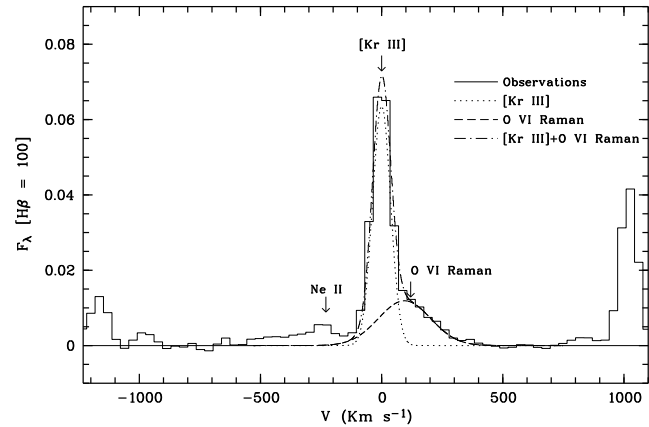


Fig. 2. Detailed spectrum showing the region centered at 6828 \AA . The histogram is the observed spectrum. The dotted-dashed line represents a two-Gaussian fit, with the narrow and broad components represented by dotted and dashed lines respectively. The broad feature redwards of the [Kr III] line is identified as the O VI Raman line (see text).

sured $\lambda\lambda 7088/\lambda\lambda 6830$ intensity ratio in NGC 7027 may suffer from large uncertainties because of the weakness of the $\lambda\lambda 7088$ feature, its small value seems to suggest that the environs from which these Raman lines arise in NGC 7027 may differ from those in symbiotic systems. In symbiotic binaries, the ultraviolet O VI doublet emission from the vicinity of a very hot white dwarf is Raman scattered in the H I atmosphere of a giant star companion. The nucleus of NGC 7027 is not known as a binary star. By analogy with the He II Raman lines observed by Péquignot et al. (1997, 2003), the O VI Raman lines may be formed in the photodissociation region (PDR) that corresponds to the interface between the H $^+$ region and the large molecular envelope of NGC 7027. The relatively small column density of this PDR, compared to the atmosphere of a giant, may be compensated by the large covering factor. The theoretical ratio of the O VI $\lambda\lambda 1032, 1038$ lines is 2 and the ratio of the Raman cross sections is about 3.3. In a small optical depth approximation, the intensity ratio of the Raman components should be of order 6.6, in agreement with the observed intensities. The smaller ratio observed in symbiotics may reflect a departure from the 2:1 ratio of the O VI lines (a similar departure is observed for C IV and N V in these objects; see Schmid 1989). In NGC 7027, the red O VI Raman lines may allow one to indirectly determine the intensity of the UV O VI lines, which presumably arise from the high ionization region of the PN, and thus provide a new useful constraint on the properties of the nucleus.

Raman features have also been detected in the spectrum of the PN NGC 6302 (Groves et al., 2002). Both NGC 7027 and NGC 6302 have a very high excitation class and show strong molecular emission. They thus may share some common evolutionary properties.

4. Reddening summary

It is generally believed that a significant amount of dust coexists with the ionized and neutral gas in NGC 7027 (see, e.g., Woodward et al., 1992). Large variations of extinction across the nebula, caused by local dust, have been detected by optical and radio imaging (Walton et al., 1988). It follows that emission lines arising from different ionized zones may suffer different amounts of reddening. A comprehensive treatment of the dust extinction for the emission lines observed from NGC 7027 requires detailed photoionization modeling and an accurate treatment of the dust component (its spatial and size distributions, chemical composition etc.), which is beyond the scope of the current work. Efforts to correct for the effects of dust extinction on observed line fluxes assuming a simplified geometry have been attempted previously by Seaton (1979) and Middlemass (1990).

On the other hand, our previous study shows that it is still a good approximation to use the standard Galactic extinction curve for the diffuse interstellar medium (ISM) to deredden the integrated spectrum of NGC 7027 (Zhang et al., 2003). Accordingly, we have dereddened all line fluxes by

$$I(\lambda) = 10^{c(H\beta)f(\lambda)} F(\lambda), \quad (1)$$

where $f(\lambda)$ is the standard Galactic extinction curve for a total-to-selective extinction ratio of $R = 3.2$ (Howarth, 1983), and $c(H\beta)$ is the logarithmic extinction at $H\beta$.

From the observed Balmer $H\alpha/H\beta$ and $H\gamma/H\beta$ ratios, we deduce an average value of $c(H\beta) = 1.34 \pm 0.02$. For $T_e = 12\,800\text{ K}$, $\text{He}^{2+}/\text{H}^+ = 0.041$ and $\text{He}^+/\text{H}^+ = 0.058$ (see below), the 5-GHz free-free radio continuum flux density, $S(5\text{ GHz}) = 6.921\text{ Jy}$, combined with the total $H\beta$ flux, $\log F(H\beta) = -10.12\text{ (erg cm}^{-2}\text{ s}^{-1}\text{)}$ (Cahn et al., 1992), yield $c(H\beta) = 1.37$, consistent with the value derived from the Balmer decrement within the uncertainties. The observed $\text{He II } \lambda 1640/\lambda 4686$ ratio gives a slightly higher value, $c(H\beta) = 1.42$. As an alternative way to determine c , we plot in Fig. 3 a synthesized spectrum of NGC 7027, computed taking into account contributions from the CS and from the free-free and free-bound emission of ionized hydrogen and helium (c.f. Zhang et al. 2004 for details). By comparing the synthesized spectrum with the observed one dereddened with a varying value of c , especially around the 2200 \AA region of the UV extinction bump, as shown in Fig. 3, we derive $c(H\beta) = 1.44$. Although the $\text{He II } \lambda 1640/\lambda 4686$ ratio and the dip at 2200 \AA yield slightly higher extinction constants compared to the values given by the Balmer decrement and by the radio continuum flux density, presumably caused by the presence of small dust grains within the nebula, we do not regard this as significant and opt to use $c(H\beta) = 1.37$ to deredden all measurements from the UV to the IR.

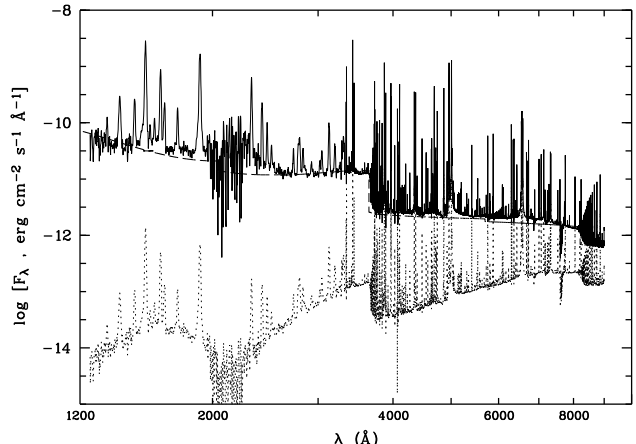


Fig. 3. The UV and optical spectrum showing the 2200 \AA extinction bump which can be used to estimate total reddening towards NGC 7027. The solid and dotted lines show respectively the observed spectrum and that dereddened assuming $c(H\beta) = 1.44$. The dashed line is a synthesized theoretical spectrum of recombination line and continuum emission from ionized hydrogen and helium.

5. Physical conditions

5.1. CEL diagnostics

The spectrum of NGC 7027 reveals a large number of CELs, useful for nebular electron density and temperature diagnostics and abundance determinations. Adopting atomic data from the references given in Appendix B and solving the level populations for multilevel (≥ 5) atomic models, we have determined electron temperatures and densities from a variety of CEL ratios and list the results in Table 5. Electron temperatures were derived assuming a constant electron density of $\log N_e = 4.67\text{ (cm}^{-3}\text{)}$, the average value yielded by a number of density-sensitive diagnostic ratios. Likewise, an average electron temperature of $14\,000\text{ K}$ was assumed when determining electron densities. A plasma diagnostic diagram based on CEL ratios is plotted in Fig. 4.

Liu et al. (2000) showed that the $[\text{N II}] \lambda 5754$ line can be enhanced by recombination excitation, leading to an overestimated electron temperature being determined from the $[\text{N II}] (\lambda 6548 + \lambda 6584)/\lambda 5754$ ratio. Using the formula given by Liu et al. (2000), we find that for this particular PN, the contribution by recombination to the intensity of the $[\text{N II}] \lambda 5754$ line is negligible (< 1%). We also find the presence of a weak He II Raman line at 6546 \AA hardly affects our estimate of the $[\text{N II}] \lambda 6548$ line flux – our measurements yield a $[\text{N II}] \lambda 6548/\lambda 6584$ ratio which is in excellent agreement with the theoretical value of 2.9.

The electron temperature derived from the $[\text{O III}] \lambda 4363/\lambda 1663$ ratio is 2100 K higher than the value deduced from the $[\text{O III}] (\lambda 4959 + \lambda 5007)/\lambda 4363$ ratio. This may be due to measurement uncertainties in the $[\text{O III}] \lambda 1663$ line flux. The $[\text{O II}]$ nebular to auroral line ratio, $(\lambda 3726 + \lambda 3729)/(\lambda 7320 + \lambda 7330)$, yields an abnormally

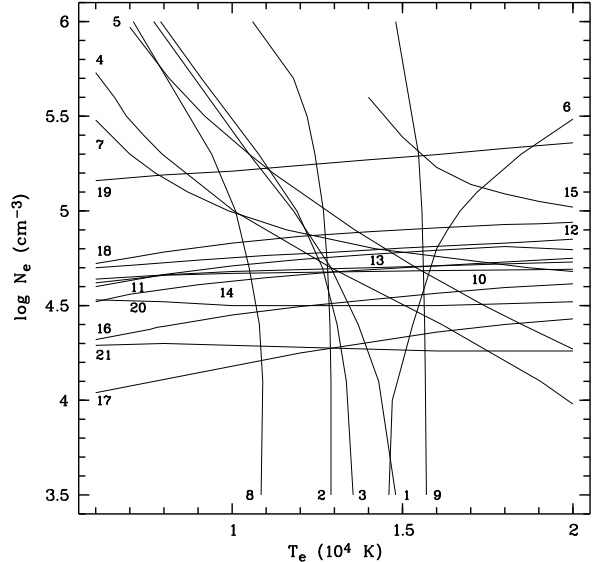
Table 5. Plasma diagnostics.

ID	Diagnostic	Result
		T_e (K)
1	[Ne III] $15\mu\text{m}/(\lambda3868 + \lambda3967)$	12900
2	[Ar III] $\lambda7135/\lambda5192$	12800
3	[O III] $(\lambda4959 + \lambda5007)/\lambda4363$	12600
4	[N II] $(\lambda6548 + \lambda6584)/\lambda5754$	12900
5	[Ne IV] $\lambda1602/(\lambda2422 + \lambda2425)$	15300
6	[O III] $\lambda4363/\lambda1663$	14700
7	[O II] $(\lambda7320 + \lambda7330)/\lambda3726$	18700
8	[O I] $\lambda5577/(\lambda6300 + \lambda6363)$	10400
9	[Mg V] $\lambda2783/5.6\mu\text{m}$	15600
	He I $\lambda6678/\lambda4471$	9430
	He I $\lambda6678/\lambda5876$	12700
	He I $\lambda7281/\lambda5876$	8800
	He I $\lambda7281/\lambda6678$	10530
	BJ/H 11	12800
		$\log N_e$ (cm^{-3})
10	[Ar IV] $\lambda4740/\lambda4711$	4.77
11	[C III] $\lambda1906/\lambda1909$	4.80
12	[Cl III] $\lambda5537/\lambda5517$	4.70
13	[Ne IV] $\lambda2425/\lambda2423$	4.69
14	[Si III] $\lambda1884/\lambda1892$	4.54
15	[S II] $\lambda6731/\lambda6716$	$\gtrsim 5$
16	[Ne V] $24\mu\text{m}/14\mu\text{m}$	4.31
17	[Ne III] $15\mu\text{m}/36\mu\text{m}$	4.89
18	[O II] $\lambda3726/\lambda3729$	4.68
19	[Fe III] $\lambda4881/\lambda4701$	5.27
20	[Fe III] $\lambda4701/\lambda4733$	4.50
21	[Fe III] $\lambda4733/\lambda4754$	4.27
	H I Balmer decrement	~ 5
	He II Pfund decrement	~ 5

high temperature of 18 700 K, 5800 K higher than that determined from the [N II] $(\lambda6548 + \lambda6584)/\lambda5754$ ratio. Similar discrepancies have also been found in M 1-42, M 2-36 (Liu et al., 2001b) and NGC 6153 (Liu et al., 2000). This is most likely caused by the presence of high density clumps in the nebula. The [O II] $\lambda\lambda3726, 3729$ nebular lines have much lower critical densities ($\sim 10^3 \text{ cm}^{-3}$) than the [O II] $\lambda\lambda7320, 7330$ auroral lines ($\sim 10^6 \text{ cm}^{-3}$), and are thus susceptible to suppression by collisional de-excitation in dense regions, leading to an apparently high ($\lambda3726 + \lambda3729$)/($\lambda7320 + \lambda7330$) temperature.

The line ratios of highly ionized species, [Ne IV] $\lambda1602/(\lambda2422 + \lambda2425)$ and [Mg V] $\lambda2783/5.6\mu\text{m}$, yield high electron temperatures of 15 300 K and 15 600 K, respectively. For comparison, the line ratio of neutral species, [O I] $\lambda5577/(\lambda6300 + \lambda6363)$, yields a much lower value of 10 400 K. In addition, the [C I] nebular to auroral line ratio $(\lambda9824 + \lambda9850)/\lambda8727$ gives a temperature of only 8100 K for the warm transition regions around the nebula (Liu & Barlow, 1996). Our results thus suggest a negative temperature gradient across the nebula. A similar trend was previously found by Bernard-Salas et al. (2001).

All density diagnostic ratios analyzed here yield compatible results. The only exception is the [S II]

**Fig. 4.** Plasma diagnostic diagram. Each curve is labelled with an ID number given in Table 5.

$\lambda6731/\lambda6716$ doublet ratio, which falls outside the high density limit for $T_e < 14\,000$ K. The [S II] $\lambda6731$ and $\lambda6716$ lines have relatively low critical densities, $\log N_{\text{crit}} = 3.62$ and 3.21 (cm^{-3}), respectively, at $T_e = 10\,000$ K. The doublet is thus not suitable for density determination for such a compact nebula. Nevertheless, Fig. 4 shows that the observed [S II] $\lambda6731/\lambda6716$ ratio implies a density higher than 10^5 cm^{-3} , which is at least a factor of two higher than that derived from the [O II] $\lambda3726/\lambda3729$ doublet ratio. Stanghellini & Kaler (1989) have found that the [S II] densities of PNe are systematically higher than the corresponding values derived from the [O II] lines. Rubin (1989) ascribes this to the effects from a dynamical plow by the ionization front, since S⁰ has a lower ionization potential than O⁰ and thus the S⁺ zone is closer to the H⁺ edge. Alternatively, this may also be caused by uncertainties in the atomic parameters (Copetti & Writzl, 2002; Wang et al., 2004). Note that Liu et al. (2001a) find that densities derived from the low critical density [O III] $88\mu\text{m}/52\mu\text{m}$ ratio are systematically lower than given by high critical density optical diagnostic ratios, such as the [Cl III] and [Ar IV] doublet ratios, indicating that density inhomogeneities are ubiquitous amongst PNe.

The [Fe III] $\lambda4881/\lambda4701$ ratio yields a relatively high electron density of $\log N_e = 5.27 (\text{cm}^{-3})$. We note that the N III V9 $\lambda4882$ line is blended with the [Fe III] $\lambda4881$ line. However, assuming N III $I(\lambda4881)/I(\lambda4884) = 0.05$, we find that the contribution of the N III line to the $\lambda4881$ feature is negligible ($\sim 0.2\%$). On the other hand, the flux of the [Fe III] $\lambda4881$ line could also be underestimated due to the possible effects of absorption by the diffuse interstellar band (DIB) at 4882.56 Å (Tuairisg et al., 2000), as suggested by our detections in the spectrum of NGC 7027 of DIBs at 5705, 5780, 6204 and 6284 Å (see Fig. 1). An

underestimated [Fe III] $\lambda 4881$ line flux will lead to an overestimated [Fe III] $\lambda 4881/\lambda 4701$ density.

5.2. ORL diagnostics

Table 5 gives the Balmer jump temperature, derived from the ratio of the nebular continuum Balmer discontinuity at 3646 \AA to H I $\lambda 3770$ using the following equation (Liu et al., 2001b)

$$T_e(\text{BJ}) = 368 \times (1 + 0.259Y^+ + 3.409Y^{++}) \times \left(\frac{\text{BJ}}{\text{H I} 3770} \right)^{-1.5} \text{ K}, \quad (2)$$

where $\text{BJ}/\text{H I} 3770$ is in units of \AA^{-1} and Y^+ and Y^{++} are He^+/H^+ and $\text{He}^{++}/\text{H}^+$ abundance ratios, respectively. Using He^+/H^+ and $\text{He}^{++}/\text{H}^+$ ratios determined from He I and He II recombination lines (see next section), we obtain a $T_e(\text{BJ})$ of 12 800 K.

We have also used the He I line ratios to determine the average He I line emission electron temperature. In Fig. 5, we plot He I $\lambda 6678/\lambda 4471$, $\lambda 6678/\lambda 5876$, $\lambda 7281/\lambda 5876$ and $\lambda 7281/\lambda 6678$ ratios as a function of electron temperature. The measured line ratios along with their uncertainties are overplotted. The He I line emission coefficients used here are from Benjamin et al. (1999) under the assumption of Case B recombination. An electron density of $N_e = 10^5 \text{ cm}^{-3}$, as deduced by the H I Balmer decrement and the He II Pfund decrement (see below), was assumed when determining temperatures, although the results are insensitive to the adopted electron density, as shown in Fig. 5. The results are presented in Table 5. Fig. 5 shows that the temperatures derived from the He I line ratios range between 7500 and 14700 K. Considering certain advantages over other He I ratios, as discussed in Zhang et al. (2005), the He I $\lambda 7281/\lambda 6678$ ratio gives the most reliable result, which is only 1.5σ lower than the value derived from the [O III] forbidden line ratio.

Electron densities have been derived from the H I Balmer decrement and the He II Pfund decrement. Fig. 6 shows the observed intensity ratio of the high-order H I Balmer lines ($n \rightarrow 2, n = 12, 13, \dots, 24$) to H I $\lambda 3770$ and the He II Pfund lines ($n \rightarrow 5, n = 15, 17, \dots, 25$) to He II $\lambda 4686$ as a function of the principal quantum number n of the upper level. Theoretical intensity ratios for different electron densities are overplotted assuming an electron temperature of 12 800 K, as deduced from the H I Balmer discontinuity. As shown in Fig. 6, both the H I Balmer decrement and the He II Pfund decrement yield a best fit at $N_e \sim 10^5 \text{ cm}^{-3}$, in reasonable agreement with densities derived from CEL diagnostics. The result rules out the possibility that H I and He II lines arise from dense regions with an electron density in excess of 10^7 cm^{-3} as proposed by Kaler et al. (1976). In principle the H I Paschen decrement and the He II Pickering decrement may also be used to probe electron density (Péquignot & Baluteau, 1988). However, both series are strongly affected by telluric absorption and line blending, and thus are omitted in the current analysis.

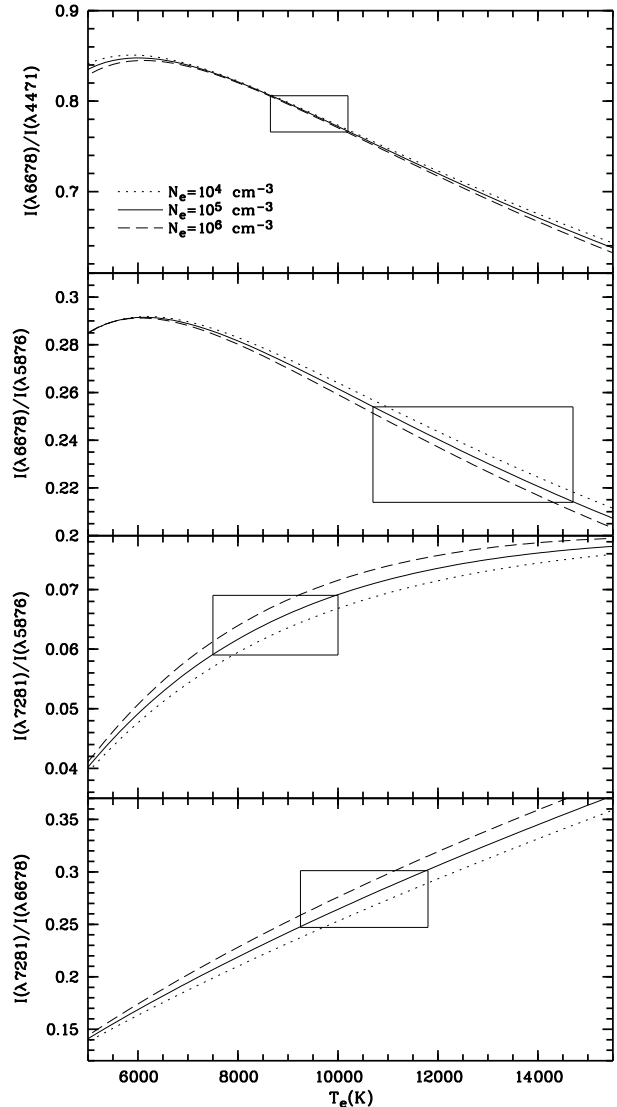


Fig. 5. The He I $\lambda 6678/\lambda 4471$, $\lambda 6678/\lambda 5876$, $\lambda 7281/\lambda 5876$ and $\lambda 7281/\lambda 6678$ ratios as a function of electron temperature for $\log N_e = 4$ (dotted line), 5 (solid line) and 6 (dashed line) (cm^{-3}). The boxes are the observed values with measurement uncertainties.

6. Elemental abundances

6.1. Ionic abundances from CELs

Ionic abundances are derived from CELs by

$$\frac{N(\text{X}^{i+})}{N(\text{H}^+)} = \frac{I_{jk}}{I_{\text{H}\beta}} \frac{\lambda_{jk}}{\lambda_{\text{H}\beta}} \frac{\alpha_{\text{H}\beta}}{A_{jk}} \left[\frac{N_j}{N(\text{X}^{i+})} \right]^{-1} N_e, \quad (3)$$

where $I_{jk}/I_{\text{H}\beta}$ is the intensity ratio of the ionic line to $\text{H}\beta$, $\lambda_{jk}/\lambda_{\text{H}\beta}$ is the wavelength ratio of the ionic line to $\text{H}\beta$, $\alpha_{\text{H}\beta}$ is the effective recombination coefficient for $\text{H}\beta$, A_{jk} is the Einstein spontaneous transition rate of the ionic line, and $N_j/N(\text{X}^{i+})$ is the fractional population of the upper level where the ionic line arises and is a function of electron temperature and density.

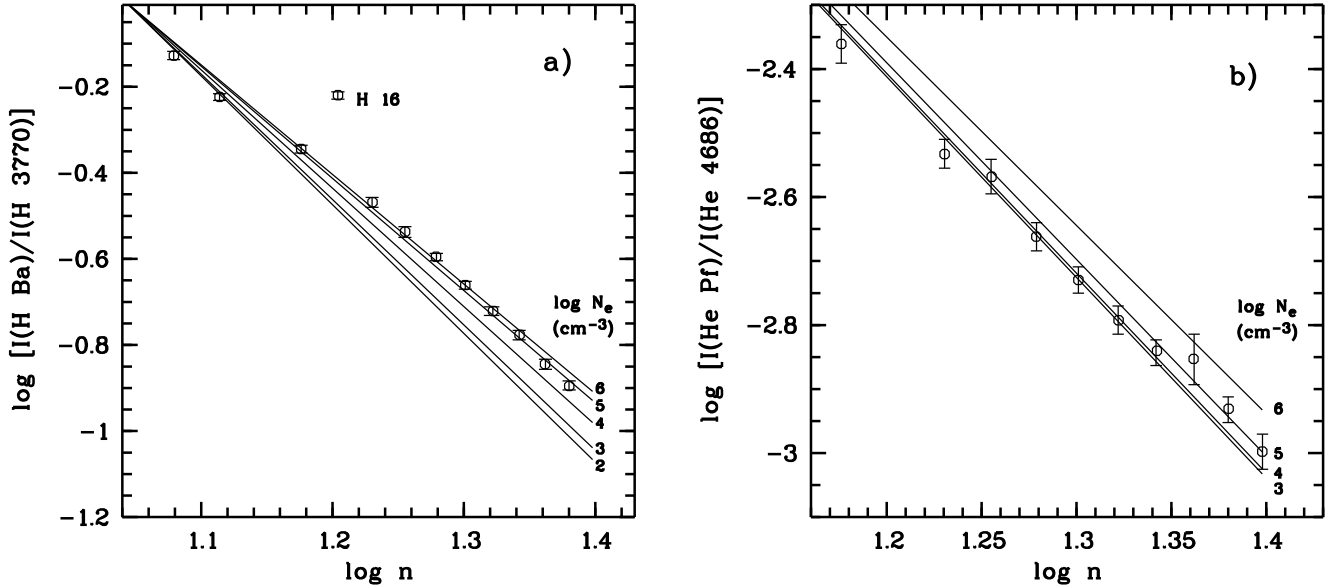


Fig. 6. Intensity ratios of a) H I Balmer lines to H II $\lambda 3770$ and b) He II Pfund lines to He II $\lambda 4686$, as a function of the principal quantum number n of the upper level of the transition. H 16 at 3703.86 \AA is blended with the He I $\lambda 3705.12$ line. Solid lines are theoretical values for electron densities of $N_e = 10^2$ to 10^6 cm^{-3} at a constant electron temperature of 12800 K .

Ionic abundances derived from UV, optical and infrared CELs are presented in Table 6. Based on plasma diagnostic results presented in the previous section, a constant electron density of $\log N_e = 4.67\text{ cm}^{-3}$ was assumed for all ionic species. Electron temperatures of 12600 K and 15500 K were assumed throughout for ions with ionization potentials lower and higher than 50 eV , respectively. In Table 6, the ‘adopted’ denotes average and adopted values derived from individual lines weighted by intensity.

Note that Mg^+ and Fe^+ exist mainly in the PDR outside the ionized zone (defined by H^+), given the very low ($< 8\text{ eV}$) ionization potentials of neutral magnesium and iron. Thus Mg^+ and Fe^+ ionic abundances are not listed in Table 6, even though several Mg II and $[\text{Fe II}]$ CELs have been detected. Similarly, the C II $158\text{-}\mu\text{m}$ line should also arise mainly from the PDR, rather than the ionized region. In fact, the C^+/H^+ ionic abundance ratio derived from the far-IR fine-structure line is a factor of six higher than the value derived from the UV CEL $\lambda 2324$. The large discrepancy remains even if one adopts the lower $158\text{-}\mu\text{m}$ line flux given by Liu et al. (1996), rather than the more recent flux presented in Liu et al. (2001a) based on a more recent version of the LWS data processing pipeline.

6.2. Ionic abundances from ORLs

From measured intensities of ORLs, ionic abundances can be derived using the following equation

$$\frac{N(\text{X}^{i+})}{N(\text{H}^+)} = \frac{I_{jk}}{I_{\text{H}\beta}} \frac{\lambda_{jk}}{\lambda_{\text{H}\beta}} \frac{\alpha_{\text{H}\beta}}{\alpha_{jk}}, \quad (4)$$

where α_{jk} is the effective recombination coefficient for the ionic ORL and is taken from the references listed in

Table 8. Comparison of ionic abundances.

Ion	$N(\text{X}^{i+})/N(\text{H}^+)$		ORL/CEL
	CEL	ORL	
C^{2+}	3.85×10^{-4}	5.54×10^{-4}	1.4
C^{3+}	4.18×10^{-4}	3.87×10^{-4}	0.9
N^{2+}	5.95×10^{-5}	1.03×10^{-4}	1.7
N^{3+}	4.85×10^{-5}	2.56×10^{-5}	0.5
N^{4+}	1.46×10^{-5}	1.68×10^{-5}	1.2
O^{2+}	3.06×10^{-4}	3.95×10^{-4}	1.3
O^{3+}	6.63×10^{-5}	4.04×10^{-5}	0.6
Ne^{2+}	5.35×10^{-5}	8.63×10^{-5}	1.6

Appendix B. Ionic abundances derived from ORLs depend only weakly on the adopted temperature ($\sim T_e^\alpha$, $|\alpha| < 1$), and are essentially independent of N_e . A constant temperature of $T_e = 12800\text{ K}$, as deduced from the H I Balmer jump, was assumed throughout. Ionic abundances derived from ORLs are presented in Table 7.

6.3. Comparison of ionic abundances derived from CELs and ORLs

In Table 8 and Fig. 7 we compare C, N, O and Ne ionic abundances derived from CELs with those derived from ORLs. Table 8 and Fig. 7 show that the ionic abundances of doubly ionized species derived from ORLs, namely those of C^{2+}/H^+ , N^{2+}/H^+ , O^{2+}/H^+ and $\text{Ne}^{2+}/\text{H}^+$, are only slightly higher than those derived from CELs, with an abundance discrepancy factor of about 1.5.

The dichotomy between the ORL and the CEL abundances is an open problem in nebular astrophysics (see

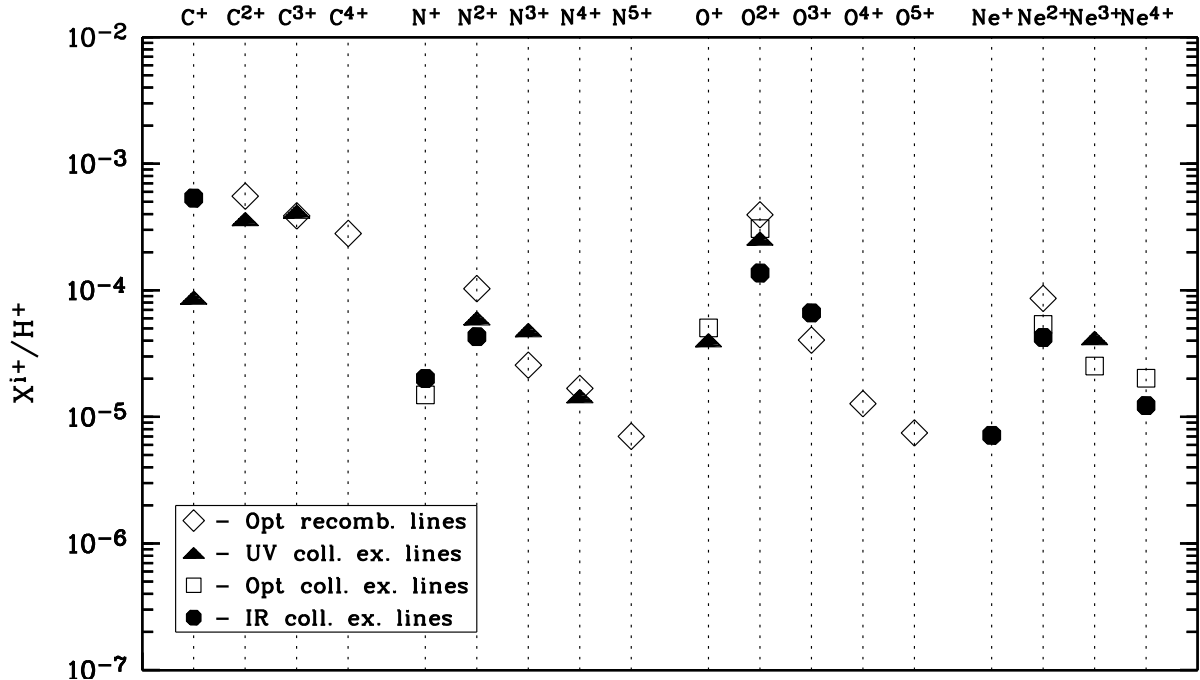


Fig. 7. Comparison of C, N, O and Ne ionic abundances derived from ORLs with those from UV, optical and IR CELs.

Liu 2003 and references therein). A chemically homogeneous nebula with temperature and density variations fails to account for the discrepancy (c.f. Liu, 2003). Instead detailed multi-waveband analyses of a large sample of PNe point to the presence of H-deficient inclusions embedded in the diffuse nebular gas (Tsamis et al., 2003, 2004; Liu et al., 2004a,b; Wesson et al., 2004). A two-abundance model, first proposed by Liu et al. (2000), provides the most plausible explanation for this problem. The model predicts $T_e(\text{He I}) \lesssim T_e(\text{BJ}) \lesssim T_e([\text{O III}])$. Liu et al. (2001b) found that the ORL/CEL abundance discrepancy is positively correlated with the difference between $T_e([\text{O III}])$ and $T_e(\text{BJ})$. It has also been found that the discrepancy increases as the nebula expands and ages (Garnett & Dinerstein, 2001; Tsamis et al., 2004; Zhang et al., 2004). NGC 7027 is a relatively young and compact PN. The small ORL to CEL discrepancies, both for temperature determinations and for abundance determinations, are therefore consistent with the general picture found for other PNe.

Interestingly, it seems that compared to doubly ionized species, abundance discrepancy factors for ionic species of even higher ionization degree, such as C^{3+} , N^{3+} , N^{4+} and O^{3+} , are even smaller. This result is however arguable considering uncertainties in both measurements and in the analysis. If real, then it may indicate that the postulated ultra-cold H-deficient inclusions have a lower ionization degree compared to the diffuse nebula of “normal” chemical composition.

6.4. Total abundances

Total elemental abundances derived for NGC 7027 are presented and compared to values published in the literature in Table 9. Except for helium, all elemental abundances given in the table are based on CEL analyses. The average abundances deduced for a large sample of Galactic PNe by Kingsburgh & Barlow (1994) and the solar photospheric abundances compiled by Lodders (2003) are also given in the table.

The helium elemental abundance is calculated from $\text{He/H} = \text{He}^+/\text{H}^+ + \text{He}^{2+}/\text{H}^+$. For a high-excitation PN such as NGC 7027, very little neutral helium is expected to exist within the ionized region, and can therefore be ignored.

Whenever available, ionization correction factors (*ICFs*) given by Kingsburgh & Barlow (1994) were used to compute the CEL elemental abundances.

The carbon abundance is calculated using the equation

$$\frac{\text{C}}{\text{H}} = ICF(\text{C}) \times \left(\frac{\text{C}^+}{\text{H}^+} + \frac{\text{C}^{2+}}{\text{H}^+} + \frac{\text{C}^{3+}}{\text{H}^+} \right), \quad (5)$$

where

$$ICF(\text{C}) = \left(1 - \frac{2.7\text{N}^{4+}}{\text{N}^+ + \text{N}^{2+} + \text{N}^{3+} + \text{N}^{4+}} \right)^{-1} \quad (6)$$

$$= 1.40.$$

For oxygen, we use

$$\frac{\text{O}}{\text{H}} = ICF(\text{O}) \times \left(\frac{\text{O}^+}{\text{H}^+} + \frac{\text{O}^{2+}}{\text{H}^+} + \frac{\text{O}^{3+}}{\text{H}^+} \right), \quad (7)$$

Table 9. Elemental abundances in NGC 7027, in units such that $\log N(\text{H}) = 12.0$.

Element	This paper	(1)	(2)	(3)	(4)	(5)	Average ^a	Solar ^b
He	11.00	11.03	11.00	11.05	11.02	11.00	11.06	10.90
C	9.10	8.78	8.98	8.84	9.11	8.98	8.74	8.39
N	8.14	8.20	8.21	8.10	8.28		8.35	7.83
O	8.66	8.61	8.71	8.49	8.75	8.66	8.68	8.69
Ne	8.07	8.00	8.14	8.00	8.04		8.09	7.87
Mg	7.60	7.34		7.41	7.33			7.55
S	6.92	6.97		6.86	6.90		6.92	7.19
Cl	5.21	5.04		5.30				5.26
Ar	6.30	6.36		6.32	6.40		6.39	6.55
Fe	5.58				6.00			7.47

^a Average abundances of Galactic PNe (Kingsburgh & Barlow, 1994);

^b Lodders (2003).

Reference: (1) Bernard-Salas et al. 2001; (2) Kwinter & Henry 1996; (3) Keyes et al. 1990; (4) Middlemass 1990; (5) Gruenwald & Péquignot 1989.

where

$$\begin{aligned} ICF(O) &= \left(1 - \frac{0.95N^{4+}}{N^+ + N^{2+} + N^{3+} + N^{4+}}\right)^{-1} \\ &= 1.11. \end{aligned} \quad (8)$$

For sulphur, Kingsburgh & Barlow (1994) give an ICF formula for the case that only S^+ and S^{2+} are measured. For NGC 7027, we have detected lines from S^+ , S^{2+} and S^{3+} . Because of its high-excitation, S^{4+} and S^{5+} are also expected to be present in a significant fraction and thus need to be corrected for. From the photoionization model presented by Shields (1978), we estimate an $ICF(S)$ of 2.13. However, the photoionization model constructed by Middlemass (1990) gives a lower $ICF(S)$ of 1.31. Here we have opted for an average value of 1.72.

Kingsburgh & Barlow (1994) did not discuss magnesium and iron. For magnesium, no CELs are available to determine the Mg^{2+}/H^+ ratio. On the hand, Barlow et al. (2003) show that whatever effect is enhancing the ORL abundances of second-row elements, such as C, N, O and Ne, it seems that it does not affect magnesium, the only third-row element that has been studied using an ORL. Here we have simply added the Mg^{2+}/H^+ ionic abundance ratio derived from the Mg II $\lambda 4481$ ORL to Mg^{3+}/H^+ and Mg^{4+}/H^+ derived from IR CELs to obtain the total Mg elemental abundance. For iron, the only missing ionization stage that needs to be corrected for is Fe^{4+} . According to the photoionization model of Shields (1978), we estimate an $ICF(Fe)$ of 1.13. Note that Mg^+ and Fe^+ exist predominantly in the PDRs outside the ionized region. Although a small amount of these ions is present in the ionized region and emits CELs, we neglect the ionic concentrations in Mg^+ and Fe^+ in the calculation of the total elemental abundances of magnesium and iron in the ionized zone.

For nitrogen, neon, argon and chlorine, no ionization corrections are required and the elemental abundances are given by simply adding up individual observed ionic abundance ratios.

As can be seen from Table 9, elemental abundances derived from individual analyses are generally in good agreement. The largest discrepancy is for carbon, by a factor of 2.14. Except for Bernard-Salas et al. (2001) and the current work, where an empirical method is used, all other abundance analyses presented in Table 9 were based on photoionization modeling. Abundances deduced in the current work are within the range of values reported in previous papers, except for Ar, Mg and Fe. For Ar, although our abundance is slightly lower than values found by others, we deem the difference insignificant. The Mg abundance obtained in the current work is 74% higher than the average value of previous studies. Given that Mg^{2+} is the dominant ionic species of magnesium, owing to the very large ionization potential span of doubly ionized magnesium, from 15 eV to 80 eV, and the fact that in all the previous works the Mg^{2+} abundance was not determined and was corrected for using either an ICF or photoionization model method, we regard the Mg abundance obtained in the current work as more reliable. Amongst the previous studies, only Middlemass (1990) gives an iron abundance and his value is significantly higher than ours. Perinotto et al. (1999) recently calculated iron abundances in a number of PNe and find an Fe/H ratio of 4×10^{-7} [5.60 in units such that $\log N(\text{H}) = 12$] for NGC 7027, which is in excellent agreement with our result.

Our analysis yields a C/O ratio of 2.72. This higher than solar C/O ratio indicates that NGC 7027 is carbon-enriched. The N/O ratio is 0.5, about three times larger than the solar value. According to the criteria defined by Peimbert & Torres-Peimbert (1983), NGC 7027 is not helium and nitrogen rich enough to be a Type-I PN. Magnesium is in good agreement with the solar value. The high magnesium abundance suggests that depletion of magnesium onto dust grains is insignificant in this young PN, contrary to the result of Bernard-Salas et al. (2001). The Fe abundance is well below the solar value, by a factor of about 85, suggesting that an effective condensation

of gas phase iron into dust grains has occurred in this carbon-rich PN.

7. The central star

It is well-known that NGC 7027 is a high-excitation PN. Based on the excitation classification scheme proposed by Dopita & Meatheringham (1990), which makes use of the observed $I(\text{[O III]}\lambda 5007)/I(\text{H}\beta)$ line ratio for low and intermediate excitation PNe (E.C. ≤ 5), and the $I(\text{He II}\lambda 4686)/I(\text{H}\beta)$ ratio for higher excitation class PNe, we find that NGC 7027 has a E.C. of 6.97 from the observed $I(\text{He II}\lambda 4686)/I(\text{H}\beta)$ ratio.

The complete spectral data from the UV to IR accumulated here allow us to calculate the energy-balance temperature (the Stoy temperature) of the CS of NGC 7027. The method was first introduced by Stoy (1933) and then advanced by Kaler et al. (1976) and Preite-Martinez & Pottasch (1983). The method rests on the idea that the total flux of all CELs (which provide the major cooling rate of the nebula) relative to $\text{H}\beta$, is a measure of the average heating rate per photoionization incident (dominated by photoionization of hydrogen given its high abundance), and thus depends on the effective temperature of the central star. Unlike the Zanstra method (Zanstra, 1927), the Stoy temperature is insensitive to the nebular optical depth to ionizing photons and is thus applicable to optically thin or partly optically thin nebulae. The major drawback of this method is that it requires the fluxes of all major CELs to be measured, which poses a major observational challenge. For the current data set, essentially all major CELs have been detected. For the remaining few unseen strong lines, their fluxes can be estimated from the observed lines emitted by the same ion. Even for the very few unseen ions, fluxes of CELs emitted by those ions can be calculated once we have estimated the abundances of those ions using the ionization correction method. According to our calculation, the total contribution of all unseen CELs is less than 2%. Using the Stoy method developed by Preite-Martinez & Pottasch (1983) and assuming blackbody radiation for the CS, we derive that the CS has an effective temperature of 219 000 K.

Adopting a distance 880 pc to NGC 7027 (Masson, 1989), we obtain a luminosity of $8100 L_\odot$ and a photospheric radius of $0.063 R_\odot$ for the CS. Then, from the evolutionary tracks for hydrogen-burning post-AGB stars calculated by Vassiliadis & Wood (1994) and the approximate formula for the initial-final mass relationship given by the same authors, we estimate that the CS has a core mass $M_c = 0.74 M_\odot$ and an initial mass $M_i = 3.2 M_\odot$. For comparison, Bernard-Salas et al. (2001) estimate an initial mass between $3\text{--}4 M_\odot$ by comparing the elemental abundances of NGC 7027 with the semi-analytical models of Marigo et al. (1996).

The properties of the CS are summarized in Table 10, and compared to the values obtained by Latter et al. (2000). Note that Latter et al. (2000) determined the effective temperature using the Zanstra method and their

Table 10. Properties of the central star.

Parameter	Present paper	Latter et al.
$T_*(10^4 \text{K})$	21.9 ^a	19.8 ^b
$L_*(10^3 L_\odot)$	8.10	7.71
$R_*(10^{-2} R_\odot)$	6.3	7.5
$M_c (M_\odot)$	0.74	0.7
$M_i (M_\odot)$	3.2	4

^a Based on the Stoy method;

^b Based on the Zanstra method.

value is only slightly lower than ours, suggesting that NGC 7027 is largely optically thick, consistent with the presence of an extensive neutral and molecular envelope around the ionized region of this PN.

8. Summary

In this paper, we have presented deep optical spectrum of the bright PN NGC 7027 from 3310 Å to 9160 Å, obtained by uniformly scanning a long slit across the nebula, thus yielding average line fluxes for the whole nebula. A total of 1174 line identifications have been obtained, with intensities ranging from 10^{-5} to 10^2 of $\text{H}\beta$. The comprehensive line list should prove useful for future spectroscopic study of emission line nebulae.

The optical spectrum, together with the *IUE* spectra in the UV and the *ISO* spectra in the IR, have been used to determine the physical conditions and elemental abundances. The results show that NGC 7027 is characterized by an average electron temperature of 14 000 K and a density of $47\,000 \text{ cm}^{-3}$. The temperatures derived from the [O III] forbidden line ratio and from H I and from He I recombination line ratios are in agreement within the errors. Our analysis also yields a negative temperature gradient as a function of nebular radius. In calculating the ionic abundances, we have used a simplified two-zone model, adopting, respectively, an electron temperature of $T_e = 12\,600$ and $15\,500$ K for ions with ionization potentials lower or higher than 50 eV. Our abundance analysis show that ORLs yield only marginally higher metal abundances than CELs. This is in accord with the general pattern found for a large sample of PNe (Liu et al., 2001b, 2004a,b; Tsamis et al., 2003, 2004; Wesson et al., 2004; Zhang et al., 2004) that the ORL/CEL abundance discrepancy increases with increasing difference between the [O III] and the H I Balmer jump temperatures and with decreasing electron density.

The integrated nebular line spectra from the UV to the IR allowed us to determine precisely the effective temperature of the ionizing CS using the Stoy, or enrgy-balance, method. We find a high temperature of $T_{\text{eff}} = 219\,000$ K. For the first time, the Raman-scattered O VI features at 6830 and 7088 Å have been detected in this PN, suggesting that abundant neutral gas is present around the ionized regions of this high-excitation PNe.

The spectral data set presented in the current paper, together with extensive high resolution images in the optical and in the radio (Robberto et al., 1993; Bryce et al., 1997; Bains et al., 1993), should provide tight constraints for future photoionization modeling of NGC 7027.

Acknowledgements. We are grateful to Y.-R. Sun and Y. Liu for their help with the preparation of this paper. YZ acknowledges the award of an Institute Fellowship from STScI. The work of YZ and XWL has been supported partially by Chinese NSFC Grant No. 10325312. We thank P. J. Storey for his comments. We are also happy to thank the referee, M. Perinotto, for comments which have helped us to improve the paper.

References

- Aggarwal, K. M. 1983, *ApJS*, 52, 387
 Bains, I., Bryce, M., Mellema, G., Redman, M. P., & Thomasson, P. 2003, *MNRAS*, 340, 381
 Baluteau, J. P., Zavagno, A., Morisset, C., & Péquignot, D. 1995, *A&A*, 303, 175
 Barlow, M. J., Péquignot, D., Liu, X.-W., et al. 2003, in IAU Symp. 209, Planetary Nebulae, eds. S. Kwok, M. Dopita, R. Sutherland (San Francisco: ASP), p.373
 Bayes, F. A., Saraph, H. E., & Seaton, M. J. 1985, *MNRAS*, 215, 85
 Benjamin, R. A., Skillman, E. D., & Smits, D. P. 1999, *ApJ*, 514, 307
 Bernard-Salas, J., Pottasch, S. R., Beintema, D. A., & Wesselius, P. R. 2001, *A&A*, 367, 949
 Berrington, K. A., Nakazaki, S., & Norrington, P. H. 2000, *A&AS*, 142, 313
 Blum, R. D., & Pradhan, A. K. 1992, *ApJS*, 80, 425
 Bohin, R. C., Stecher, T. P., & Marionni, P. A. 1975, *ApJ*, 202, 415
 Bowen, I. S., & Wyse, A. B. 1939, *Lick Obs. Bull.*, 19, 1
 Brocklehurst, M. 1972, *MNRAS*, 157, 211
 Bryce, M., Pedlar, A., Muxlow, T., Thomasson, P., & Mellema, G. 1997, *MNRAS*, 284, 815
 Butler, K., & Zeippen, C. J. 1989, *A&A*, 208, 337
 Butler, K., & Zeippen, C. J. 1994, *A&AS*, 108, 1
 Cahn, J. H., Kaler, J. B., & Stanghellini, L. 1992, *A&AS*, 94, 399
 Clegg, P. E., Ade, P. A. R., Armand, C., et al. 1996, *A&A*, 315, L38
 Condal, A., Fahlman, G. G., Walker, G. A. H., & Glaspey, J. W. 1981, *PASP*, 93, 191
 Copetti, M. V. F., & Witzl, B. C. 2002, *A&A*, 382, 282
 Davey, A. R., Storey, P. J., & Kisielius, R. 2000, *A&AS*, 142, 85
 Dopita, M. A., & Meatheringham, S. J. 1990, *ApJ*, 357, 140
 Dyck, H. M., & Simon, T. 1976, *PASP*, 88, 738
 Escalante, V., & Victor, G. A. 1990, *ApJS*, 73, 513
 Fang, Z., Kwong, V. H. S., & Parkinson, W. H. 1993, *ApJ*, 413, L141
 Fischer, C. F., & Rubin, R. H. 2004, 355, 461
 Fleming, J., Bell, K. L., Hibbert, A., Vaeck, N., & Godefroid, M. R. 1996, *MNRAS*, 279, 1289
 Froese, F. C., & Saha, H. P. 1985, *Phys. Scr.*, 32, 181
 Galavis, M. E., Mendoza, C., Zeippen, C. J. 1997, *A&AS*, 312, 159
 Garnett, D. R., Dinerstein, H. L., 2001a, *RMxAA* (Ser. de Conf.), 10, 13
 Garstang, R. H. 1958, *MNRAS*, 118, 572
 Gau, J. N., & Henry, R. J. W. 1977, *Phys. Rev. A*, 16, 986
 Gee, G., Emerson, J. P., Ade, P. A. R., et al. 1984, *MNRAS*, 208, 517
 Giles, K. 1981, *MNRAS*, 195, 63
 de Graauw, T., Haser, L. N., Beintema, D. A., et al. 1996, *A&A*, 315, L45
 Groves, B., Dopita, M. A., Williams, R. E., & Hua, C.-T. 2002, *PASP*, 19, 425
 Gruenwald, R. B., & Péquignot, D. 1989, IAU Symposium 131, Planetary Nebulae, ed. S. Torres-Peimbert, Kluwer (Dordrecht), p.224
 Hayes, M. A., & Nussbaumer, H. 1984, *A&A*, 134, 94
 Howarth, I. D. 1983, *MNRAS*, 203, 301
 Johnson, C. T., & Kingston, A. E. 1990, *J. Phys. B*, 23, 3393
 Justtanont, K., Barlow, M. J., Tielens, A. G. G. M. 2000, *A&A*, 360, 1117
 Kaler, J. B. 1976, *ApJ*, 210, 843
 Kaler, J. B., Aller, L. H., Czyzak, S. J., & Epps, H. W. 1976, *ApJS*, 31, 163
 Keenan, F. P., Aller, L. H., Bell, K. L., Hyung, S., McKenna F. C., & Ramsbottom C. A. 1996, *MNRAS*, 281, 1073
 Keenan, F. P., Feibelman, W. A., & Berrington, K. A. 1992, *ApJ*, 389, 443
 Keenan, F. P., Hibbert, A., Ojha, P. C., & Conlon, E. S. 1993, *Phys. Scr*, 48, 129
 Keenan, F. P., & Norrington, P. H. 1987, *A&A*, 181, 370
 Kessler, M. F., Morris, P. W., Salama, A., et al. 1996, *A&A*, 315, L27
 Keyes, C. D., Aller, L. H., & Feibelman, W. A. 1990, *PASP*, 97, 700
 Kingsburgh, R. L., & Barlow, M. J. 1994, *MNRAS*, 271, 257
 Kisielius, R., & Storey, P. J. 2002, *A&A*, 387, 1135
 Kisielius, R., Storey, P. J., Davey, A. R., & Neale, L. T. 1998, *A&AS*, 133, 257
 Kwitter, K. B., & Henry, R. B. C. 1996, *ApJ*, 473, 304
 Latter, W. B., Dayal, A., Bieging, J. H. et al. 2000, *ApJ*, 539, 783
 Lennon D. J., & Burke V. M. 1994, *A&AS*, 103, 273
 Liu, X.-W., 2003, in IAU Symp. 209, Planetary Nebulae, eds. S. Kwok, M. Dopita, R. Sutherland (San Francisco: ASP), p.339
 Liu, X.-W., Danziger, I. J. & Murdin, P., 1993, *MNRAS*, 262, 699
 Liu, X.-W., & Barlow, M. J. 1996, *MNRAS*, 279, 511
 Liu, X.-W., Barlow, M. J., Cohen, M. et al. 2001a, *MNRAS*, 323, 343
 Liu, X.-W., Barlow, M. J., Nguyen-Q-Rieu, et al. 1996, *A&A*, 315, 257

- Liu, X.-W., Luo, S.-G., Barlow, M. J., Danziger, I. J., & Storey P. J. 2001b, MNRAS, 327, 141
- Liu, X.-W., Storey P. J., Barlow, M. J., & Clegg, R. E. S. 1995, MNRAS, 272, 369
- Liu, X.-W., Storey, P. J., Barlow, M. J., et al. 2000, MNRAS, 312, 585
- Liu, Y., Liu, X.-W., Barlow, M. J. & Luo, S.-G. 2004a, MNRAS, 353, 1251
- Liu, Y., Liu, X.-W., Luo, S.-G. & Barlow, M. J. 2004b, MNRAS, 353, 1231
- Lodders, K. 2003, ApJ, 591, 1220
- Marigo, P., Bressan, A., & Chiosi, C. 1996, A&A, 313, 545
- Masson, C. R. 1989, ApJ, 336, 294
- Melnick, G., Russell, R. W., Gull, G. E., & Harwit, M. 1981, ApJ, 243, 170
- Mendoza, C. 1983, in IAU Symp. 103, Planetary Nebulae, ed. Flower, D., Reidel, Dordrecht, p.143
- Mendoza, C., & Zeippen, C. J. 1982a, MNRAS, 199, 1025
- Mendoza, C., & Zeippen, C. J. 1982b, MNRAS, 198, 127
- Mendoza, C., & Zeippen, C. J. 1983, MNRAS, 202, 981
- Middlemass, D. 1990, MNRAS, 244, 294
- Nagatam, T., Tokunaga, A. T., Sellgren, K., et al. 1988, ApJ, 326, 157
- Nahar, S. N., & Pradhan, A. K. 1996, A&AS, 119, 509
- Nussbaumer, H., & Rusca, C. 1979, A&A, 72, 129
- Nussbaumer, H., & Storey, P. J. 1978, A&A, 70, 37
- Nussbaumer, H., & Storey, P. J. 1981a, A&A, 96, 91
- Nussbaumer, H., & Storey, P. J. 1981b, A&A, 99, 177
- Nussbaumer, H., & Storey, P. J., 1982a, A&A, 113, 21
- Nussbaumer, H., & Storey, P. J., 1982b, A&A, 115, 205
- Nussbaumer, H., & Storey, P. J. 1984, A&AS, 56, 293
- Osterbrock, D. E., & Wallace, R. K. 1977, ApJ, 19, 11
- Peimbert, M., & Torres-Peimbert, S. 1983, in IAU Symp. 103, Planetary Nebulae, ed. Flower, D., Reidel, Dordrecht, p.233
- Pelan, J., & Berrington, K.A. 1995, A&AS, 110, 209
- Péquignot, D., & Baluteau, J. P. 1988, A&A, 206, 298
- Péquignot, D., & Baluteau, J. P. 1994, A&A, 283, 593
- Péquignot, D., Baluteau, J. P., Morisset, C., & Boisson, C. 1997, A&A, 323, 217
- Péquignot, D., Petitjean, P., & Boisson, C. 1991, A&A, 251, 680
- Péquignot, D., Walsh, J. R., & Morisset, C. 2003, in IAU Symp. 209, Planetary Nebulae, eds. S. Kwok, M. Dopita, R. Sutherland (San Francisco: ASP), p.403
- Perinotto, M., Bencini, C. G., Pasquali, A., et al. 1999, A&A, 347, 967
- Pradhan, A. K. 1976, MNRAS, 177, 31
- Preite-Martinez, A., & Pottasch, S. R. 1983, A&A, 126, 31
- Roberto, M., Clampin, M., Ligori, S., Paresce, F., & Staude, H. J. 1993, A&A, 280, 241
- Roelfsema, P. R., Goss, W. M., Pottasch, S. R., & Zijlstra, A. 1991, A&A, 251, 611
- Rubin, R. H. 1989, ApJS, 69, 897
- Rudy, R. J., Erwin, P., Rossano, G. S., & Puettner, R. C. 1992, ApJ, 384, 536
- Saraph, H. E., & Tully, J. A. 1994, A&AS, 107, 29
- Saraph, H. E. & Storey, P. J. 1996, A&AS, 115, 151
- Schmid, H. M. 1989, A&A, 211, L31
- Seaton, M. J. 1979, MNRAS, 187, 785
- Shaw, R. A., & Kaler, J. B. 1982, ApJ, 261, 510
- Shields, G. A. 1978, ApJ, 219, 565
- Stafford, R. P., Bell, K. L., Hibbert, A., Wijesundera, W. P., 1994a, MNRAS, 266, 715
- Stafford, R. P., Bell, K. L., Hibbert, A., Wijesundera, W. P., 1994b, MNRAS, 268, 816
- Stanghellini, L., & Kaler, J. B. 1989, ApJ, 343, 811
- Storey, P. J. 1994, A&A, 282, 999
- Storey, P. J., & Hummer, D. G. 1995, MNRAS, 272, 41
- Stoy, R. W. 1933, MNRAS, 93, 588
- Telesco, C. M., & Harper, D. A. 1977, ApJ, 211, 475
- Tsamis, Y. G., Barlow, M. J., Liu, X.-W., Danziger, I. J., & Storey, P. 2003, MNRAS, 345, 186
- Tsamis, Y. G., Barlow, M. J., Liu, X.-W., Storey, P. & Danziger, I. J. 2004, MNRAS, 353, 953
- Tuairisg, S. O., Cami, J., Foing, B. H., Sonnentrucker, P., & Ehrenfreund, P. 2000, A&AS, 142, 225
- Vassiliadis, E., & Wood, P. R. 1994, ApJS, 92, 125
- Vujnovic, V. & Wiese, W. L. 1992, J. Phys. Chem. Ref. Data, 21, 919
- Walton, N. A., Pottasch, S. R., Reay, N. K., & Taylor, A. R. 1988, A&A, 200, L21
- Wang, W., Liu, X.-W., Zhang, Y., & Barlow, M. J. 2004, A&A, 427, 873
- Wesson, R., Liu, X.-W., & Barlow, M. J. 2004, MNRAS, submitted
- Wiese, W. L., Smith, M. W., & Glennon, B. M. 1966, NSRDS-NBS 4, US Government Printing Office, Washington DC
- Wolff, M. J., Code, A. D., & Groth, E. J. 2000, AJ, 119, 302
- Woodward, C. E., Pipher, J. L., Forrest, W. J., Moneti, A., & Shure, M. A. 1992, ApJ, 385, 567
- Wyse, A. B. 1942, ApJ, 95, 356
- Zanstra, H. 1927, ApJ, 65, 50
- Zeippen, C. J. 1982, MNRAS, 198, 111
- Zeippen, C. J., Le Bourlot, J., & Butler, K. 1987, A&A, 188, 251
- Zhang, H. L. 1996, A&AS, 119, 523
- Zhang, H. L., Graziani, M., & Pradhan, A. K. 1994, A&A, 283, 319
- Zhang, H. L., & Pradhan, A. K. 1997, A&AS, 126, 373
- Zhang, Y., Liu, X.-W., Liu, Y., & Rubin, R. H. 2005, MNRAS, 357, 458
- Zhang, Y., Liu, X.-W., & Luo, S.-G. 2003, in IAU Symp. 209, Planetary Nebulae, eds. S. Kwok, M. Dopita, R. Sutherland (San Francisco: ASP), p.319
- Zhang, Y., Liu, X.-W., Wesson, R., et al. 2004, MNRAS, 351, 935

Table 6. Ionic abundances from CELs.

Ion	λ (Å)	$I(\lambda)$	$N(X^{i+})/N(H^+)$
		[$I(H\beta) = 100$]	
C ⁺	2324	177 ^a	8.74×10^{-5}
	15.8 μ m	2.4	5.36×10^{-4}
	adopted		8.74×10^{-5}
C ²⁺	1908	726	3.85×10^{-4}
C ³⁺	1550	1125	4.18×10^{-4}
N ⁺	5754	5.76	1.60×10^{-5}
	6548	33.1	1.53×10^{-5}
	6584	93.6	1.47×10^{-5}
	122 μ m	0.028	2.01×10^{-5}
	adopted		1.49×10^{-5}
N ²⁺	1750	27.1	6.01×10^{-5}
	57 μ m	0.99	4.30×10^{-5}
	adopted		5.95×10^{-5}
N ³⁺	1485	42.3	4.85×10^{-5}
N ⁴⁺	1240	35.9	1.46×10^{-5}
O ⁺	2470	25.9	5.05×10^{-5}
	3726	20.8	3.19×10^{-5}
	3729	7.51	3.17×10^{-5}
	7320	17.9	4.72×10^{-5}
	7330	14.7	4.82×10^{-5}
	adopted		4.33×10^{-5}
	1663	34.5	2.56×10^{-4}
	4363	25.4	3.07×10^{-4}
	4931	0.254	3.33×10^{-4}
O ²⁺	4959	564.0	3.03×10^{-4}
	5007	1657.92	3.08×10^{-4}
	52 μ m	6.86	1.63×10^{-4}
	88 μ m	0.79	1.83×10^{-4}
	adopted		3.06×10^{-4}
	1400	49.5 ^b	1.39×10^{-4}
	26 μ m	40.2	6.63×10^{-5}
Ne ⁺	adopted		6.63×10^{-5}
Ne ²⁺	12.8 μ m	5.33	7.16×10^{-6}
Ne ³⁺	3869	125.8	5.37×10^{-5}
	36 μ m	2.82	4.25×10^{-5}
	adopted		5.35×10^{-5}
Ne ⁴⁺	1602	13.8	3.30×10^{-5}
	2422	120.4	4.32×10^{-5}
	2425	41.3	4.15×10^{-5}
	4714	0.903	2.82×10^{-5}
	4715	0.257	2.87×10^{-5}
	4724	0.807	2.31×10^{-5}
	4726	0.677	2.22×10^{-5}
	adopted		4.19×10^{-5}
	3346	38.0	2.02×10^{-5}
	14.3 μ m	72.2	1.23×10^{-5}
S ⁺	adopted		1.50×10^{-5}
	4068	7.61	5.06×10^{-7}
	4076	2.44	4.85×10^{-7}
	6716	1.72	6.56×10^{-7}
	6731	3.88	6.78×10^{-7}
S ²⁺	adopted		5.62×10^{-7}
	6312	4.23	3.46×10^{-6}

Table 6. continued.

Ion	λ (Å)	$I(\lambda)$	$N(X^{i+})/N(H^+)$
		[$I(H\beta) = 100$]	
	8830	0.011	3.51×10^{-6}
	$33.5\mu m$	0.494	2.13×10^{-6}
	$18.7\mu m$	4.69	2.18×10^{-6}
	adopted		2.75×10^{-6}
S^{3+}	$10.5\mu m$	22.7	1.56×10^{-6}
Cl^+	8578	0.324	2.08×10^{-8}
	9124	0.14	3.40×10^{-8}
	adopted		2.48×10^{-8}
Cl^{2+}	3353	0.099	4.55×10^{-8}
	5518	0.189	5.40×10^{-8}
	8434	0.074	7.70×10^{-8}
	8481	0.073	7.81×10^{-8}
	adopted		5.96×10^{-8}
Cl^{3+}	5324	0.06	6.07×10^{-8}
	7531	0.457	5.74×10^{-8}
	8045	1.05	5.69×10^{-8}
	$11.8\mu m$	0.46	1.01×10^{-7}
	adopted		6.71×10^{-8}
Cl^{4+}	$6.7\mu m$	0.365	1.08×10^{-8}
Ar^+	$7.0\mu m$	1.726	1.43×10^{-7}
Ar^{2+}	7136	21.4	1.09×10^{-6}
	7751	4.65	9.79×10^{-7}
	$9.0\mu m$	6.26	6.82×10^{-7}
	$21.9\mu m$	0.339	9.20×10^{-7}
	adopted		9.94×10^{-7}
Ar^{3+}	4712	2.21	5.84×10^{-7}
	4741	8.11	6.45×10^{-7}
	adopted		6.32×10^{-7}
Ar^{4+}	4626	0.07	1.63×10^{-7}
	6435	1.31	1.99×10^{-7}
	$7.9\mu m$	2.50	1.31×10^{-7}
	adopted		1.54×10^{-7}
Ar^{5+}	$4.5\mu m$	6.88	8.58×10^{-8}
Mg^{3+}	$4.4\mu m$	8.67	3.65×10^{-6}
Mg^{4+}	2783	9.53	1.39×10^{-5}
	2929	3.39	1.27×10^{-5}
	$5.6\mu m$	22.1	9.88×10^{-6}
	adopted		1.18×10^{-5}
Fe^{2+}	4702	0.067	3.09×10^{-8}
	4734	0.032	2.97×10^{-8}
	4755	0.032	3.88×10^{-8}
	4770	0.023	3.07×10^{-8}
	4778	0.018	3.46×10^{-8}
	4881	0.069 ^c	1.77×10^{-8}
	5270	0.094	3.70×10^{-8}
	adopted		3.40×10^{-8}
Fe^{3+}	6740	0.015	7.08×10^{-8}
	7183	0.016	3.93×10^{-7}
	7189	0.029	3.73×10^{-7}
	adopted		3.02×10^{-7}
Fe^{5+}	5234	0.020	1.19×10^{-9}
	5278	0.035	1.24×10^{-9}
	5335	0.102	1.97×10^{-9}
	5425	0.117	1.56×10^{-9}

Table 6. continued.

Ion	λ (Å)	$I(\lambda)$ [$I(H\beta) = 100$]	$N(X^{i+})/N(H^+)$
Fe ⁶⁺	5484	0.070	2.44×10^{-9}
	5631	0.083	1.35×10^{-9}
	adopted		1.73×10^{-9}
	4894	0.062	1.05×10^{-9}
	4989	0.089	1.68×10^{-9}
	5159	0.145	1.75×10^{-9}
	adopted		1.56×10^{-9}

^a Corrected for a 4% contribution from the [O III] $\lambda 2322$ line, assuming [O III] $I(\lambda 2322)/(\lambda 1663) = 0.14$;

^b Blended with the Si IV $\lambda 1400$ line;

^c Probably underestimated because of absorption by the DIB at 4882.56 Å.

Table 7. Ionic abundances from ORLs.

Ion	λ (Å)	$I(\lambda)$	$N(X^{i+})/N(H^+)$
		[$I(H\beta) = 100$]	
He ⁺	4471	3.222	5.63×10^{-2}
	6678	2.538	5.82×10^{-2}
	5876	10.87	5.80×10^{-2}
	adopted		5.80×10^{-2}
He ²⁺	4686	47.75	4.04×10^{-2}
	4860	2.833	4.39×10^{-2}
	adopted		4.10×10^{-2}
C ²⁺	3918	0.024	1.04×10^{-3}
	4267	0.575	6.40×10^{-4}
	4802	0.032	1.01×10^{-3}
	5342	0.034	7.15×10^{-4}
	6462	0.060	6.64×10^{-4}
	6578	0.231	3.99×10^{-4}
	7231	0.108	2.56×10^{-4}
	adopted		5.54×10^{-4}
	4070	0.425	2.70×10^{-4}
C ³⁺	4187	0.197	2.70×10^{-4}
	8196	0.289	6.20×10^{-4}
	adopted		3.87×10^{-4}
C ⁴⁺	4658	0.579 ^a	2.81×10^{-4}
N ²⁺	3995	0.009	8.49×10^{-5}
	4041	0.012	8.42×10^{-5}
	4043	0.008	7.41×10^{-5}
	4678	0.007	1.18×10^{-4}
	4179	0.005	7.62×10^{-5}
	4237	0.005	5.07×10^{-5}
	4431	0.006	9.75×10^{-5}
	4631	0.021	8.86×10^{-5}
	5667	0.014	6.03×10^{-5}
	5680	0.033	7.60×10^{-5}
	5686	0.019	2.47×10^{-4}
	5927	0.002	6.83×10^{-5}
	5940	0.004	1.37×10^{-4}
	6482	0.004	9.90×10^{-5}
N ³⁺	adopted		1.03×10^{-4}
	4379	0.059 ^b	2.56×10^{-5}
N ⁴⁺	3483	0.031	1.22×10^{-5}
	4707	0.015	2.34×10^{-5}
	7582	0.011	2.29×10^{-5}
	7703	0.021	1.66×10^{-5}
	adopted		1.68×10^{-5}
N ⁵⁺	4945	0.043	7.02×10^{-6}
O ²⁺	4072	0.134	5.55×10^{-4}
	4111	0.012	5.04×10^{-4}
	4119	0.035	3.99×10^{-4}
	4133	0.013	2.40×10^{-4}
	4153	0.021	2.72×10^{-4}
	4317	0.022	2.80×10^{-4}
	4320	0.026	3.06×10^{-4}
	4346	0.017	2.17×10^{-4}
	4349	0.041	2.08×10^{-4}
	4367	0.035	4.41×10^{-4}
	4639	0.070	6.38×10^{-4}

Table 7. continued.

Ion	λ (Å)	$I(\lambda)$ [$I(H\beta) = 100$]	$N(X^{i+})/N(H^+)$
O^{3+}	4649	0.165	3.13×10^{-4}
	4662	0.036	2.56×10^{-4}
	4676	0.037	3.14×10^{-4}
	adopted		3.95×10^{-4}
	4435	0.019	4.04×10^{-5}
	5592 ^c	0.105	6.20×10^{-5}
	adopted		4.04×10^{-5}
	3410	0.103	1.43×10^{-5}
	4632	0.188	1.19×10^{-5}
	adopted		1.27×10^{-5}
O^{5+}	7611	0.014	7.46×10^{-6}
Ne^{2+}	3327	0.016	8.86×10^{-5}
	3335	0.042	6.24×10^{-5}
	3355	0.027	7.68×10^{-5}
	3694	0.023	6.78×10^{-5}
	3777	0.011	8.35×10^{-5}
	4392	0.011	8.43×10^{-5}
	4409	0.017	1.96×10^{-4}
	adopted		8.63×10^{-5}
Mg^{2+}	4481	0.023	2.43×10^{-5}

^a Corrected for a 23% contribution from the [Fe III] $\lambda 4658$ line, assuming [Fe III] $I(\lambda 4658)/I(\lambda 4734) = 5.33$;

^b Corrected for a total of 11% contribution from the C III and Ne II $\lambda 4380$ lines, assuming C III $I(\lambda 4380)/(\lambda 4383) = 3.5$ and Ne II $I(\lambda 4380)/(\lambda 4392) = 0.61$;

^c Also excited partly by charge exchange with H⁰ (Liu, Danziger & Murdin, 1993).

Online Material

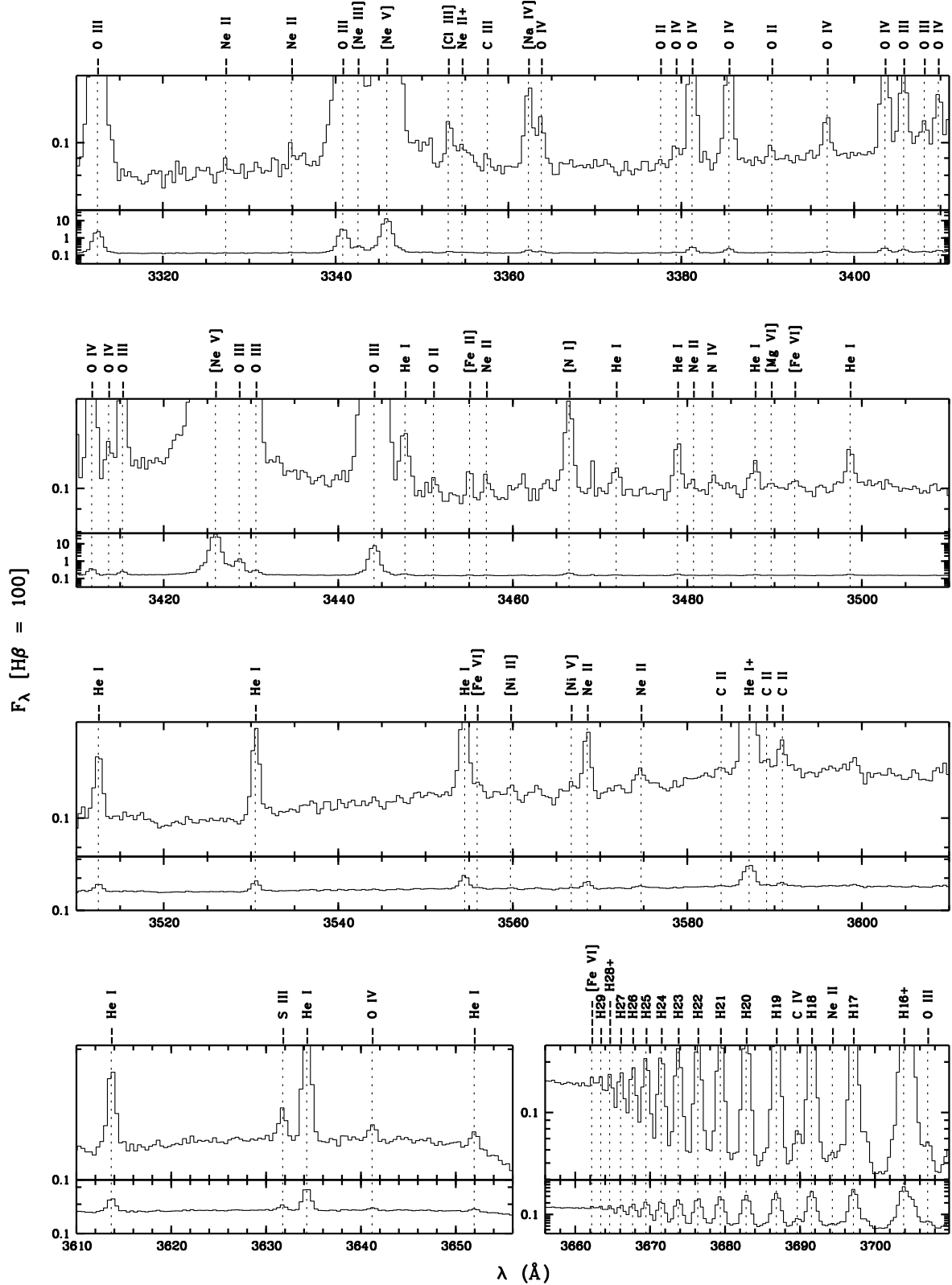
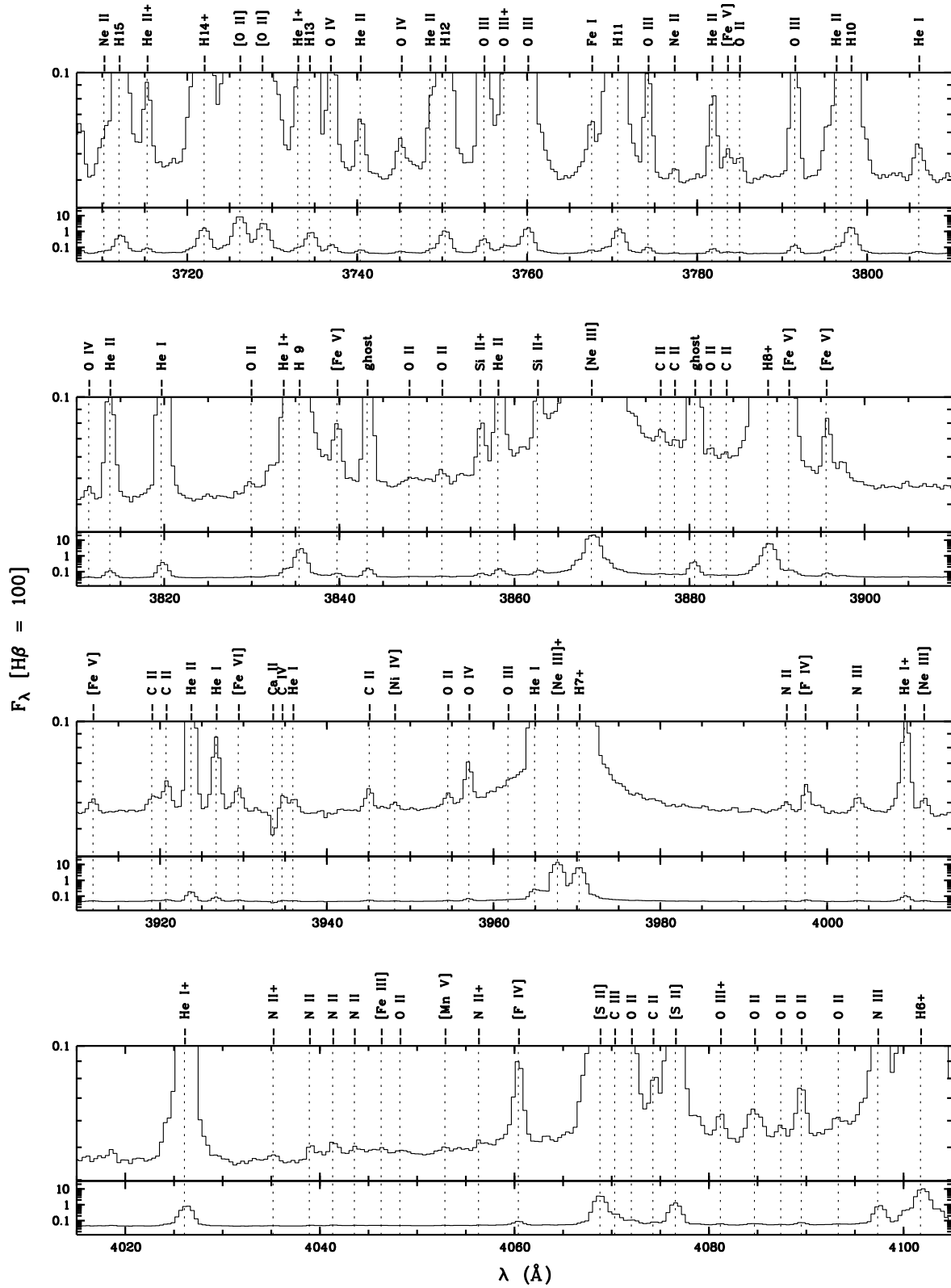
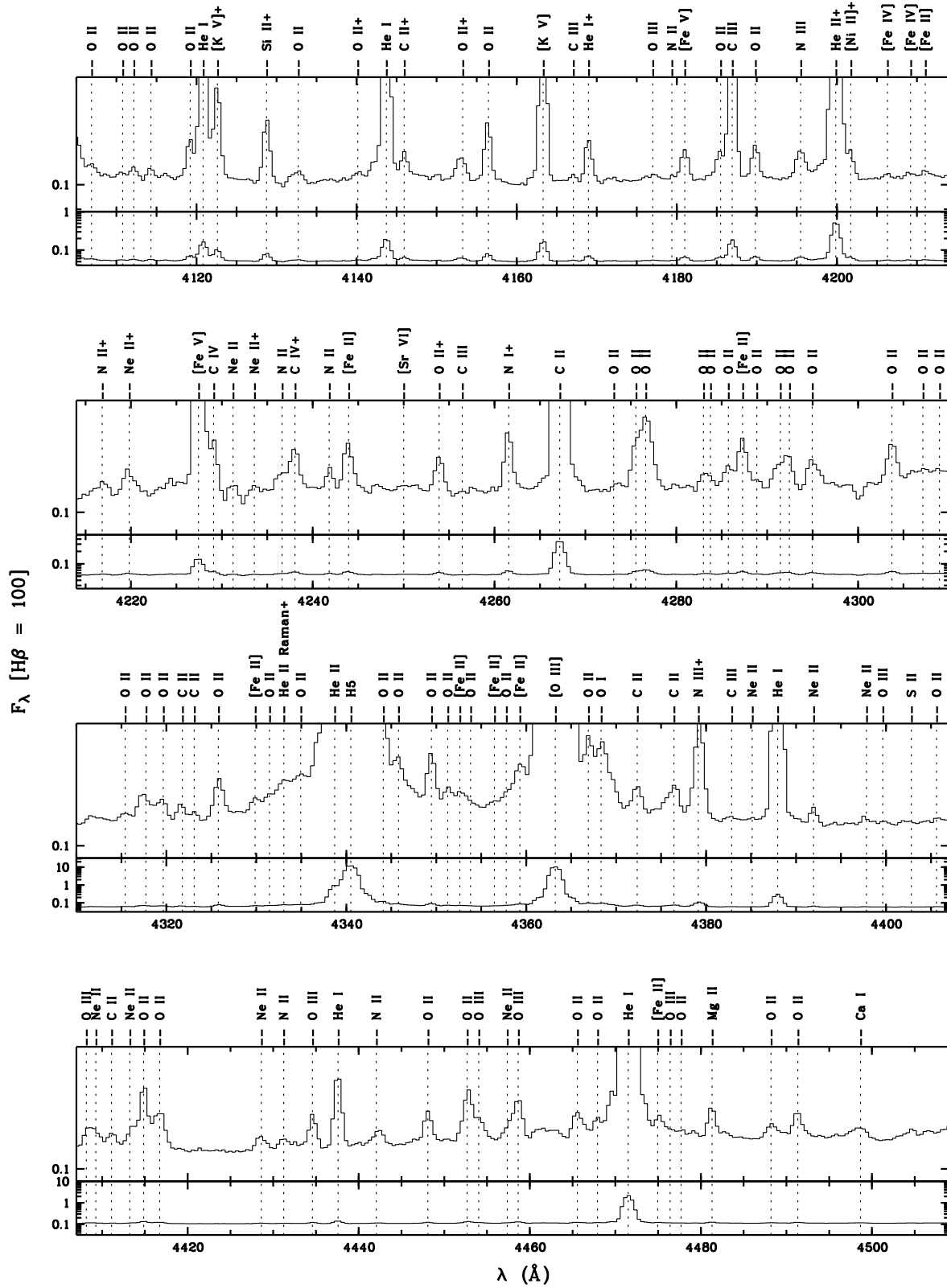
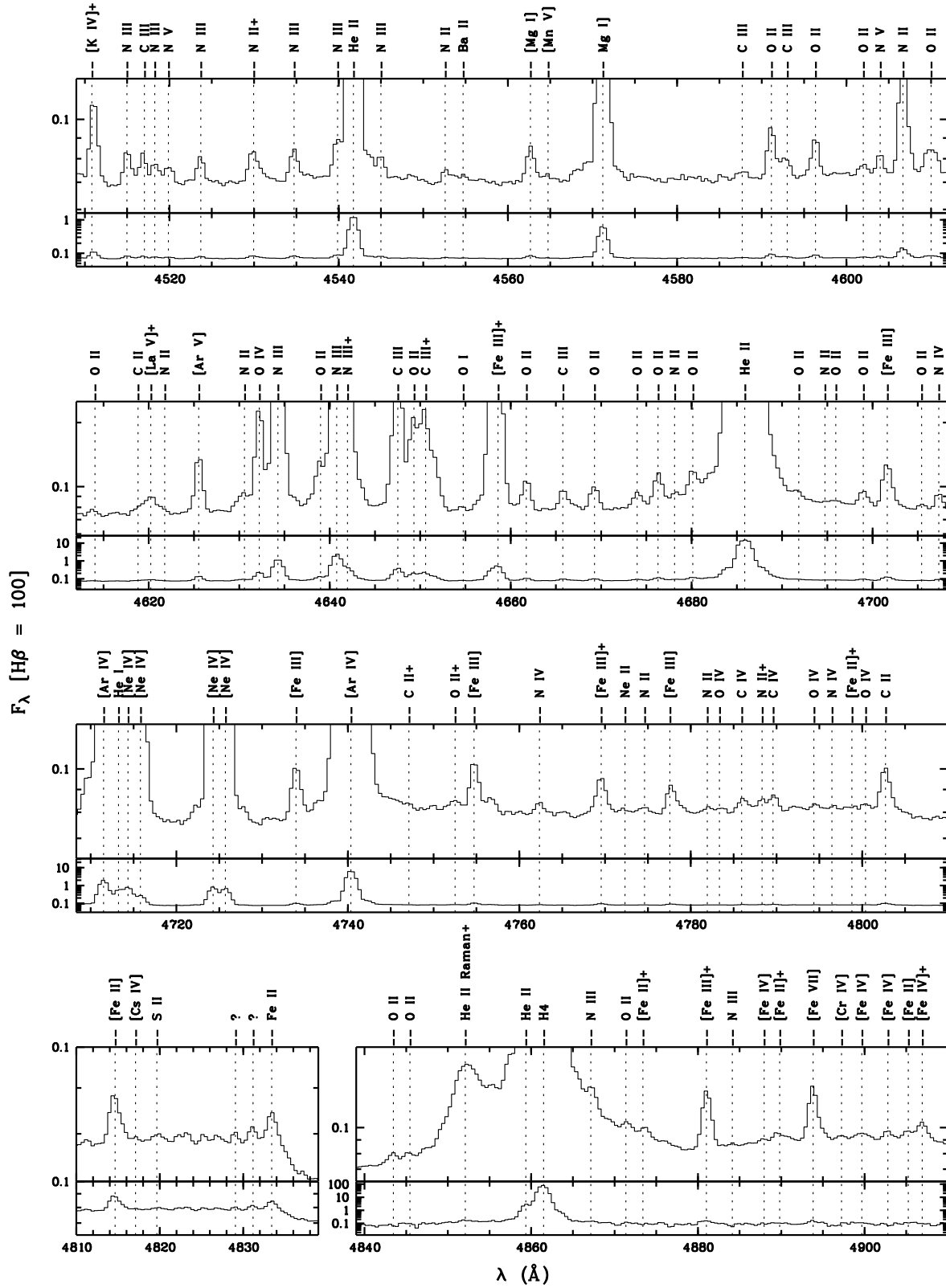
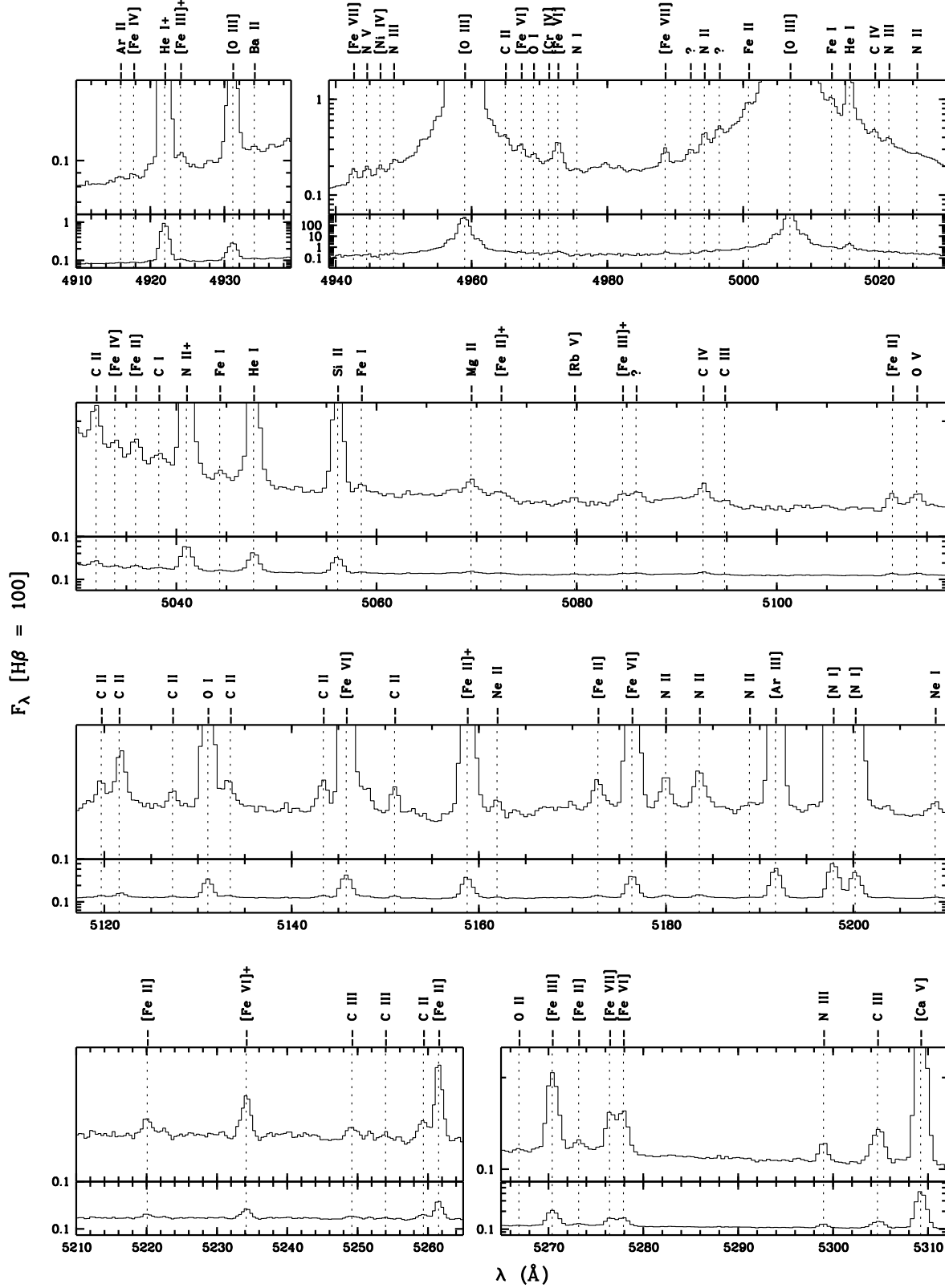


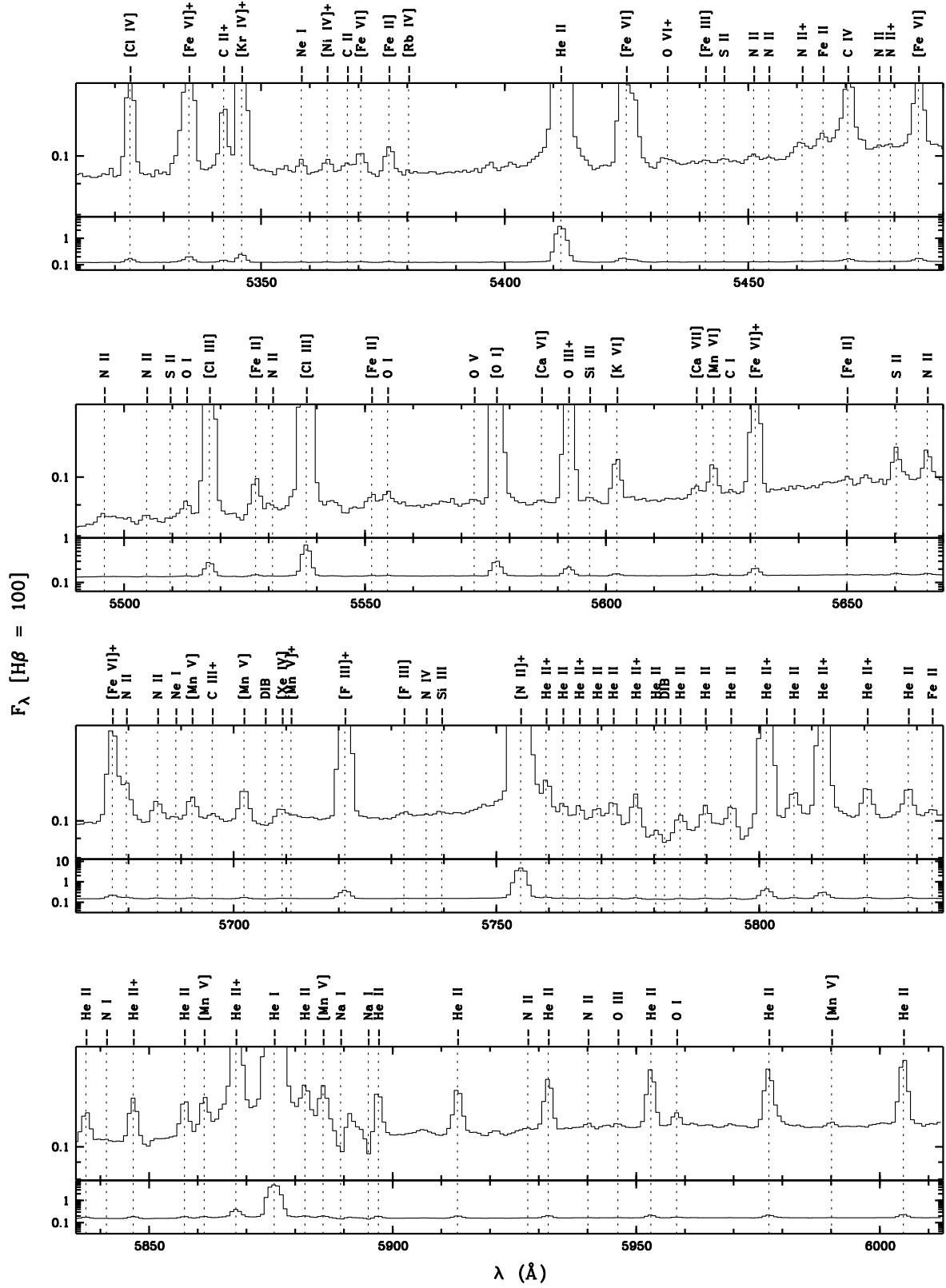
Fig. 1. Optical spectrum of NGC 7027. A '+' attached to a line identification means that the line is blended with other emission features.

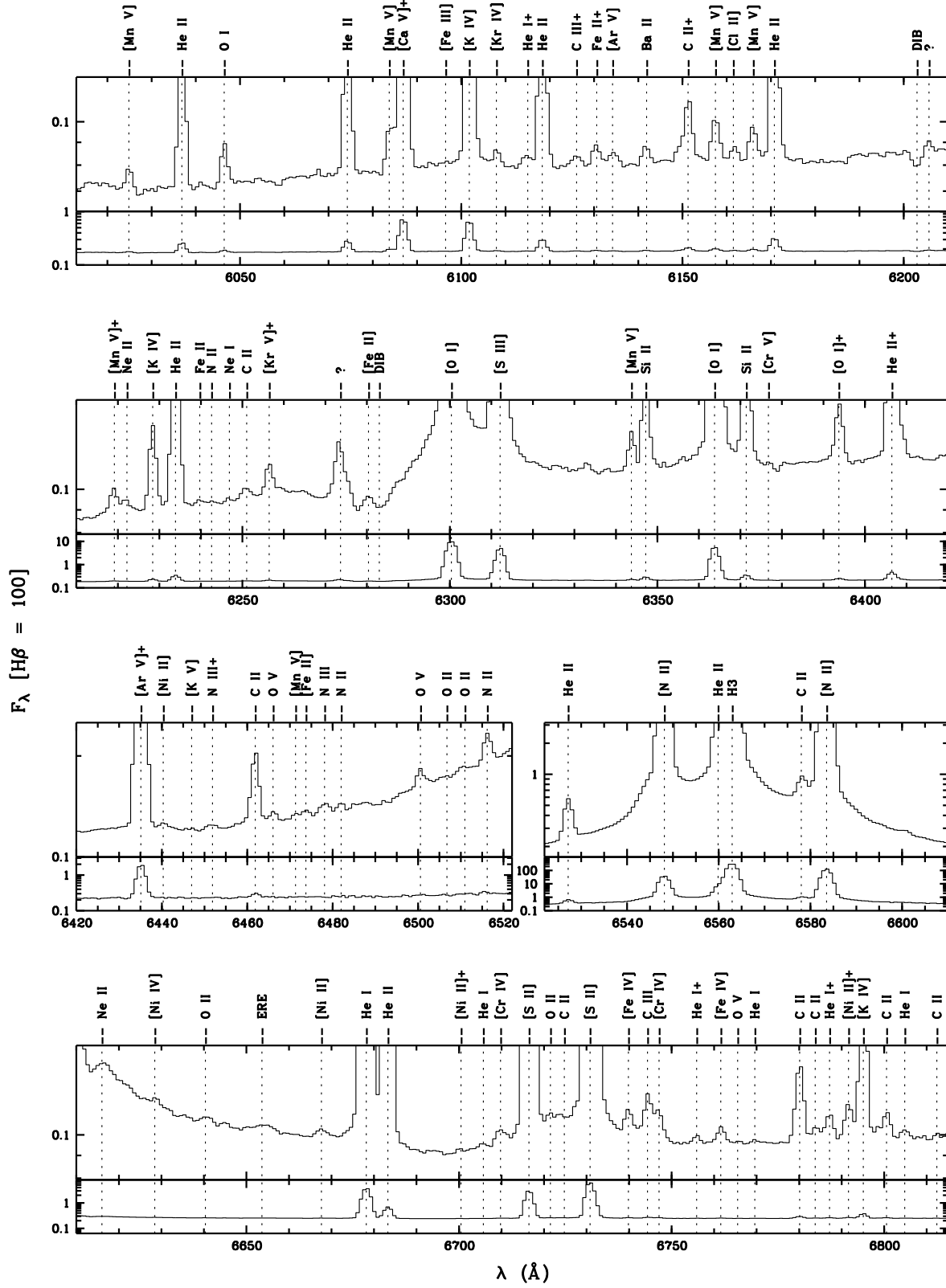


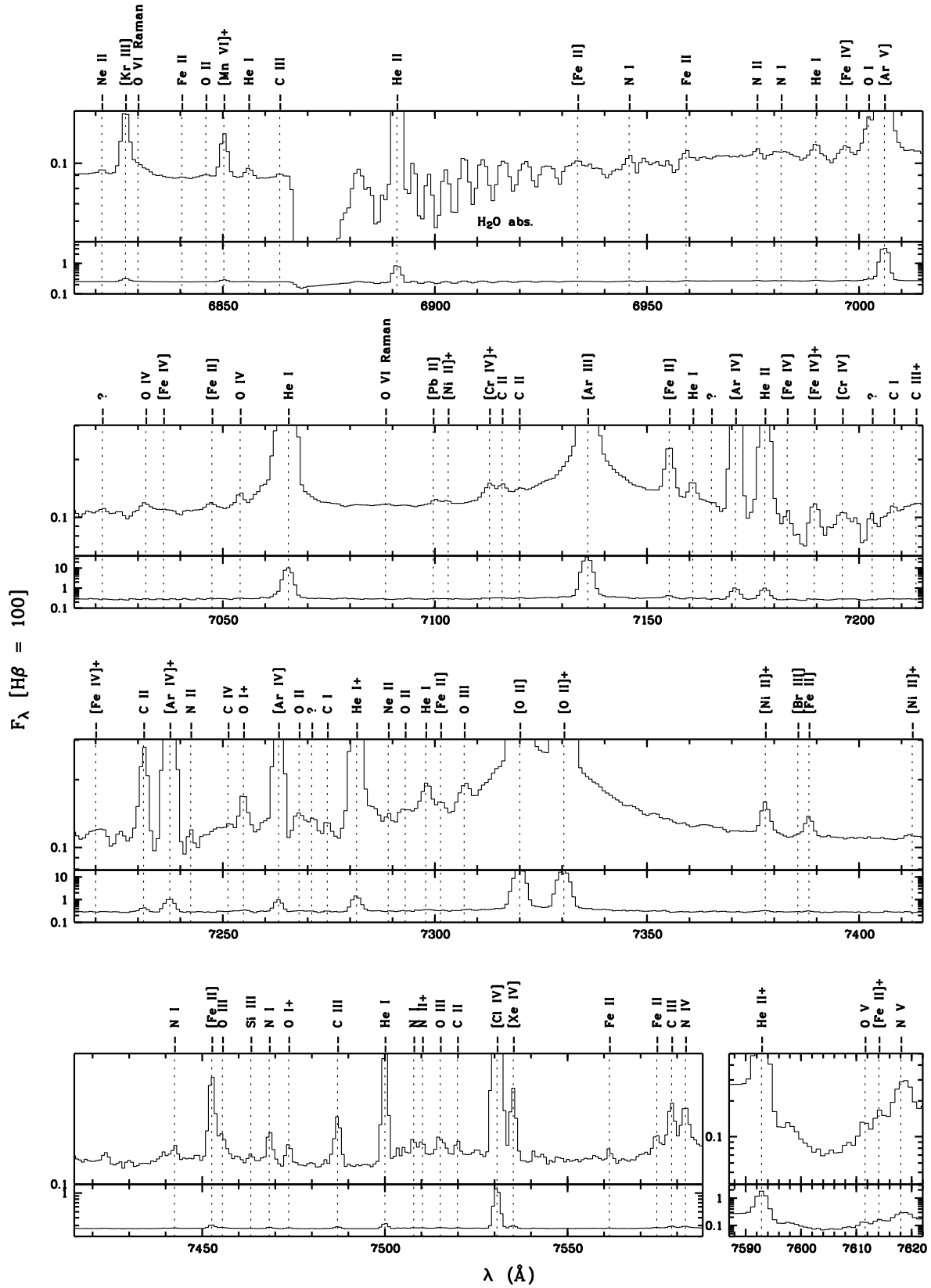


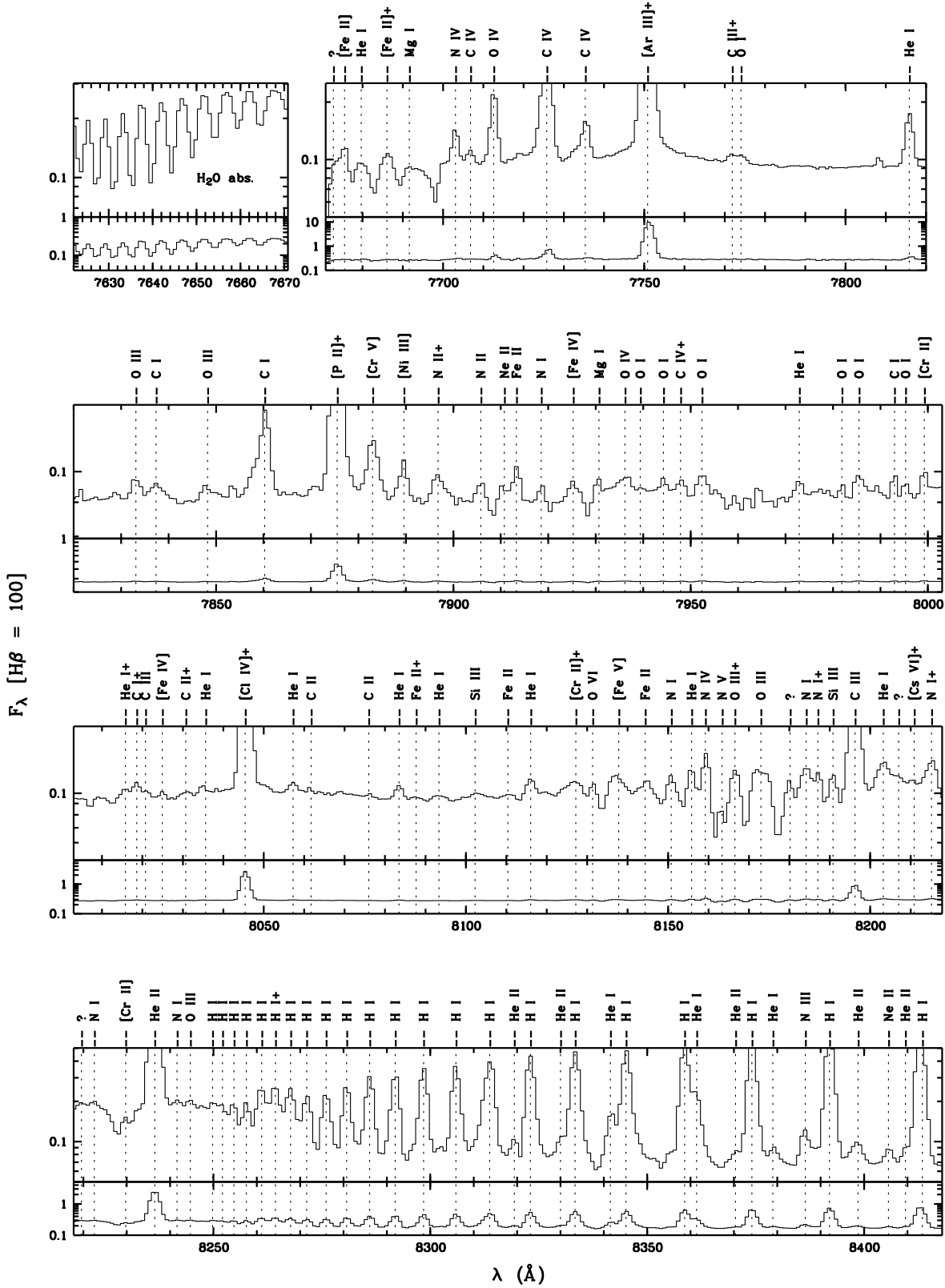












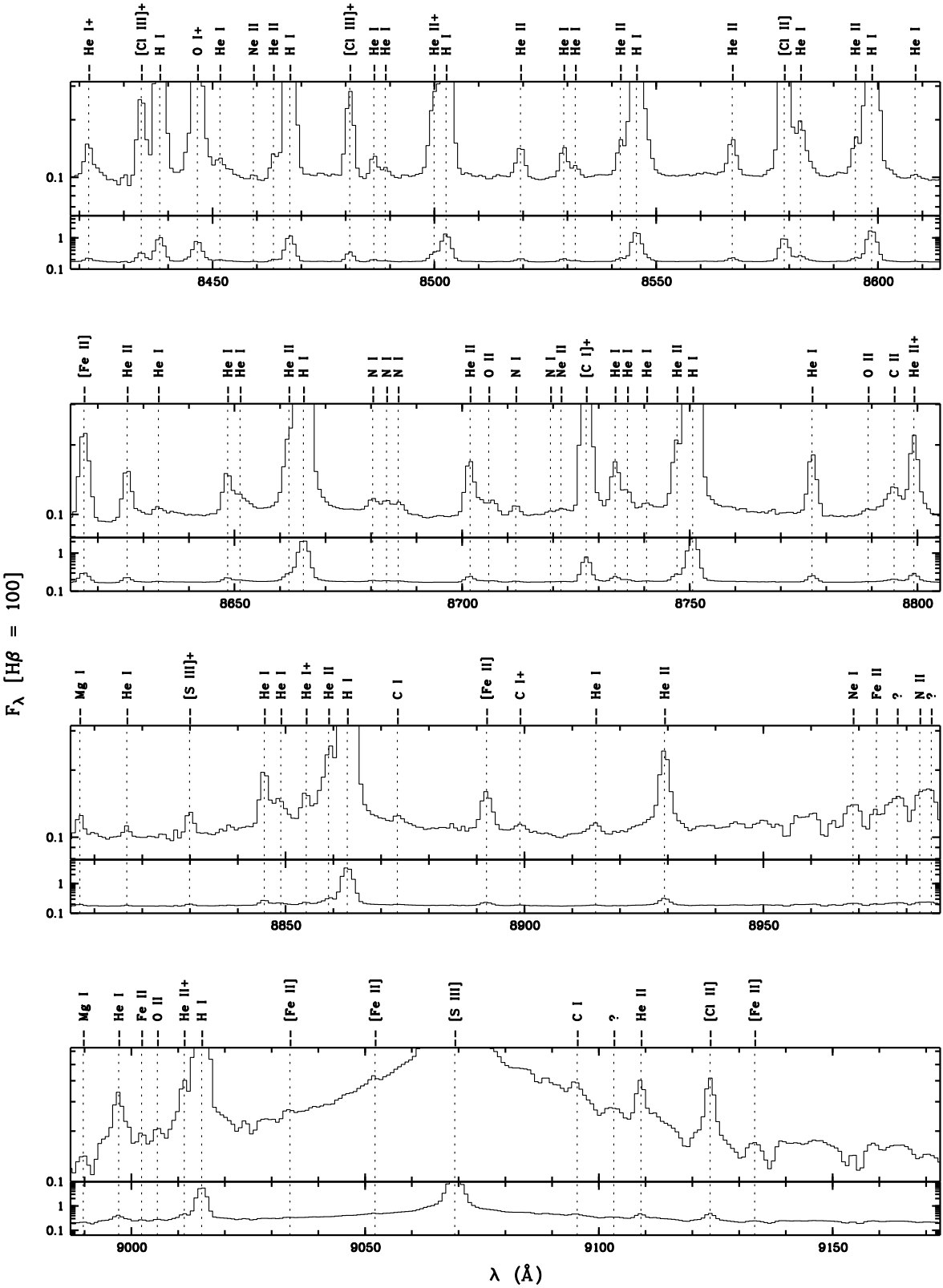


Table 1. Journal of WHT observations.

Date (UT)	λ -range (Å)	$\Delta\lambda$ (Å)	Exp. Time (sec)
1996/08/23	3620–4400	2.5	4×14 , 1200
1996/08/23	4200–4980	2.5	10, 2×7 , 2×20 , 2×600
1996/08/23	5200–6665	4.5	10, 2×7 , 2×20 , 2×600
1996/08/23	6460–7930	4.5	4×14 , 1200
1997/08/10	3310–3710	1.5	2×1200
1997/08/10	3710–4105	1.5	20 , 2×1200
1997/08/10	4110–4505	1.5	20 , 3×1200
1997/08/10	4510–4905	1.5	20 , 25 , 600 , 4×1200
1997/08/10	4910–5310	1.5	10, 2×20 , 300 , 4×600
1997/08/10	5220–6220	2.5	20 , 2×1200
1997/08/10	6020–6800	2.5	10, 2×20 , 300 , 4×600
1997/08/10	6770–7650	2.5	20 , 3×1200
1997/08/10	7620–8410	2.5	20 , 25 , 600 , 4×1200
1997/08/10	8370–9160	2.5	2×1200

Table 3. Journal of IUE observations.

Date (UT)	Image No.	Exp. Time (min)
1982/06/17	L SWP 17242 L	180
1983/05/02	L SWP 19878 L	162
1978/07/04	L SWP 01914 L	36
1978/09/01	L SWP 02430 L	30
1978/01/08	L SWP 01747 L	10
1978/03/29	H SWP 19578 L	420
1979/03/21	H SWP 04716 L	287
1979/09/17	H SWP 06541 L	60
1982/06/17	H SWP 17240 L	45
1979/03/25	H SWP 04748 L	35
1983/05/02	L LWR 15861 L	180
1978/02/24	L LWR 01024 L	120
1979/09/17	L LWR 05614 L	60
1982/06/17	L LWR 13506 L	60
1978/11/01	L LWR 02785 L	30
1978/06/08	L LWR 01639 L	25
1978/09/01	L LWR 02230 L	10
1983/01/25	H LWR 15105 L	300
1979/09/17	H LWR 05615 L	35

Appendix A: Emission from heavy elements ($Z > 30$)

Péquignot & Baluteau (1994) identify emission lines from a number of heavy elements with $Z > 30$ in NGC 7027 for the first time. As expected, many of these lines have extremely low intensities [$\sim 10^{-5}I(H\beta)$]. Table A.1 lists emission lines from heavy elements of $Z > 30$ identified by Péquignot & Baluteau (1994) (PB) that have also been detected in our optical spectrum. The measured fluxes are in general consistent with those reported by Péquignot & Baluteau (1994). These emission features should provide vital information about r- and s-processes in late evolution stages of AGB stars.

Table A.1. Emission lines from elements of $Z > 30$.

Ion	$\lambda(\text{\AA})$	$10^5 I/I(H\beta)$	
		This	PB
[Se II]	7592.00	blend ^a	blend
[Se III]	8854.20	< 9	15.0 ± 2.3
[Br III]	6131.00	< 11	7.6 ± 1.1
[Br III]	7385.1	2	< 2.5
[Kr III]	6826.90	44 ^b	41 ± 2
[Kr IV]	5346.10	148 ^c	187 ± 6
[Kr IV]	5868.00	231 ^d	255 ± 15
[Kr IV]	6107.80	5	6.3 ± 1.6
[Kr V]	6256.50	18 ^e	15.1 ± 1.5
[Rb IV]	5759.40	23 ^f	17.4 ± 2.6
[Rb V]	5080.20	7	< 4
[Sr VI]	4249.30	1	7 ± 5
[Sr VI]	5434.40	< 6	8 ± 4
[Sr V]	4922.20	blend	blend
[Zr VII]	7379.70	< 35	blend
[Te II]	8049.60	blend	< 1.5
[I II]	7282.90	blend	blend
[Xe III]	5846.70	12 ^g	9.3 ± 2
[Xe IV]	5709.20	9	10.6 ± 2
[Xe IV]	7535.40	14	15.8 ± 0.6
[Xe VI]	6408.89	blend	13.2 ± 1.6
[Cs II]	7219.70	< 19	< 10
[Cs VI]	8210.60	< 14	3 ± 2
Ba II	4554.00	2	7.8:
Ba II	4934.10	4	< 5.6
Ba II	6141.70	7	7.5
[Ba IV]	5696.60	8 ^h	7.3 ± 2.2
[Ba VIII]	4233.60	< 3	5 ± 4
[Pb II]	7099.80	10	3.5 ± 1.0
[La V]	4621.00	< 26	blend

^a Blended with a strong line;

^b Ignore contribution from the C I $\lambda 6828.11$ line;

^c Ignore contribution from the C III $\lambda 5345.80$ line;

^d Corrected for a 9% contribution from the He II $\lambda 5869.00$ line, assuming He II $I(\lambda 5869.00)/I(\lambda 5869.79) = 0.58$;

^e Corrected for a 28% contribution from the C II $\lambda 6256.54$ line, assuming C II $I(\lambda 6256.54)/I(\lambda 6250.74) = 0.56$;

^f Corrected for a 18% contribution from the He II $\lambda 5759.44$ line, assuming He II $I(\lambda 5759.44)/I(\lambda 5762.63) = 0.71$;

^g Corrected for a 69% contribution from the He II $\lambda 5847.10$ line, assuming He II $I(\lambda 5847.10)/I(\lambda 5857.27) = 0.93$;

^h Neglect contribution from the C III $\lambda 5695.9$ line.

Appendix B: Atomic data references

Table B.1 and Table B.2 list references of atomic data for CEL and ORL analyses, respectively.

Table B.1. Atomic data references for CEL analysis.

Ion	Transition probabilities	Collision strengths
C II	Nussbaumer & Storey 1981a	Blum & Pradhan 1992
C III	Keenan et al. 1992	Keenan et al. 1992
	Fleming et al. 1996	
C IV	Wiese et al. 1966	Gau & Henry 1977
N II	Nussbaumer & Rusca 1979	Stafford et al. 1994b
N III	Fang et al. 1993	Blum & Pradhan 1992
		Stafford et al. 1994a
N IV	Nussbaumer & Rusca 1979	Mendoza 1983
N V	Wiese et al. 1966	Osterbrock & Wallace 1977
O II	Zeippen 1982	Pradhan 1976
O III	Nussbaumer & Storey 1981b	Aggarwal 1983
O IV	Nussbaumer & Storey 1982b	Zhang et al. 1994
		Hayes & Nussbaumer 1984
Ne II	Mendoza 1983	Bayes et al. 1985
Ne III	Mendoza 1983	Butler & Zeippen 1994
Ne IV	Zeippen 1982	Giles 1981
Ne V	Froese & Saha 1985	Lennon & Burke 1994
S II	Mendoza & Zeippen 1982b	Keenan et al. 1996
	Keenan et al. 1993	
S III	Mendoza & Zeippen 1982a	Mendoza 1983
S IV	Storey (unpublished)	Butler & Zeippen 1989
Cl III	Mendoza 1983	Mendoza 1983
Cl IV	Mendoza & Zeippen 1982b	Butler & Zeippen 1989
Cl V	Mendoza 1983	Mendoza 1983
Ar II	Pelan & Berrington 1995	Vujnovic & Wiese 1992
Ar III	Mendoza & Zeippen 1983	Johnson & Kingston 1990
Ar IV	Mendoza & Zeippen 1982b	Zeippen et al. 1987
Ar V	Mendoza & Zeippen 1982a	Mendoza 1983
Ar VI	Storey (unpublished)	Saraph & Storey 1996
Mg IV	Mendoza & Zeippen 1983	Saraph & Tully 1994
Mg V	Galavis et al. 1997	Butler & Zeippen 1994
Fe III	Nahar & Pradhan 1996	Zhang 1996
Fe IV	Garstang 1958	Zhang & Pradhan 1997
	Fischer & Rubin 2004	
Fe VI	Nussbaumer & Storey 1978	Nussbaumer & Storey 1978
Fe VII	Nussbaumer & Storey 1982a	Keenan & Norrington 1987
		Berrington et al. 2000

Table B.2. Atomic data references for ORL analysis.

Ion	Effective recomb. coeffs.	Comment
H I	Storey & Hummer 1995	Case B
He I	Benjamin et al. 1999	Case B; singlets
	Brocklehurst 1972	Case A; triplets
He II	Storey & Hummer 1995	Case B
C II	Davey et al. 2000	Case B
C III	Péquignot et al. 1991	Case A
	Nussbaumer & Storey 1984	Dielectronic recom.
C IV	Péquignot et al. 1991	Case A
N II	Kisielius & Storey 2002	Case B; triplets
	Escalante & Victor 1990	Case A; singlets
N III	Péquignot et al. 1991	Case A
	Nussbaumer & Storey 1984	Dielectronic recom.
N IV	Péquignot et al. 1991	Case A
	Nussbaumer & Storey 1984	Dielectronic recom.
N V	Péquignot et al. 1991	Case A
O II	Storey 1994	Case B; quartets
	Liu et al. 1995	Case A; doublets
O III	Péquignot et al. 1991	Case A
O IV	Péquignot et al. 1991	Case A
	Nussbaumer & Storey 1984	Dielectronic recom.
O V	Péquignot et al. 1991	Case A
Ne II	Kisielius et al. 1998	Case B; doublets
	Storey (unpublished)	Case A; quartets
Mg II	Davey et al. 2000 ^a	Case B

^a Given the similarity between the atomic structure of Mg II and C II, we have assumed that the Mg II 3d–4f λ 4481 line has an effective recombination coefficient equal to that of the C II 3d–4f λ 4267 line.

Table 2. Optical line fluxes on a scale where H β = 100.

λ_{obs}	$F(\lambda)$	$I(\lambda)$	Ion	λ_{lab}	Mult	Lower Term	Upper Term	g_1^a	g_2^a
3312.43	2.385	7.760	O III	3312.30	V3	3s 3P*	3p 3S	3	3
3327.27	0.005:	0.017	Ne II	3327.15	V2	3s 4P	3p 4D*	4	4
3334.88	0.014	0.045	Ne II	3334.84	V2	3s 4P	3p 4D*	6	8
3340.82	3.345	10.547	O III	3340.74	V3	3s 3P*	3p 3S	5	3
3342.58	0.277	0.869	[Ne III]	3342.50		2p4 1D	2p4 1S	5	1
3345.91	12.858	40.282	[Ne V]	3345.83		2p2 3P	2p2 1D	3	5
3353.44	0.034	0.105	[Cl III]	3353.33		3p3 4S*	3p3 2P*	4	2
3354.62	0.028	0.086	Ne II	3355.05	V2	3s 4P	3p 4D*	4	6
*	*	He I	3354.55	V8		2s 1S	7p 1P*	1	3
3357.56	0.008	0.028	C III	3357.91		3p 3S	6p 3P*	9	9
3362.31	0.077	0.238	[Na IV]	3362.20		2p4 3P	2p4 1D	3	5
3363.80	0.038	0.118	O IV	3363.21		3s 4P	3p 4P*	2	4
3377.60	0.006	0.019	O II	3377.15	V9	3p 2S*	3d 2p	2	2
3379.40	0.019	0.056	O IV	3379.58		3s 4P	3p 4P*	4	4
3381.25	0.170	0.511	O IV	3381.28	V3	3s' 4P*	3p' 4D	6	10
3385.52	0.119	0.354	O IV	3385.55	V3	3s' 4P*	3p' 4D	6	8
3390.47	0.009	0.027	O II	3390.21	V9	3p 2S*	3d 2p	2	4
3396.88	0.037	0.108	O IV	3396.80	V3	3s' 4P*	3p' 4D	4	4
3403.57	0.114	0.337	O IV	3403.58	V2	3p 2P*	3d 2D	2	4
3405.73	0.068	0.198	O III	3405.74	V15	3p 3P	3d 3P*	1	3
3408.12	0.014	0.041	O III	3408.13	V15	3p 3P	3d 3P*	3	1
3409.74	0.035	0.103	O IV	3409.75	V3	3s' 4P*	3p' 4D	6	6
3411.75	0.202	0.590	O IV	3411.76	V2	3p 2P*	3d 2D	4	6
3413.69	0.012	0.035	O IV	3413.71	V2	3p 2P*	3d 2D	4	4
3415.28	0.102	0.296	O III	3415.29	V15	3p 3P	3d 3P*	3	3
3425.93	_ ^b	-	[Ne V]	3425.87		2p2 3P	2p2 1D	5	5
3428.64	1.349	3.870	O III	3428.65	V15	3p 3P	3d 3P*	3	5
3430.56	0.208	0.594	O III	3430.60	V15	3p 3P	3d 3P*	5	3
3444.10	7.725	21.809	O III	3444.07	V15	3p 3P	3d 3P*	5	5
3447.65	0.050	0.139	He I	3447.59	V7	2s 1S	6p 1P*	1	3
3450.91	0.013	0.035	O II	3451.27	V26.01	3p 3S	4s 1P*	3	3
3455.05	0.013	0.035	[Fe II]	3455.11		3d7 4F	4s 4D	8	4
3456.97	0.014	0.038	Ne II	3456.61	V28	3p 2S*	3d 2P	2	4
3466.44	0.072	0.199	[N I]	3466.38	V2F	2p3 4S*	2p3 2P*	4	4
3471.85	0.034	0.092	He I	3471.83	V44	2p 3P*	16d 3D	9	15
3478.88	0.043	0.118	He I	3478.97	V43	2p 3P*	15d 3D	9	15
3480.70	0.019	0.051	Ne II	3480.72	V49	3s'' 2S	3p'' 2P*	2	4
3482.84	0.018	0.050	N IV	3482.99	V1	3s 3S	3p 3P*	3	3
3487.75	0.029	0.076	He I	3487.73	V42	2p 3P*	14d 3D	9	15
3489.60	0.004	0.013	[Mg VI]	3488.72		2p3 2D*	2p3 2P*	4	4
3492.31	0.006	0.019	[Fe VI]	3492.10		3d3 4F	3d3 2D2	4	4
3498.65	0.029	0.075	He I	3498.66	V40	2p 3P*	13d 3D	9	15
3512.51	0.036	0.095	He I	3512.52	V38	2p 3P*	12d 3D	9	15
3530.49	0.042	0.110	He I	3530.50	V36	2p 3P*	11d 3D	9	15
3554.48	0.081	0.204	He I	3554.42	V34	2p 3P*	10d 3D	9	15
3555.92	0.008	0.020	[Fe VI]	3555.60		3d3 4F	3d3 2D2	6	4
3559.74	0.010	0.025	[Ni II]	3559.41		3d9 2D	4s 2P	4	2
3566.69	0.006	0.017	[Ni V]	3566.50		3d6 5D	3d6 3F2	3	5
3568.53	0.034	0.085	Ne II	3568.50	V9	3s' 2D	3p' 2F*	6	8
3574.69	0.018	0.046	Ne II	3574.61	V9	3s' 2D	3p' 2F*	4	6
3583.87	0.018	0.043	C II	3584.98	V23	3p' 4D	4s' 4P*	6	6
3587.07	0.165	0.407	He I	3587.28	V32	2p 3P*	9d 3D	9	15
*	*	C II	3585.81	V23		3p' 4D	4s' 4P*	2	4
*	*	[Fe VII]	3586.32			3d2 3P	3d2 1G	7	9

Table 2. continued.

λ_{obs}	$F(\lambda)$	$I(\lambda)$	Ion	λ_{lab}	Mult	Lower Term	Upper Term	g_1^a	g_2^a
3589.08	0.007	0.018	C II	3588.92	V23	3p' 4D	4s' 4P*	2	2
3590.89	0.024	0.059	C II	3590.86	V23	3p' 4D	4s' 4P*	10	6
3613.67	0.069	0.164	He I	3613.64	V6	2s 1S	5p 1P*	1	3
3631.74	0.030	0.071	S III	3632.02	V1	3d 3P*	4p 3D	5	7
3634.28	0.135	0.318	He I	3634.25	V28	2p 3P*	8d 3D	9	15
3641.16	0.012	0.026	O IV	3641.59		3p 2D	6f 2F*	12	14
3651.93	0.014	0.032	He I	3651.98	V27	2p 3P*	8s 3S	5	3
3662.22	0.011:	0.024	[Fe VI]	3662.50		3d3 4F	3d3 2D2	8	6
3663.41	0.018	0.041	H 29	3663.40	H29	2p+ 2P*	29d+ 2D	8	*
3664.60	0.032	0.073	H 28	3664.68	H28	2p+ 2P*	28d+ 2D	8	*
	*	*	[Fe II]	3664.70		4s 4D	4s 2D	2	4
3666.07	0.072	0.165	H 27	3666.10	H27	2p+ 2P*	27d+ 2D	8	*
3667.68	0.097	0.223	H 26	3667.68	H26	2p+ 2P*	26d+ 2D	8	*
3669.45	0.147	0.338	H 25	3669.46	H25	2p+ 2P*	25d+ 2D	8	*
3671.49	0.177	0.409	H 24	3671.48	H24	2p+ 2P*	24d+ 2D	8	*
3673.75	0.199	0.460	H 23	3673.74	H23	2p+ 2P*	23d+ 2D	8	*
3676.37	0.233	0.538	H 22	3676.36	H22	2p+ 2P*	22d+ 2D	8	*
3679.37	0.265	0.611	H 21	3679.36	H21	2p+ 2P*	21d+ 2D	8	*
3682.82	0.305	0.702	H 20	3682.81	H20	2p+ 2P*	20d+ 2D	8	*
3686.84	0.356	0.817	H 19	3686.83	H19	2p+ 2P*	19d+ 2D	8	*
3689.63	0.034	0.077	C IV	3689.78		6g 2G	9f 2F*	18	14
3691.53	0.407	0.934	H 18	3691.56	H18	2p+ 2P*	18d+ 2D	8	*
3694.32	0.011	0.024	Ne II	3694.21	V1	3s 4P	3p 4P*	6	6
3697.12	0.478	1.094	H 17	3697.15	H17	2p+ 2P*	17d+ 2D	8	*
3703.83	0.853	1.939	H 16	3703.86	H16	2p+ 2P*	16d+ 2D	8	*
	*	*	He I	3705.02	V25	2p 3P*	7d 3D	9	15
3707.03	0.018	0.041	O III	3707.25	V14	2p 3P	3d 3D*	3	5
3709.86	0.025	0.057	Ne II	3709.62	V1	3s 4P	3p 4P*	4	2
3711.98	0.642	1.454	H 15	3711.97	H15	2p+ 2P*	15d+ 2D	8	*
3715.28	0.053	0.120	He II	3715.16	4.29	4f+ 2F*	29g+ 2G	32	*
	*	*	N IV	3714.43	V12	3p' 3D	3d' 3P*	5	5
3721.99	1.753	3.943	H 14	3721.94	H14	2p+ 2P*	14d+ 2D	8	*
	*	*	He II	3720.41	4.28	4f+ 2F*	28g+ 2G	32	*
	*	*	[S III]	3721.63	F2	3p2 3P	3p2 1S	3	1
3726.19	9.230	20.763	[O II]	3726.03	F1	2p3 4S*	2p3 2D*	4	4
	*	*	He II	3726.27	4.27	4f+ 2F*	27g+ 2G	32	*
3728.79	3.350	7.512	[O II]	3728.82	F1	2p3 4S*	2p3 2D*	4	6
3733.00	0.049	0.110	He I	3732.86	V24	2p 3P*	7s 3S	3	3
	*	*	He II	3732.80	4.26	4f+ 2F*	26g+ 2G	32	*
3734.37	0.859	1.921	H 13	3734.37	H13	2p+ 2P*	13d+ 2D	8	*
3736.83	0.112	0.251	O IV	3736.85	V6	3p' 4D	3d' 4F*	12	14
3740.35	0.032	0.071	He II	3740.30	4.25	4f+ 2F*	25g+ 2G	32	*
3745.18	0.018	0.040	O IV	3744.89	V6	3p' 4D	3d' 4F*	6	6
3748.56	0.045	0.101	He II	3748.55	4.24	4f+ 2F*	24g+ 2G	32	*
3750.34	1.079	2.397	H 12	3750.15	H12	2p+ 2P*	12d+ 2D	8	*
3754.90	0.304	0.672	O III	3754.69	V2	3s 3P*	3p 3D	3	5
3757.25	0.111	0.245	O III	3757.24	V2	3s 3P*	3p 3D	1	3
	*	*	He II	3758.15	4.23	4f+ 2F*	23g+ 2G	32	*
3760.07	1.701	3.755	O III	3759.87	V2	3s 3P*	3p 3D	5	7
3767.58	0.015	0.033	Fe I	3767.19	V21	a5F	y5F*	3	3
3770.64	1.502	3.295	H 11	3770.63	H11	2p+ 2P*	11d+ 2D	8	*
	*	*	He II	3769.08	4.22	4f+ 2F*	22g+ 2G	32	*
3774.21	0.058	0.127	O III	3774.02	V2	3s 3P*	3p 3D	3	3
3777.29	0.005	0.011	Ne II	3777.14	V1	3s 4P	3p 4P*	2	4
3781.74	0.041	0.090	He II	3781.72	4.21	4f+ 2F*	21g+ 2G	32	*

Table 2. continued.

λ_{obs}	$F(\lambda)$	$I(\lambda)$	Ion	λ_{lab}	Mult	Lower Term	Upper Term	g_1^a	g_2^a
3783.55	0.013	0.029	[Fe V]	3783.22		3d4 5D	3d4 3F2	5	7
3784.98	0.008	0.017	O II	3784.98		4p 2P*	4d 2D*	4	6
3791.48	0.076	0.164	O III	3791.27	V2	3s 3P*	3p 3D	5	5
3796.34	0.072	0.155	He II	3796.33	4.20	4f+ 2F*	20g+ 2G	32	*
3798.10	2.038	4.400	H 10	3797.90	H10	2p+ 2P*	10d+ 2D	8	*
3806.06	0.017	0.036	He I	3805.74	V63	2p 1P*	11d 1D	3	5
3811.38	0.005	0.011	O VI	3811.35	V1	3s 2S	3p 2P*	2	4
3813.79	0.081	0.173	He II	3813.50	4.19	4f+ 2F*	19g+ 2G	32	*
3819.83	0.358	0.764	He I	3819.62	V22	2p 3P*	6d 3D	9	15
3829.91	0.006	0.013	O II	3830.29	V34	3p 2P*	4s 2P	4	2
3833.58	0.139	0.294	He I	3833.57	V62	2p 1P*	10d 1D	3	5
*	*		He II	3833.80	4.18	4f+ 2F*	18g+ 2G	32	*
3835.40	3.075	6.494	H 9	3835.39	H9	2p+ 2P*	9d+ 2D	8	*
3839.73	0.035	0.074	[Fe V]	3839.27		3d4 5D	3d4 3F2	7	7
3847.95	0.005	0.010	O II	3847.89	V12	3p 4D*	3d 4D	2	2
3851.71	0.007	0.014	O II	3851.03	V12	3p 4D*	3d 4D	4	4
3856.05	0.030	0.062	Si II	3856.02	V1	3p2 2D	4p 2P*	6	4
*	*		O II	3856.13	V12	3p 4D*	3d 4D	4	2
3858.10	0.098	0.205	He II	3858.07	4.17	4f+ 2F*	15g+ 2G	32	*
3862.63	0.054	0.113	Si II	3862.60	V1	3p2 2D	4p 2P*	4	2
*	*		O II	3863.50	V12	3p 4D*	3d 4D	6	8
3868.78	60.880	125.769	[Ne III]	3868.75	F1	2p4 3P	2p4 1D	5	5
*	*		[Fe VI]	3870.13		3d3 2F	3d3 2D1	7	4
3876.65	0.013	0.026	C II	3876.66	V33	3d' 4F*	4f' 4G	6	8
3878.28	0.007	0.015	C II	3878.03	V33	3d' 4F*	4f' 4G	6	6
3882.38	0.004	0.008	O II	3882.19	V12	3p 4D*	3d 4D	8	8
*	*		O II	3882.44	V11	3p 4D*	3d 4P	4	4
3884.19	0.003	0.006	C II	3883.82	V33	3d' 4F*	4f' 4G	10	8
3888.91	7.748	15.855	H 8	3889.05	H8	2p+ 2P*	8d+ 2D	8	*
*	*		He I	3888.65	V2	2s 3S	3p 3P*	3	9
*	*		He II	3887.44	4.16	4f+ 2F*	16g+ 2G	32	*
3891.32	0.083	0.169	[Fe V]	3891.28		3d4 5D	3d4 3F2	9	9
3895.60	0.036	0.073	[Fe V]	3895.22		3d4 5D	3d4 3P2	7	5
3911.95	0.010	0.020	[Fe V]	3911.86		3d4 5D	3d4 3F2	9	7
3919.00	0.012	0.024	C II	3918.98	V4	3p 2P*	4s 2S	2	2
3920.71	0.017	0.034	C II	3920.69	V4	3p 2P*	4s 2S	4	2
3923.70	0.159	0.319	He II	3923.48	4.15	4f+ 2F*	15g+ 2G	32	*
3926.72	0.046	0.091	He I	3926.54	V58	2p 1P*	8d 1D	3	5
3929.38	0.014	0.028	[Fe VI]	3928.90		3d3 2F	3d3 2D1	6	4
3934.62	0.010	0.021	C IV	3934.29	V2	5s 2S	6p 2P*	2	4
*	*		C IV	3934.89	V2	5s 2S	6p 2P*	2	2
3935.92	0.009	0.018	He I	3935.91	V57	2p 1P*	8s 1S	3	1
3945.08	0.014	0.028	C II	3945.00	V32	3d' 4F*	4f' 4F	4	4
*	*		C II	3945.20	V32	3d' 4F*	4f' 4F	6	8
3948.13	0.003	0.006	[Ni IV]	3948.50		3d7 4P	3d7 4F	6	10
3954.51	0.006	0.012	O II	3954.37	V6	3s 2P	3p 2P*	2	2
3957.03	0.022	0.043	O IV	3956.74	V10	3p' 4P	3d' 4P*	4	4
3961.73	0.007	0.013	O III	3961.59	V17	3p 1D	3d 1F*	5	7
3964.92	0.285	0.554	He I	3964.92	V5	2s 1S	4p 1P*	1	3
3967.66	19.330	37.610	[Ne III]	3967.46	F1	2p4 3P	2p4 1D	3	5
*	*		He II	3968.43	4.14	4f+ 2F*	14g+ 2G	32	*
3970.26	7.502	14.550	H 7	3970.07	H7	2p+ 2P*	7d+ 2D	8	98
*	*		[Fe IV]	3970.90		3d5 2G2	3d5 2G1	10	8
3995.10	0.005	0.009	N II	3994.98	V12	3s 1P*	3p 1D	3	5
3997.35	0.013	0.025	[F IV]	3996.90		2p2 3P	2p2 1D	3	5

Table 2. continued.

λ_{obs}	$F(\lambda)$	$I(\lambda)$	Ion	λ_{lab}	Mult	Lower Term	Upper Term	g_1^a	g_2^a
4003.58	0.010	0.020	N III	4003.58	V17	4d 2D	5f 2F*	6	8
4009.26	0.070	0.132	He I	4009.26	V55	2p 1P*	7d 1D	3	5
*	*	[Fe III]		4008.30		3d6 5D	3d6 3G	9	9
4011.58	0.008	0.016	[Ne III]	4011.70		2p4 3P	2p4 1D	1	5
4026.08	1.017	1.899	He I	4026.19	V18	2p 3P*	5d 3D	18	*
*	*	He II		4025.60	4.13	4f+ 2F*	13g+ 2G	32	*
*	*	N II		4026.08	V39b	3d 3F*	4f 2[5]	7	9
*	*	O II		4026.31	V50b	3d 4F	4f F3*	4	6
4035.19	0.003	0.006	N II	4035.08	V39a	3d 3F*	4f 2[5]	5	7
*	*	O II		4035.07	V50b	3d 4F	4f F3*	6	6
*	*	O II		4035.46	V50b	3d 4F	4f F3*	6	8
4038.92	0.005	0.009	N II	4039.35	V39b	3d 3F*	4f 2[5]	9	9
4041.32	0.007	0.013	N II	4041.31	V39b	3d 3F*	4f 2[5]	9	11
4043.54	0.004	0.008	N II	4043.53	V39a	3d 3F*	4f 2[4]	7	9
4046.30	0.003	0.006	[Fe III]	4046.40		3d6 5D	3d6 3G	7	7
4048.22	0.001	0.002	O II	4048.21	V50b	3d 4F	4f F3*	8	8
4052.85	0.002	0.003	[Mn V]	4052.30		3d3 4F	3d3 2D	4	4
4056.30	0.003	0.005	N II	4056.90	V39a	3d 3F*	4f 2[4]	9	9
*	*	C III		4056.06	V24	4d 1D	5f 1F*	5	7
4060.41	0.050	0.091	[F IV]	4060.22		2p2 3P	2p2 1D	5	5
4068.80	4.193	7.611	[S II]	4068.60	F1	2p3 4S*	2p3 2P*	4	4
*	*	C III		4067.94	V16	4f 3F*	5g 3G	5	7
*	*	C III		4068.91	V16	4f 3F*	5g 3G	7	9
*	*	O II		4069.62	V10	3p 4D*	3d 4F	2	4
*	*	O II		4069.87	V10	3p 4D*	3d 4F	4	6
4070.30	0.234	0.425	C III	4070.26	V16	4f 3F*	5g 3G	9	11
4072.02	0.074	0.134	O II	4072.16	V10	3p 4D*	3d 4F	6	8
4074.24	0.035	0.063	C II	4074.52	V36	3d' 4D*	4f' 4F	6	10
4076.55	1.354	2.442	[S II]	4076.35	F1	2p3 4S*	2p3 2P*	2	4
*	*	O II		4075.86	V10	3p 4D*	3d 4F	8	10
4081.17	0.013	0.023	O III	4081.04	V23	3s' 3P	3p' 3D*	5	7
4084.68	0.021	0.037	O II	4084.65	V21	3p 4P*	3d 2F	6	8
*	*	O II		4085.11	V10	3p 4D*	3d 4F	6	6
4087.38	0.004	0.007	O II	4087.15	V48c	3d 4F	4f G3*	4	6
4089.48	0.025	0.046	O II	4089.29	V48a	3d 4F	4f G5*	10	12
4093.29	0.005	0.009	O II	4092.93	V10	3p 4D*	3d 4F	8	8
4097.34	0.919	1.637	N III	4097.33	V1	3s 2S	3p 2P*	2	4
4101.75	14.670	26.048	H 6	4101.74	H6	2p+ 2P*	6d+ 2D	8	72
*	*	He II		4100.04	4.12	4f+ 2F*	12g+ 2G	32	*
*	*	O II		4103.00	V20	3p 4P*	3d 4D	2	2
*	*	N III		4103.43	V1	3s 2S	3p 2P*	2	2
4106.89	0.006	0.010	O II	4106.02	V10	3p 4D*	3d 4F	8	6
4110.77	0.007	0.012	O II	4110.78	V20	3p 4P*	3d 4D	4	2
4112.16	0.007	0.013	O II	4112.02	V21	3p 4P*	3d 2F	6	6
4114.31	0.007	0.012	O II	4114.18	V48b	3d 4F	4f G4*	10	8
*	*	O II		4114.50	V48b	3d 4F	4f G4*	10	10
4119.21	0.020	0.035	O II	4119.22	V20	3p 4P*	3d 4D	6	8
4120.83	0.120	0.210	He I	4120.84	V16	2p 3P*	5s 3S	9	3
4122.62	0.051	0.089	[K V]	4122.63		3p3 4S*	3p3 2D*	4	6
*	*	O II		4121.46	V19	3p 4P*	3d 4P	2	2
4128.75	0.029	0.051	Si II	4128.07	V3	3d 2D	4f 2F*	6	8
*	*	O II		4129.32	V19	3p 4P*	3d 4P	4	2
4132.71	0.008	0.013	O II	4132.80	V19	3p 4P*	3d 4P	2	4
4140.14	0.007	0.012	O II	4140.70	V19	3p 4P*	3d 4P	4	4
*	*	N II		4131.78	V43.01	3d 1D*	4f 2[4]	5	7

Table 2. continued.

λ_{obs}	$F(\lambda)$	$I(\lambda)$	Ion	λ_{lab}	Mult	Lower Term	Upper Term	g_1^a	g_2^a
4143.71	0.158	0.272	He I	4143.76	V53	2p 1P*	6d 1D	3	5
4145.94	0.011	0.019	C II	4145.00		3d' 4F	4p' 2P*	*	*
	*	*	N II	4145.77	V65	3s' 5P	3p' 5S*	7	5
4153.25	0.013	0.021	O II	4153.30	V19	3p 4P*	3d 4P	4	6
	*	*	C III	4152.43	V21	3p' 3D	5f 3F*	3	5
4156.48	0.033	0.056	O II	4156.53	V19	3p 4P*	3d 4P	6	4
4163.30	0.105	0.179	[K V]	4163.30		3p3 4S*	3p3 2D*	4	4
4167.07	0.006	0.011	C III	4166.95	V33	3p' 1D	6p 1P*	5	3
4168.96	0.020	0.034	He I	4168.97	V52	2p 1P*	6s 1S	3	1
	*	*	O II	4169.22	V19	3p 4P*	3d 4P	6	6
4176.99	0.003	0.005	O III	4177.60	V36b	4d 3D*	5f F[4]	5	7
4179.38	0.003	0.005	N II	4179.67	V50a	3d 3D*	4f 2[3]	7	7
4180.99	0.015	0.025	[Fe V]	4180.60		3d4 5D	3d4 3P2	3	1
4185.47	0.013	0.022	O II	4185.45	V36	3p' 2F*	3d' 2G	6	8
4186.92	0.118	0.197	C III	4186.90	V18	4f 1F*	5g 1G	7	9
4189.81	0.017	0.028	O II	4189.79	V36	3p' 2F*	3d' 2G	8	10
4195.48	0.010	0.017	N III	4195.76	V6	3s' 2P*	3p' 2D	2	4
4199.86	0.518	0.859	He II	4199.83	4.11	4f+ 2F*	11g+ 2G	32	*
	*	*	N III	4200.10	V6	3s' 2P*	3p' 2D	4	6
4201.73	0.012	0.020	[Ni II]	4201.17		3d9 2D	4s 2D	6	4
	*	*	[Mn V]	4201.40		3d3 4F	3d3 2D2	8	6
4206.31	0.002	0.003	[Fe IV]	4206.60		3d5 4G	3d5 2H	10	10
4209.20	0.003	0.005	[Fe IV]	4208.90		3d5 4G	3d5 2H	8	10
4211.04	0.005	0.008	[Fe II]	4211.10		3d7 4F	4s 2H	8	12
4216.84	0.006	0.010	N II	4217.10		4d 3D*	10p 3P	15	9
	*	*	N III	4215.77	V6	3s' 2P*	3p' 2D	4	4
4219.80	0.007	0.011	Ne II	4219.74	V52a	3d 4D	4f 2[4]*	8	10
	*	*	C IV	4219.34		6s 2S	8p 2P*	4	6
4227.43	0.096	0.156	[Fe V]	4227.20		3d4 5D	3d4 3H	9	9
4229.09	0.013	0.021	C IV	4229.02		7g 2G	12f 2F*	18	14
4231.22	0.003	0.005	Ne II	4231.53	V52b	3d 4D	4f 2[3]*	6	6
	*	*	Ne II	4231.64	V52b	3d 4D	4f 2[3]*	6	8
4233.58	0.002	0.003	Ne II	4233.85	52a	3d 4D	4f 2[4]*	6	8
	*	*	[Ba VIII]	4233.60		5p 2P	6p 2P	2	4
4236.49	0.003	0.005	N II	4236.91	V48a	3d 3D*	4f 1[3]	3	5
	*	*	N II	4237.05	V48b	3d 3D*	4f 1[4]	5	7
4238.05	0.012	0.020	C IV	4238.70		7d 2D	12p 2P*	10	6
	*	*	O II	4237.93		3d 4P	4f F3*	4	6
4241.27	0.0005:	0.001	N II	4241.24	V48a	3d 3D*	4f 1[3]	5	5
4241.81	0.005	0.009	N II	4241.78	V48a	3d 3D*	4f 1[3]	5	7
	*	*	N II	4241.78	V48b	3d 3D*	4f 1[4]	7	9
4243.95	0.014	0.022	[Fe II]	4243.97		3d7 4F	4s 4G	10	12
4250.00	0.0008:	0.001	[Sr VI]	4249.30		4p3 4S	4p3 2D	4	6
4253.90	0.010	0.016	O II	4253.90	V101	3d' 2G	4f' H5*	10	12
	*	*	O II	4253.91	V101	3d' 2G	4f' H5*	10	10
	*	*	N III	4253.99		4d 4P*	3d 4P	6	6
4256.45	0.001	0.002	C III	4256.46	V15.01	4f 3F*	5d 3D	7	5
4261.56	0.015	0.023	N I	4261.28		3s 4P	4p 4D*	4	4
	*	*	N II	4261.62		3s 3P	11d 3P*	5	3
4267.17	0.365	0.575	C II	4267.00	V6	3d 2D	4f 2F*	4	6
	*	*	C II	4267.26	V6	3d 2D	4f 2F*	12	14
4273.11	0.001	0.002	O II	4273.11	V67a	3d 4D	4f F4*	6	8
4275.56	0.015	0.023	O II	4275.55	V67a	3d 4D	4f F4*	8	10
	*	*	O II	4276.00	V67b	3d 4D	4f F3*	4	6
	*	*	O II	4276.29	V67b	3d 4D	4f F3*	6	6

Table 2. continued.

λ_{obs}	$F(\lambda)$	$I(\lambda)$	Ion	λ_{lab}	Mult	Lower Term	Upper Term	g_1^a	g_2^a
	*	*	O II	4276.63	V53c	3d 4P	4f D1*	4	4
4276.75	0.020	0.031	O II	4276.75	V67b	3d 4D	4f F3*	6	8
	*	*	O II	4277.44	V67c	3d 4D	4f F2*	2	4
	*	*	O II	4277.90	V67b	3d 4D	4f F3*	8	8
4282.99	0.003	0.005	O II	4282.96	V67c	3d 4D	4f F2*	4	6
4283.76	0.002	0.004	O II	4283.73	V67c	3d 4D	4f F2*	4	4
4285.72	0.006	0.010	O II	4285.69	V78b	3d 2F	4f F3*	6	8
4287.29	0.014	0.021	[Fe II]	4287.39		4s 6D	4s2 6S	10	6
4288.85	0.002	0.003	O II	4288.82	V53c	3d 4P	4f D1*	2	4
4291.49	0.007	0.010	O II	4291.25	V55	3d 4P	4f G3*	6	8
4292.45	0.009	0.014	O II	4292.21	V78c	3d 2F	4f F2*	6	6
4295.02	0.008	0.012	O II	4294.78	V53b	3d 4P	4f D2*	4	6
4295.16	0.002	0.003	O II	4294.92	V53b	3d 4P	4f D2*	4	4
4303.72	0.014	0.021	O II	4303.82	V53a	3d 4P	4f D3*	6	8
	*	*	O II	4303.61	V65a	3d 4D	4f G5*	8	10
4307.13	0.006	0.009	O II	4307.23	V53b	3d 4P	4f D2*	2	4
4308.96	0.005	0.008	O II	4308.99	V63c	3d 4D	4f D1*	2	2
4315.41	0.010	0.016	O II	4315.39	V78b	3d 2F	4f F3*	8	6
	*	*	O II	4315.39	V63c	3d 4D	4f D1*	4	2
	*	*	O II	4315.40	V63c	3d 4D	4f D1*	4	4
	*	*	O II	4315.69	V63c	3d 4D	4f D1*	6	4
4317.72	0.015	0.022	O II	4317.70	V53a	3d 4P	4f D3*	4	6
4319.65	0.017	0.026	O II	4319.63	V2	3s 4P	3p 4P*	4	6
4321.77	0.014	0.022	C II	4321.65	V28	3p' 4P	4s' 4P*	4	4
4323.09	0.003	0.004	C II	4323.10	V28	3p' 4P	4s' 4P*	2	2
4325.78	0.023	0.035	O II	4325.76	V2	3s 4P	3p 4P*	2	2
4329.86	0.006	0.008	[Fe II]	4329.43		4s 4D	4s 4D	6	8
4331.46	0.002	0.003	O II	4331.47	V41	3p' 2D*	3d' 2D	4	6
4333.05	0.008	0.012	He II	4332.00			Raman line		
	*	*	O II	4332.71	V65b	3d 4D	4f G4*	8	10
4334.94	0.004	0.006	O II	4335.36	V63b	3d 4D	4f D2*	8	6
4338.70	0.836	1.248	He II	4338.67	4.10	4f+ 2F*	11g+ 2G*	32	*
4340.50	31.930	47.664	H 5	4340.47	H5	2p+ 2P*	5d+ 2D	8	50
4344.11	0.023	0.034	O II	4344.42	V65c	3d 4D	4f G3*	6	8
4345.80	0.011	0.017	O II	4345.56	V2	3s 4P	3p 4P*	4	2
	*	*	O II	4345.55	V65c	3d 4D	4f G3*	8	8
4349.46	0.028	0.041	O II	4349.43	V2	3s 4P	3p 4P*	6	6
4351.28	0.008	0.012	O II	4351.26	V16	3s' 2D	3p' 2D*	6	6
4352.62	0.008	0.012	[Fe II]	4352.78		3d7 4F	4s 4G	6	10
4353.62	0.004	0.005	O II	4353.59	V76c	3d 2F	4f G3*	6	8
4356.46	0.003	0.004	[Fe II]	4356.14		3d7 4F	4s 2P	6	4
4357.78	0.003	0.004	O II	4357.25	V18	3p 4P*	3d 4F	6	8
	*	*	O II	4357.25	V63a	3d 4D	4f D3*	10	14
	*	*	O II	4357.52	V63a	3d 4D	4f D3*	6	6
4359.29	0.012	0.018	[Fe II]	4359.33		4s 6D	4s2 6S	8	6
4363.23	17.330	25.384	[O III]	4363.23	2F	2p2 1D	2p2 1S	5	1
4366.91	0.024	0.035	O II	4366.89	V2	3s 4P	3p 4P*	6	4
4368.32	0.033	0.048	O I	4368.30	V5	3s 3S*	4p 3P	3	1
4372.34	0.018	0.026	C II	4372.35	V45	3d' 4P*	4f' 4D	4	4
4376.42	0.022	0.031	C II	4376.56	V45	3d' 4P*	4f' 4D	4	6
4379.13	0.045	0.066	N III	4379.11	V18	4f 2F*	5g 2G	16	18
	*	*	Ne II	4379.55	V60b	3d 2F	4f 1[4]*	8	10
	*	*	C III	4379.48	V14	4d 3D	5p 3P*	3	1
4382.84	0.001	0.002	C III	4382.90	V14	4d 3D	5p 3P*	5	3
4385.12	0.0004:	0.0006	Ne II	4384.98	V59	3d 2F	4f 2[3]*	6	6

Table 2. continued.

λ_{obs}	$F(\lambda)$	$I(\lambda)$	Ion	λ_{lab}	Mult	Lower Term	Upper Term	g_1^a	g_2^a
4387.95	0.256	0.369	He I	4387.93	V51	2p 1P*	5d 1D	3	5
4391.94	0.008	0.011	Ne II	4391.99	V55e	3d 4F	4f 2[5]*	10	12
*	*		Ne II	4392.00	V55e	3d 4F	4f 2[5]*	10	10
4397.82	0.003	0.004	Ne II	4397.99	V57b	3d 4F	4f 1[4]*	6	8
4399.64	0.003	0.004	O III	4399.60	V47	4f G[4]	5g F[4]*	7	16
4402.82	0.008:	0.011	S II	4402.84	V43	4p 4D*	5s 4P	2	4
4405.62	0.009	0.013	O II	4405.98	V26	3p 2D*	3d 2D	6	4
4408.15	0.011	0.015	O III	4408.29	V46a	4f G[4]	5g H[5]*	7	9
4409.26	0.012	0.017	Ne II	4409.30	V55e	3d 4F	4f 2[5]*	8	10
4411.11	0.013	0.019	C II	4411.16	V39	3d' 2D*	4f' 2F	4	6
4413.24	0.012	0.017	Ne II	4413.22	V65	3d 4P	4f 0[3]*	6	8
4414.86	0.037	0.052	O II	4414.90	V5	3s 2P	3p 2D*	4	6
4416.73	0.025	0.035	O II	4416.97	V5	3s 2P	3p 2D*	2	4
4428.62	0.008	0.011	Ne II	4428.52	V61b	3d 2D	4f 2[3]*	6	8
*	*		Ne II	4428.64	V60c	3d 2F	4f 1[3]*	6	8
*	*		Ne II	4428.64	V60c	3d 2F	4f 1[3]*	6	8
4431.22	0.004	0.006	N II	4431.82	V55a	3d 3P*	4f 2[3]	5	5
4434.59	0.014	0.019	O III	4434.60	V46b	4f G[5]	5g H[6]*	11	24
4437.58	0.036	0.050	He I	4437.55	V50	2p 1P*	5s 1S	3	1
4442.05	0.007	0.009	N II	4442.02	V55a	3d 3P*	4f 2[3]	3	5
4448.09	0.020	0.028	O II	4448.19	V35	3p' 2F*	3d' 2F	8	8
4452.68	0.042	0.058	O II	4452.37	V5	3s 2P	3p 2D*	4	4
*	*		O III	4454.03	V49a	4f D[3]	5g F[4]*	7	16
*	*		O V	4454.97	V21	6g 3G	7h 3H*	9	11
4457.36	0.009	0.012	Ne II	4457.36	V66c	3d 4P	4f 1[3]*	6	8
4458.65	0.027	0.038	O III	4458.55	V49a	4f D[3]	5g F[4]*	5	7
4465.56	0.023	0.032	O II	4465.42	V94	3s''' 6S*	3p''' 6P	6	8
4467.92	0.018	0.025	O II	4467.92	V94	3s''' 6S*	3p''' 6P	6	6
4471.50	2.388	3.222	He I	4471.50	V14	2p 3P*	4d 3D	9	15
4474.95	0.016	0.022	[Fe II]	4474.90		4s 4F	4p 4F*	6	4
4476.40	0.008	0.010	O III	4476.11	V45b	4f G[4]	5g G[5]	7	9
4477.68	0.006	0.008	O II	4477.90	V88	3d 2P	4f G3*	4	6
4481.30	0.017	0.023	Mg II	4481.21	V4	3d 2D	4f 2F*	10	14
4488.20	0.009	0.012	O II	4488.20	V104	3d' 2P	4f' D2*	8	10
4491.33	0.016	0.021	O II	4491.23	V86a	3d 2P	4f 3D*	4	6
4498.66	0.012	0.016	Ca I	4498.73		4p2 1D	40p 1P*	5	3
4510.83	0.049	0.064	[K IV]	4510.90		3p4 1D	3p4 1S	5	1
*	*		N III	4510.91	V3	3s' 4P*	3p' 4D	6	10
4514.97	0.017	0.022	N III	4514.86	V3	3s' 4P*	3p' 4D	6	8
4517.04	0.013	0.017	C III	4516.93	V9	4p 3P*	5s 3S	5	3
4518.26	0.010	0.013	N III	4518.15	V3	3s' 4P*	3p' 4D	2	2
4519.88	0.009	0.012	N V	4520.04		7g 2G	9f 2F*	18	14
4523.70	0.012	0.016	N III	4523.58	V3	3s' 4P*	3p' 4D	4	4
4529.95	0.019	0.024	N II	4530.41	V58b	3d 1F*	4f 2[5]	7	9
*	*		N III	4530.86	V3	3s' 4P*	3p' 4D	4	2
4534.72	0.014	0.018	N III	4534.58	V3	3s' 4P*	3p' 4D	6	6
4539.87	0.022	0.029	N III	4539.71	V12	4p 2P*	5s 2S	2	2
4541.74	1.291	1.651	He II	4541.59	4.9	4f+ 2F*	9g+ 2G	32	*
4545.00	0.012	0.015	N III	4544.85	V12	4p 2P*	5s 2S	4	2
4552.58	0.005	0.007	N II	4552.53	V58a	3d 1F*	4f 2[4]	7	9
4554.70	0.002	0.002	Ba II	4554.00		6s 2S	6p 2P*	2	4
4562.65	0.017	0.021	[Mg I]	4562.60		3s2 1S	3s3p 3P*	1	5
4564.74	0.003	0.004	[Mn V]	4564.70		3d3 2F	3d3 2D1	6	6
4571.21	0.629	0.787	Mg I]	4571.10		3s2 1S	3s3p 3P*	1	3
4587.69	0.005	0.006	C III	4587.60	V51	4f' 3D	5g' 3F*	*	*

Table 2. continued.

λ_{obs}	$F(\lambda)$	$I(\lambda)$	Ion	λ_{lab}	Mult	Lower Term	Upper Term	g_1^a	g_2^a
4591.13	0.026	0.032	O II	4590.97	V15	3s' 2D	3p' 2F*	6	8
4593.00	0.010	0.012	C III	4593.30	V51	4f' 3D	5g' 3F*	7	9
4596.34	0.018	0.022	O II	4596.18	V15	3s' 2D	3p' 2F*	4	6
4601.99	0.007	0.009	O II	4602.13	V92b	3d 2D	4f F3*	4	6
4603.99	0.012	0.015	N V	4603.70	V1	3s 2S	3p 2P*	2	4
4606.68	0.077	0.094	N II	4607.16	V5	3s 3P*	3p 3P	1	3
4609.44	0.019	0.022	O II	4609.44	V92a	3d 2D	4f F4*	6	8
4610.43	0.011	0.014	O II	4610.20	V92c	3d 2D	4f F2*	4	6
4614.05	0.006	0.008	O II	4613.68	V92b	3d 2D	4f F3*	6	8
4618.81	0.008:	0.009	C II	4618.40	V50	3d' 2F*	4f' 2G	6	8
4620.22	0.022	0.026	N V	4620.00		3s 2S	3p 2P*	2	2
*	*	[La V]	4621.00			4p5 2P	5p5 2P	4	2
4621.76	0.006:	0.007	N II	4621.39	V5	3s 3P*	3p 3P	3	1
4625.52	0.059	0.070	[Ar V]	4625.54		3p2 1D	3p2 1S	5	1
4630.58	0.018	0.021	N II	4630.54	V5	3s 3P*	3p 3P	5	5
4632.22	0.158	0.188	O IV	4631.89		5g 2G	6h 2H*	18	32
4634.27	1.178	1.406	N III	4634.14	V2	3p 2P*	3d 2D	2	4
4638.99	0.059	0.070	O II	4638.86	V1	3s 4P	3p 4D*	2	4
4640.77	2.156	2.556	N III	4640.64	V2	3p 2P*	3d 2D	4	6
4641.97	0.216	0.256	N III	4641.84	V2	3p 2P*	3d 2D	4	4
*	*	O II	4641.81	V1		3s 4P	3p 4D*	4	6
*	*	N II	4643.08	V5		3s 3P*	3p 3P	5	3
4647.52	0.322	0.381	C III	4647.42	V1	3s 3S	3p 3P*	3	5
4649.31	0.140	0.165	O II	4649.13	V1	3s 4P	3p 4D*	6	8
4650.60	0.237	0.279	C III	4650.25	V1	3s 3S	3p 3P*	3	3
*	*	O II	4650.84	V1		3s 4P	3p 4D*	2	2
4654.75	0.002	0.002	O I	4654.56	V18	3p 5P	8d 5D*	5	*
4658.60	0.641	0.750	[Fe III]	4658.10	F3	3d6 5D	3d6 3F2	9	9
*	*	C IV	4657.15			5f 2F*	6g 2G	14	18
4661.73	0.031	0.036	O II	4661.63	V1	3s 4P	3p 4D*	4	4
4665.77	0.020	0.023	C III	4665.86	V5	3s' 3P*	3p' 3P	5	5
4669.26	0.024	0.028	O II	4669.27	V89b	3d 2D	4f D2*	4	6
4673.97	0.017	0.020	O II	4673.73	V1	3s 4P	3p 4D*	4	2
4676.29	0.032	0.037	O II	4676.24	V1	3s 4P	3p 4D*	6	6
4678.12	0.006	0.007	N II	4678.14	V61b	3d 1P*	4f 2[2]	3	5
4680.13	0.025	0.029	O II	4680.58	V89b	3d 2D	4f D2*	6	6
4685.87	41.690	47.747	He II	4685.68	3.4	3d+ 2D	4f+ 2F*	18	32
4691.84	0.006	0.007	O II	4691.42	V58	3p' 2P*	3d' 2P	2	2
4694.73	0.002	0.002	N II	4694.64	V61a	3d 1P*	4f 2[3]	3	5
4695.93	0.005	0.005	O II	4696.35	V1	3s 4P	3p 4D*	6	4
4698.97	0.016	0.018	O II	4699.00	V40	3p' 2D*	3d' 2F	6	8
4701.63	0.059	0.067	[Fe III]	4701.62	F3	3d6 5D	3d6 3F2	7	7
4705.41	0.004	0.004	O II	4705.35	V25	3p 2D*	3d 2F	6	8
4707.31	0.013	0.015	N IV	4707.31	V21	5f 3F*	6g 3G	*	*
4711.50	1.967	2.211	[Ar IV]	4711.37	F1	3p3 4S*	3p3 2D*	4	6
4713.24	0.567	0.635	He I	4713.17	V12	2p 3P*	4s 3S	9	3
4714.36	0.807	0.903	[Ne IV]	4714.36		2p3 2D*	2p3 2P*	6	2
4715.80	0.230	0.257	[Ne IV]	4715.80		2p3 2D*	2p3 2P*	6	4
4724.28	0.725	0.807	[Ne IV]	4724.15	F1	2p3 2D*	2p3 2P*	4	4
4725.72	0.610	0.677	[Ne IV]	4725.62	F1	2p3 2D*	2p3 2P*	4	2
4733.95	0.029	0.032	[Fe III]	4733.93		3d6 5D	3d6 3F2	5	5
4740.35	7.380	8.113	[Ar IV]	4740.17	F1	3p3 4S*	3p3 2D*	4	4
*	*	N IV	4740.26	V11		3p' 3D	3d' 3D*	3	5
4747.12	0.004	0.005	C II	4747.28	V1	2p2 2P	3p 2P*	4	2
*	*	N IV	4747.96	V11		3p' 3D	3d' 3D*	3	3

Table 2. continued.

λ_{obs}	$F(\lambda)$	$I(\lambda)$	Ion	λ_{lab}	Mult	Lower Term	Upper Term	g_1^a	g_2^a
4752.50	0.006	0.007	O II	4752.68	V24	3p 2D*	3d 4D	6	6
*	*		N IV	4752.49	V11	3p' 3D	3d' 3D*	5	7
4754.72	0.030	0.032	[Fe III]	4754.72		3d6 5D	3d6 3F2	7	9
4762.35	0.006	0.007	N IV	4762.09	V11	3p' 3D	3d' 3D*	5	5
4769.54	0.022	0.023	[Fe III]	4769.60		3d6 5D	3d6 3F2	5	7
*	*		N IV	4769.86	V11	3p' 3D	3d' 3D*	5	3
4772.32	0.002	0.003	Ne II	4772.93		4p 4D*	5d 4F	6	8
4774.61	0.004	0.004	N II	4774.24	V20	3p 3D	3d 3D*	3	5
4777.56	0.016	0.018	[Fe III]	4777.88		3d6 5D	3d6 3F2	3	5
4781.92	0.005	0.005	N II	4781.19	V20	3p 3D	3d 3D*	5	7
4783.34	0.005	0.005	O IV	4783.34	V9	3p 4P	3d 4D*	4	6
4785.93	0.009	0.009	C IV	4785.90	V5	5d 2D	6p 2P*	6	4
4788.31	0.005	0.005	N II	4788.13	V20	3p 3D	3d 3D*	5	5
*	*		N IV	4786.92	V11	3p' 3D	3d' 3D*	7	7
4789.60	0.011	0.011	C IV	4789.79		6p 2P*	8s 2S	4	2
4794.36	0.005	0.005	O IV	4794.26	V9	3p' 4P	3d' 4D*	4	4
4796.47	0.002	0.002	N IV	4796.70	V11	3p' 3D	3d' 3D*	7	5
4798.79	0.004	0.004	[Fe II]	4798.27		4s 6D	4s 4P	2	4
*	*		O IV	4798.25	V9	3p 4P	3d 4D*	6	8
4800.39	0.004	0.004	O IV	4800.77	V9	3p 4P	3d 4D*	4	2
4802.72	0.030	0.032	C II	4802.70	V17.08	4f 2F*	8g 2G	22	26
4814.64	0.016	0.017	[Fe II]	4814.53		3d7 4F	4s 4F	10	10
4817.09	0.002	0.002	[Cs IV]	4817.07		5p4 3P	5p4 1D	5	5
4819.64	0.003	0.003	S II	4819.58	V52	4p 2D*	5s 2P	4	2
4829.06	0.003	0.003	?	*				*	*
4831.17	0.004	0.004	?	*				*	*
4833.39	0.007	0.007	Fe II	4833.13	V30	a4H	z6F*	12	10
4843.46	0.008	0.008	O II	4843.37	V105	3d' 2S	4f' P1*	4	6
4845.45	0.004	0.004	O II	4844.91	V30	3p 2S*	3d 2F	2	6
4852.09	0.244	0.245	He II	4852.00			Raman line		
*	*	[Fe II]	4852.73			3d7 4F	4s 4F	8	4
4859.35	2.833	2.833	He II	4859.32	4.8	4f+ 2F*	8g+ 2G	32	*
*	*	N III	4858.82	V9		3p' 4D	3d' 4F*	6	10
4861.49	100	100	H 4	4861.33	H4	2p+ 2P*	4d+ 2D	8	32
*	*	N III	4861.30	V9		3p' 4D	3d' 4F*	6	8
4867.16	0.015	0.015	N III	4867.18	V9	3p' 4D	3d' 4F*	12	14
4871.36	0.008	0.008	O II	4871.52	V57	3p' 2P*	3d' 2D	4	6
4873.41	0.007	0.007	N III	4873.57	V9	3p' 4D	3d' 4F*	6	6
*	*	[Fe II]	4874.49			3d7 4F	4s 4F	8	6
4881.03	0.070	0.069	[Fe III]	4881.11	F2	3d6 5D	3d6 3H	9	9
*	*	N III	4881.81	V9		3p' 4D	3d' 4F*	6	4
4884.13	0.002	0.002	N III	4884.13	V9	3p' 4D	3d' 4F*	8	8
4887.94	0.002	0.002	[Fe IV]	4888.60		3d5 4G	3d5 4F	12	8
4889.81	0.014	0.013	[Fe II]	4889.62		4s 6D	4s 4P	8	6
*	*	O II	4890.85	V28		3p 4S*	3d 4P	4	2
4893.83	0.064	0.062	[Fe VII]	4893.83		3d2 3F	3d2 3P	5	3
4897.23	0.004	0.004	[Cr IV]	4897.30		3d3 4F	3d3 2D2	6	4
4899.66	0.010	0.010	[Fe IV]	4900.00		3d5 4G	3d5 4F	10	8
4902.79	0.008	0.008	[Fe IV]	4903.10		3d5 4G	3d5 4F	8	8
4905.25	0.011	0.011	[Fe II]	4905.34		3d7 4F	4s 4F	8	8
4906.91	0.023	0.022	O II	4906.83	V28	3p 4S*	3d 4P	4	4
*	*	[Fe IV]	4906.60			3d5 4G	3d5 4F	12	10
4915.97	0.003	0.003	Ar II	4915.83		4d 2G	5f 2[5]*	20	22
4917.74	0.004	0.004	[Fe IV]	4817.90		3d5 4G	3d5 4F	10	10
4921.92	0.978	0.933	He I	4921.93	V48	2p 1P*	4d 1D	3	5

Table 2. continued.

λ_{obs}	$F(\lambda)$	$I(\lambda)$	Ion	λ_{lab}	Mult	Lower Term	Upper Term	g_1^a	g_2^a
	*	*	[Sr V]	4922.20		4p4 3P	4p4 1D	5	5
4924.06	0.013	0.012	O II	4924.53	V28	3p 4S*	3d 4P	4	6
	*	*	[Fe III]	4924.66		3d6 5D	3d6 3H	9	11
4931.11	0.268	0.254	[O III]	4931.80	F1	2p2 3P	2p2 1D	1	5
4934.01	0.004	0.004	Ba II	4934.10		6s 2S	6p 2P*	2	2
4942.62	0.051	0.048	[Fe VII]	4942.50		3d2 3F	3d2 3P	7	5
4944.56	0.046	0.043	N V	4944.56	V9	6f+ 2F*	7g+ 2G	*	*
4946.52	0.028	0.026	[Ni IV]	4946.70		3d7 2P	3d7 2F	4	8
4948.53	0.027	0.026	N III	4948.80		7p 2D	4d 2D*	4	4
4958.98	608.300	563.946	[O III]	4958.91	F1	2p2 3P	2p2 1D	3	5
4964.97	0.077	0.071	C II	4964.73	V25	3p' 2P	3d' 2P*	4	4
4967.32	0.064	0.059	[Fe VI]	4967.32		3d3 4F	3d3 2G	8	10
4969.11	0.050	0.046	O I	4968.79	V14	3p 5P	6d 5D*	7	5
4971.36	0.032	0.030	[Cr IV]	4971.50		3d3 4F	3d3 2D2	8	6
4972.71	0.184	0.169	[Fe VI]	4972.50		3d3 4F	3d3 2G	6	8
4975.51	0.017	0.016	N I	4975.04	V77	3p 4P*	8d 4D	12	10
4988.50	0.098	0.089	[Fe VII]	4988.80		3d7 3F	3d2 3P	5	1
4992.22	0.073	0.066	?	*				*	*
4994.27	0.151	0.136	N II	4994.36	V24	3p 3S	3d 3P*	3	3
4996.47	0.125	0.112	?	*				*	*
5000.78	0.207	0.186	Fe II	5000.74	V25	b4P	z6F*	2	4
5006.88	1845.10	1657.92	[O III]	5006.84	F1	2p2 3P	2p2 1D	5	5
5012.99	0.203	0.180	Fe I	5012.68	V1093	y5F*	e5H	5	7
5015.65	1.465	1.300	He I	5015.68	V4	2s 1S	3p 1P*	1	3
	*	*	C IV	5016.58	V3	5p 2P*	6s 2S	2	2
5019.36	0.066	0.059	C IV	5018.39	V3	5p 2P*	6s 2S	4	2
5021.45	0.045	0.040	N III	5021.70		4d 2D*	5p 2D	6	6
5025.57	0.020	0.018	N II	5025.66	V19	3p 3D	3d 3F*	7	7
5031.98	0.034	0.030	C II	5032.07	V17	2p3 2P*	3p' 2D	4	6
5033.84	0.012	0.011	[Fe IV]	5033.60		3d5 2F2	3d5 4G	8	6
5035.92	0.028	0.024	[Fe II]	5035.40		3d7 2P	4s 2D	4	4
5038.24	0.016	0.014	C I	5039.07	V18.01b	2p3 3D*	4f 1[4]	7	*
5041.00	0.278	0.242	Si II	5041.03	V5	4p 2P*	4d 2D	2	4
	*	*	N II	5040.72	V19	3p 3D	3d 3F*	7	5
5044.33	0.010	0.009	Fe I	5044.21	V318	z7F*	e7D	9	11
5047.71	0.178	0.154	He I	5047.74	V47	2p 1P*	4s 1S	3	1
5056.11	0.137	0.117	Si II	5056.31	V5	4p 2P*	4d 2D	4	4
5058.48	0.007	0.006	Fe I	5058.50	V884	b3D	v3D*	7	7
5069.44	0.027	0.023	Mg II	5069.07		4d 2D	8p 2P*	4	4
	*	*	Mg II	5069.80		4d 2D	8p 2P*	4	2
5072.43	0.019	0.016	[Fe II]	5072.39		3d7 4F	4s 4H	10	10
	*	*	C IV	5073.20		7s 2S	10p 2P*	2	6
5079.78	0.008	0.007	[Rb V]	5080.20		5p3 2D	5p3 2P	4	4
5084.58	0.008	0.007	[Fe III]	5084.85		3d6 5D	3d6 3P2	1	3
	*	*	O VI	5084.00	V11	7p 2P*	8d 2D	6	10
5085.93	0.012	0.010	?	*				*	*
5092.63	0.019	0.016	C IV	5093.10		8g 2G	15h 2H*	*	*
5094.78	0.003	0.002	C III	5095.20		4d' 1P*	5f' 1D	*	*
5111.55	0.013	0.011	[Fe II]	5111.63		3d7 4F	4s 4H	10	12
5113.97	0.019	0.015	O V	5114.10		3s 1S	3p 1P*	1	3
5119.67	0.016	0.014	C II	5120.10	V12	4p 2P*	3p' 2P	2	4
5121.57	0.046	0.038	C II	5121.69	V12	4p 2P*	3p' 2P	4	4
5127.28	0.009	0.007	C II	5126.93	V12	4p 2P*	3p' 2P	4	2
5131.06	0.142	0.115	O I	5131.30		3p 3P	8d 3D*	*	*
5133.46	0.016	0.013	C II	5133.28	V16	3s' 4P*	3p' 4P	4	6

Table 2. continued.

λ_{obs}	$F(\lambda)$	$I(\lambda)$	Ion	λ_{lab}	Mult	Lower Term	Upper Term	g_1^a	g_2^a
5143.38	0.016	0.013	C II	5143.38	V16	3s' 4P*	3p' 4P	4	2
5145.83	0.219	0.176	[Fe VI]	5146.80		3d3 4F	3d3 2G	8	8
5151.00	0.011	0.009	C II	5151.09	V16	3s' 4P*	3p' 4P	6	4
5158.75	0.183	0.145	[Fe II]	5158.78		3d7 4F	4s 4H	10	14
*	*		[Fe VII]	5158.89		3d2 3F	3d2 3P	7	3
5161.94	0.007	0.006	Ne II	5161.96		3d 2D	9f 1[3]*	6	8
5172.72	0.019	0.015	[Fe II]	5172.47		3d7 2P	4s 2D	2	4
5176.35	0.203	0.159	[Fe VI]	5176.43		3d3 4F	3d3 2G	10	10
5179.94	0.018	0.014	N II	5179.35	V70	3p' 5P*	3d' 5D	7	9
5183.55	0.022	0.017	N II	5183.21	V70	3p' 5P*	3d' 5D	7	7
5189.03	0.002	0.002	N II	5190.38	V66	3p' 5D*	3d' 5F	9	9
5191.68	0.343	0.266	[Ar III]	5191.82	F3	2p4 1D	2p4 1S	5	1
5197.85	0.417	0.322	[N I]	5197.51	V1F	2p3 4S*	2p3 2D*	4	4
5200.20	0.243	0.187	[N I]	5200.26	F1	2p3 4S*	2p3 2D*	4	6
5208.74	0.005	0.004	Ne I	5208.87	V25.1	3p 2[2]	5d 2[2]*	5	5
5220.08	0.012	0.009	[Fe II]	5220.06		3d7 4F	4s 4H	8	10
5234.14	0.027	0.020	[Fe VI]	5234.30		3d3 4F	3d3 4P	6	6
*	*		[Fe IV]	5233.80		3d5 4G	3d5 2F2	10	8
5249.17	0.007	0.005	C III	5249.11	V23	4d 1D	5p 1P*	5	3
5253.95	0.004	0.003	C III	5253.58	V4	3s' 3P*	3p' 3S	3	3
5259.34	0.013	0.009	C II	5259.06	V30	3d' 4F*	4p' 4D	8	6
*	*		C II	5259.71	V30	3d' 4F*	4p' 4D	10	6
5261.51	0.041	0.030	[Fe II]	5261.62		3d7 4F	4s 4H	8	12
5266.90	0.004	0.003	O II	5267.27		4f G3*	4d' 2F	8	6
5270.41	0.129	0.094	[Fe III]	5270.40		3d6 5D	3d6 3P2	7	5
5273.19	0.011	0.008	[Fe II]	5273.35		3d7 4F	4s 4P	10	6
5276.45	0.045	0.033	[Fe VII]	5276.40		3d2 3F	3d2 3P	9	5
5277.91	0.049	0.035	[Fe VI]	5277.80		3d3 4F	3d3 4P	4	4
5298.99	0.021	0.015	N III	5298.95	V15	3p 4P	3d 4P	6	4
5304.68	0.038	0.027	C III	5305.10	V46	5f 3F*	7g 3G	*	*
5309.23	0.337	0.239	[Ca V]	5308.90		3p4 3P	3p4 1D	5	5
5323.09	0.086	0.060	[Cl IV]	5323.27		3p2 1D	3p2 1S	5	1
5335.19	0.147	0.102	[Fe VI]	5335.23		3d3 4F	3d3 4P	4	2
*	*		C II	5332.89	V11	4p 2P*	6s 2S	2	2
*	*		[Fe II]	5333.45		3d7 4F	4s 4H	6	10
5342.30	0.050	0.034	C II	5342.38	V17.06	4f 2F*	7g 2G	22	26
*	*		[P I]	5339.62		3p3 4S*	3p3 2P*	4	2
5345.99	0.215	0.148	C III	5345.80	V13.01	4d 3D	3d' 3P*	5	3
*	*		[Kr IV]	5346.10		4p3 4S	4p3 2D	4	6
5358.24	0.007	0.005	Ne I	5358.00		3p 2[3/2]	5d 2[3/2]*	5	3
5363.55	0.006	0.004	[Ni IV]	5363.30		3d7 4F	3d7 2G	8	10
*	*		C II	5364.67	V54	4s' 4P*	5p' 4D	4	6
5367.70	0.005	0.003	C II	5367.67	V54	4s' 4P*	5p' 4D	6	8
5370.45	0.009	0.006	[Fe VI]	5370.30		3d3 4F	3d3 2G	10	8
5376.24	0.015	0.010	[Fe II]	5376.40		3F 4d4H	4f 4[5]*	10	10
5380.28	0.001:	0.0007	[Rb IV]	5380.00		4p2 3P	4p2 1D	3	5
5411.52	5.500	3.615	He II	5411.52	4.7	4f+ 2F*	7g+ 2G	32	98
5424.96	0.179	0.117	[Fe VI]	5424.40		3d3 4F	3d3 4P	6	4
*	*		[Fe VI]	5426.60		3d3 4F	3d3 4P	8	6
5433.37	0.009	0.006	O VI	5433.00	V12	7d 2D	8p 2P*	10	6
*	*		[Sr VI]	5434.40		4p3 2D	5p3 2P	4	2
5441.20	0.003	0.002	[Fe III]	5440.02		3d6 5D	3d6 3P	1	5
5445.00	0.003	0.002	S II	5444.97	V2	3d 5D*	4p 5P	*	*
5451.09	0.006	0.004	N II	5452.08	V29	3p 3P	3d 3P*	1	3
5454.21	0.003	0.002	N II	5454.22	V29	3p 3P	3d 3P*	3	1

Table 2. continued.

λ_{obs}	$F(\lambda)$	$I(\lambda)$	Ion	λ_{lab}	Mult	Lower Term	Upper Term	g_1^a	g_2^a
5461.04	0.012	0.008	[Ca VI]	5460.70		3p3 2D*	3p3 2P*	4	4
*	*		N II	5462.60	V29	3p 3P	3d 3P*	3	3
5465.33	0.009	0.006	Fe II	5465.56		4p sp6D*	4p2 6D	8	10
5470.42	0.106	0.067	C IV	5470.68		7g 2G	10f 2F*	18	14
5476.82	0.002	0.001	N II	5476.13		3s' 3P	7d 3D*	5	5
5479.16	0.002	0.001	N II	5480.06	V29	3p 3P	3d 3P*	8	8
*	*		C II	5478.59	V34	3d' 4D*	4p' 4D	8	8
5484.92	0.111	0.070	[Fe VI]	5484.80		3d3 4F	3d3 4P	6	2
5495.88	0.012:	0.007	N II	5495.65	V29	3p 3P	3d 3P*	5	5
5504.67	0.007	0.004	N II	5504.67		4p 3D	5d 3P*	5	3
5509.54	0.006:	0.004	S II	5509.71	V6	4s 4P	4p 4D*	4	4
5512.95	0.017	0.010	O I	5512.60	V25	3p 3P	6d 3D*	8	8
*	*		O I	5512.77	V25	3p 3P	6d 3D*	15	15
*	*		O I	5512.82	V25	3p 3P	6d 3D*	1	3
5517.68	0.308	0.189	[Cl III]	5517.66	F1	2p3 4S*	2p3 2D*	4	6
5527.30	0.028	0.017	[Fe II]	5527.61		4s 4D	4s 2P	2	2
5530.80	0.011	0.007	N II	5530.24	V63	3s' 5P	3pd' 5D*	5	7
5537.80	1.063	0.646	[Cl III]	5537.60	F1	2p3 4S*	2p3 2D*	4	4
*	*		C II	5535.35	V10	4s 2S	5p 2P*	2	4
*	*		[Mn VI]	5536.50		3d2 3F	3d2 3P	5	3
5551.36	0.011	0.007	[Fe II]	5551.31		3d7 4P	4s 4D	6	8
5554.68	0.012	0.007	O I	5554.83	V24	3p 3P	7s 3S*	3	3
5572.64	0.003	0.002	O V	5571.84	V3	3p 3P*	3d 3D	1	3
5577.27	0.356	0.212	[O I]	5577.34	F3	2p4 1D	2p4 1S	5	1
5586.62	0.004	0.003	[Ca VI]	5586.30		3p3 2D*	3p3 2P*	6	4
5592.23	0.178	0.105	O III	5592.37	V5	3s 1P*	3p 1P	3	3
*	*		[Mn VI]	5590.70		3d2 3F	3d2 3P	7	5
5596.60	0.004	0.003	Si III	5596.89	V18	5d 3D	7p 3P*	3	5
5602.27	0.034	0.020	[K VI]	5602.40		3p2 3P	3p2 1D	3	5
5618.75	0.006	0.003	[Ca VII]	5618.80		3p2 3P	3p2 1D	5	5
5622.27	0.025	0.014	[Mn VI]	5622.10		3d2 3F	3d2 3P	5	1
5625.76	0.002	0.001	C I	5625.80		3p 3P	8d 1F*	5	7
5631.00	0.143	0.083	[Fe VI]	5631.10		3d3 4F	3d3 4P	8	4
*	*		[Ca VI]	5631.70		3p3 2D*	3p3 2P*	4	2
5650.05	0.007:	0.004	[Fe II]	5649.66		3d7 4P	3d6 4D	4	2
5660.27	0.035	0.020	S II	5659.95	V11	3d 4F	4p 4D*	6	4
5666.71	0.025	0.014	N II	5666.63	V3	3s 3P*	3p 3D	3	5
5676.91	0.167	0.094	N II	5676.02	V3	3s 3P*	3p 3D	1	3
*	*		[Fe VI]	5677.00		3d3 4F	3d3 4P	10	6
5679.57	0.058	0.033	N II	5679.56	V3	3s 3P*	3p 3D	5	7
5685.51	0.034	0.019	N II	5686.21	V3	3s 3P*	3p 3D	3	3
5689.00	0.002	0.001	Ne I	5689.82		3p 2[1]	5s 2[2]*	3	5
5692.08	0.039	0.022	[Mn V]	5692.00		3d3 4F	3d3 2G	8	10
5695.92	0.014	0.008	C III	5695.92		3p 1P*	3d 1D	3	5
*	*		[Ba IV]	5696.60		4p5 2P	5p5 2P	4	2
5701.95	0.048	0.026	[Mn V]	5701.80		3d3 4F	3d3 2G	6	8
5709.23	0.015	0.009	[Xe IV]	5709.20		5p3 4S	5p3 2D	4	6
5710.90	0.007:	0.004	N II	5710.77	V3	3s 3P*	3p 3D	5	5
*	*		[Mn V]	5711.20		3d3 2P	3d3 2F	4	8
5721.17	0.504	0.278	[F III]	5721.20		2p3 2D*	2p3 2P*	6	4
*	*		[Fe VII]	5720.70		3d2 3F	3d2 3F	5	5
5732.40	0.021	0.012	[F III]	5732.90		2p3 2D*	2p3 2P*	4	4
5736.63	0.002	0.001	N IV	5736.94	V9	3p' 1P	3d' 1D*	3	5
5739.58	0.004	0.002	Si III	5739.73	V4	4s 1S	4p 1P*	1	3
5754.60	10.630	5.764	[N II]	5754.60	F3	2p2 1D	2p2 1S	5	1

Table 2. continued.

λ_{obs}	$F(\lambda)$	$I(\lambda)$	Ion	λ_{lab}	Mult	Lower Term	Upper Term	g_1^a	g_2^a
	*	*	He II	5752.00	5.50	5g+ 2G	50h+ 2H*	50	*
	*	*	He II	5754.40	5.49	5g+ 2G	49h+ 2H*	50	*
	*	*	He II	5757.00	5.48	5g+ 2G	48h+ 2H*	50	*
5759.44	0.051	0.028	He II	5759.44	5.47	5g+ 2G	47h+ 2H*	50	*
	*	*	[Rb IV]	5759.40		4p4 3P	4p4 1D	5	5
5762.63	0.013	0.007	He II	5762.63	5.46	5g+ 2G	46h+ 2H*	50	*
5765.78	0.009	0.005	[Ca VI]	5765.40		3p3 2D*	3p3 2P*	6	2
	*	*	He II	5765.70	5.45	5g+ 2G	45h+ 2H*	50	*
5769.20	0.011	0.006	He II	5769.20	5.44	5g+ 2G	44h+ 2H*	50	*
5772.20	0.018	0.009	He II	5772.20	5.43	5g+ 2G	43h+ 2H*	50	*
5776.56	0.035	0.019	He II	5776.40	5.42	5g+ 2G	42h+ 2H*	50	*
	*	*	[Mn VI]	5775.00		3d2 3F	3d2 3P	7	3
5780.31	0.011	0.006	He II	5780.50	5.41	5g+ 2G	41h+ 2H*	50	*
5784.94	0.024	0.013	He II	5784.94	5.40	5g+ 2G	40h+ 2H*	50	*
5789.73	0.026	0.014	He II	5789.65	5.39	5g+ 2G	39h+ 2H*	50	*
5794.57	0.031	0.016	He II	5794.57	5.38	5g+ 2G	38h+ 2H*	50	*
5801.35	0.624	0.328	C IV	5801.33	V1	3s 2S	3p 2P*	2	4
	*	*	He II	5800.40	5.37	5g+ 2G	37h+ 2H*	50	*
5806.63	0.039	0.020	He II	5806.50	5.36	5g+ 2G	36h+ 2H*	50	*
5812.11	0.402	0.211	C IV	5811.98	V1	3s 2S	3p 2P*	2	2
	*	*	He II	5813.10	5.35	5g+ 2G	35h+ 2H*	50	*
5820.55	0.041	0.022	[Ni IV]	5820.10		3d7 4F	3d7 4P	8	4
	*	*	He II	5820.40	5.34	5g+ 2G	34h+ 2H*	50	*
5828.37	0.041	0.021	He II	5828.60	5.33	5g+ 2G	33h+ 2H*	50	*
5832.91	0.007	0.004	Fe II	5832.89		3F 4p4G*	3F 4d4F	6	6
5837.04	0.051	0.026	He II	5836.50	5.32	5g+ 2G	32h+ 2H*	50	*
5841.25	0.002	0.001	N I	5840.89	V60	3p 4P*	6s 4P	4	4
5846.76	0.075	0.039	He II	5847.10	5.31	5g+ 2G	31h+ 2H*	50	*
	*	*	[Xe III]	5846.70		5p3 3P	5p3 1D	5	5
5857.26	0.057	0.029	He II	5857.27	5.30	5g+ 2G	30h+ 2H*	50	*
5861.31	0.052	0.026	[Mn V]	5861.00		3d3 4F	3d3 2G	8	8
5867.82	0.495	0.253	[Kr IV]	5868.00		4p3 4S	3d3 2G	4	4
	*	*	He II	5869.00	5.29	5g+ 2G	29h+ 2H*	50	*
5875.68	21.410	10.866	He I	5875.66	V11	2p 3P*	3d 3D	9	15
5882.00	0.041	0.021	He II	5882.14	5.28	5g+ 2G	28h+ 2H*	50	*
5885.71	0.074	0.038	[Mn V]	5885.40		3d3 4F	3d3 2G	10	10
5897.09	0.071	0.035	He II	5896.79	5.27	5g+ 2G	27h+ 2H*	50	*
5913.32	0.084	0.042	He II	5913.26	5.26	5g+ 2G	26h+ 2H*	50	*
5927.73	0.004	0.002	N II	5927.81	V28	3p 3P	3d 3D*	1	3
5931.94	0.098	0.048	He II	5931.84	5.25	5g+ 2G	25h+ 2H*	50	*
5940.09	0.008	0.004	N II	5940.24	V28	3p 3P	3d 3D*	3	3
5946.22	0.006	0.003	O III	5946.37		4d 3F*	3s 3D	5	7
5953.01	0.112	0.056	He II	5952.94	5.24	5g+ 2G	24h+ 2H*	50	*
5958.28	0.023	0.011	O I	5958.39	V23	3p 3P	5d 3D*	6	8
	*	*	O I	5958.58	V23	3p 3P	5d 3D*	15	15
	*	*	O I	5958.58	V23	3p 3P	5d 3D*	1	3
5977.23	0.139	0.067	He II	5977.03	5.23	5g+ 2G	23h+ 2H*	50	*
5990.10	0.008	0.004	[Mn V]	5990.10		3d3 4F	3d3 4P	6	6
6004.85	0.146	0.069	He II	6004.73	5.22	5g+ 2G	22h+ 2H*	50	*
6024.87	0.018	0.009	[Mn V]	6024.40		3d3 4F	3d3 4P	4	4
6036.86	0.165	0.077	He II	6036.70	5.21	5g+ 2G	21h+ 2H*	50	*
6046.42	0.032	0.015	O I	6046.23	V22	3p 3P	6s 3S*	3	3
	*	*	O I	6046.44	V22	3p 3P	6s 3S*	5	3
	*	*	O I	6046.49	V22	3p 3P	6s 3S*	1	3
6074.26	0.195	0.089	He II	6074.10	5.20	5g+ 2G	20h+ 2H*	50	*

Table 2. continued.

λ_{obs}	$F(\lambda)$	$I(\lambda)$	Ion	λ_{lab}	Mult	Lower Term	Upper Term	g_1^a	g_2^a
6083.73	0.039	0.018	[Mn V]	6083.73		3d3 4F	3d3 4P	4	2
6086.86	1.022	0.461	[Ca V]	6086.92		3p4 3P	3p4 1D	3	5
*	*		[Fe VII]	6086.90		3d2 3F	3d2 1D	7	5
*	*		[Ba V]	6085.08		5p4 3P	5p4 3P	5	3
6096.47	0.003	0.001	[Fe III]	6096.30		3d6 3P2	3d6 1D2	5	5
6101.80	0.897	0.406	[K IV]	6101.83	F1	3p4 3P	3d4 1D	5	5
6107.94	0.011	0.005	[Kr IV]	6107.80		5p3 2D	5d3 2P	4	4
6115.01	0.011	0.005	N II	6114.60	V36	3d 3F*	4p 3D	5	7
6118.31	0.232	0.104	He II	6118.20	5.19	5g+ 2G	19h+ 2H*	50	*
6126.05	0.012	0.006	C III	6126.30		7h 1H*	16i 1I	11	13
*	*		C III	6126.30		7h 3H*	16i 3I	*	*
*	*		[Ni IV]	6124.10		3d7 4F	3d7 4P	6	4
6130.63	0.024	0.011	[Br III]	6131.00		4p3 4S	4p3 2D	4	4
*	*		Fe II	6129.71		c4P	x4F*	6	6
6134.20	0.016	0.007	[Ar V]	6133.50		3p2 3P	3p2 1D	1	5
6141.88	0.016	0.007	Ba II	6141.70		5d 2D	6p 2P*	6	4
6151.26	0.064	0.028	C II	6151.43	V16.04	4d 2D	6f 2F*	16	20
*	*		C IV	6150.20		8s 2S	12p 2P*	2	6
6157.44	0.042	0.019	[Mn V]	6157.60		3d3 4F	3d3 4P	6	4
6161.48	0.009	0.004	[Cl II]	6161.84		3p4 1D	3p4 1S	5	1
6165.99	0.028	0.012	[Mn V]	6166.00		3d3 4F	3d3 4P	8	6
6170.75	0.296	0.129	He II	6170.60	5.18	5g+ 2G	18h+ 2H*	50	*
6205.73	0.009	0.004	?	*				*	*
6219.17	0.029	0.013	[Mn V]	6219.10		3d3 2D2	3d3 2F	6	2
*	*		[Ni IV]	6218.70		3d7 4F	3d7 4P	6	6
6222.20	0.015	0.006	Ne II	6221.65		4p 2D*	4s' 2D	6	4
*	*		Ne II	6221.79		4p 2D*	4s' 2D	6	6
6228.41	0.097	0.041	[K IV]	6228.60		3p2 3P	3p2 1D	5	5
6233.89	0.329	0.140	He II	6233.80	5.17	5g+ 2G	17h+ 2H*	50	*
6239.75	0.004	0.002	Fe II	6239.95	V74	4s 4D	4s 4P*	2	4
6242.57	0.002	0.001	N II	6242.41	V57	3d 1F*	4p 1D	7	5
6246.87	0.003	0.001	Ne I	6246.73		3p 2[3]	5s 2[2]*	5	5
6251.03	0.030	0.013	C II	6250.74	V38.03	3d' 2D*	4p' 2P	6	4
6256.47	0.059	0.025	C II	6256.54	V38.03	3d' 2D*	4p' 2P	4	2
*	*		[Kr V]	6256.50		5p2 3P	5p2 1D	3	5
6273.63	0.110	0.046	?	*				*	*
6280.40	0.023	0.009	[Fe II]	6279.95		3d6 2D2	4s 2S	4	2
6300.35	33.060	13.582	[O I]	6300.34	F1	2p4 3P	2p4 1D	5	5
6312.10	10.330	4.230	[S III]	6312.10	F3	2p2 1D	2p2 1S	5	1
*	*		He II	6310.80	5.16	5g+ 2G	16h+ 2H*	50	*
6343.73	0.046	0.019	[Mn V]	6343.60		3d3 4F	3d3 4P	8	4
6347.17	0.158	0.063	Si II	6347.09	V2	4s 2S	4p 2P*	2	4
6363.78	11.070	4.421	[O I]	6363.78	F1	2p4 3P	2p4 1D	3	5
6371.39	0.292	0.116	Si II	6371.38	V2	4s 2S	4p 2P*	2	2
6376.75	0.008	0.003	[Cr V]	6377.20		3d2 3F	3d2 3P	5	3
6393.70	0.093	0.037	[Mn V]	6393.60		3d3 4F	3d3 4P	10	6
*	*		[O I]	6391.73	F1	2p4 3P	2p4 1D	1	5
6406.48	0.530	0.208	He II	6406.30	5.15	5g+ 2G	15h+ 2H*	50	*
*	*		[Xe VI]	6408.89		5p 2P	6p 2P	2	4
6435.10	3.391	1.308	[Ar V]	6435.10		3p2 3P	3p2 1D	3	5
*	*		[Cr V]	6436.20		3d2 3F	3d2 3P	7	5
6440.34	0.010	0.004	[Ni II]	6441.29		4s 2F	4s 2P	8	4
6446.98	0.003	0.001	[K V]	6446.30		3p3 2D*	3p3 2P*	6	2
6451.86	0.013	0.005	[Ni IV]	6450.90		3d7 4F	3d7 4P	4	6
*	*		N III	6450.78		3p 4P	3d 4D*	2	2

Table 2. continued.

λ_{obs}	$F(\lambda)$	$I(\lambda)$	Ion	λ_{lab}	Mult	Lower Term	Upper Term	g_1^a	g_2^a
	*	*	[Cr V]	6453.20		2d2 3F	2d2 3P	5	1
6461.86	0.159	0.060	C II	6461.95		4f 2F*	6g 2G	22	26
6466.04	0.022	0.008	O V	6466.13	V7.01	3p' 3D	3d' 3F*	5	7
6471.31	0.009	0.004	[Mn V]	6471.30		3d3 2H	3d3 2F	10	8
6473.73	0.011	0.004	[Fe II]	6473.86		3d7 2G	3d7 2F	8	6
6478.08	0.022	0.008	N III	6478.69		3p 4P	3d 4D*	6	6
6481.97	0.012	0.004	N II	6482.05	V8	3s 1P*	3p 1P	3	3
6500.55	0.049	0.018	O V	6500.24	V7.01	3p' 3D	3d' 3F*	7	9
6506.72	0.006	0.002	O II	6506.03		3d' 2F	4p' 2F*	8	8
6510.94	0.010	0.004	O II	6510.75		3d' 2F	4p' 2F*	6	6
6516.16	0.090	0.034	N II	6516.15		4d 1P*	6f 2[3]	3	5
6527.16	0.683	0.253	He II	6527.11	5.14	5g+ 2G	14h+ 2H*	50	*
6548.14	90.220	33.086	[N II]	6548.10	F1	2p2 3P	2p2 1D	3	5
6559.86	15.910	5.798	He II	6560.00	4.6	4f+ 2F*	6g+ 2G	32	72
6562.94	744.000	271.127	H 3	6562.77	H3	2p+ 2P*	3d+ 2D	8	18
6578.01	0.637	0.231	C II	6578.01	V2	3s 2S	3p 2P*	2	4
6583.53	259.200	93.567	[N II]	6583.50	F1	2p2 3P	2p2 1D	5	5
6616.02	0.041	0.014	Ne II	6615.72		5g 1[3]	4f' 2[1]*	6	4
6628.45	0.005	0.002	[Ni IV]	6629.10		3d7 2D2	3d7 2F	4	8
6640.34	0.009	0.003	O II	6641.03	V4	3s 2P	3p 2S*	2	2
6653.65	0.018	0.006	ERE						
6667.64	0.013	0.004	[Ni II]	6666.8		3d9 2D	4s 2F	6	6
6678.19	7.324	2.538	He I	6678.16	V46	2p 1P*	3d 1D	3	5
6683.28	0.933	0.322	He II	6683.20	5.13	5g+ 2G	13h+ 2H*	50	*
6700.46	0.003	0.001	[Ni II]	6700.24		4s 4F	4s 2D	6	6
	*	*	[Fe II]	6700.64		3d7 2G	4s 2G	10	8
6705.71	0.005	0.002	He I	6704.60		3s 3S	26p 3P*	9	9
6709.76	0.019	0.006	[Cr IV]	6709.90		3d2 3F	3d2 3P	9	5
6716.44	5.060	1.720	[S II]	6716.44	F2	2p3 4S*	2p3 2D*	4	6
6721.50	0.006	0.002	O II	6721.39	V4	3s 2P	3p 2S*	4	2
6724.76	0.004	0.001	C II	6724.56	V21	3p' 4D	3d' 4D*	2	4
6730.81	11.470	3.875	[S II]	6730.82	F2	2p3 4S*	2p3 2D*	4	4
6739.83	0.045	0.015	[Fe IV]	6740.63		3d5 4G	3d5 2I	12	12
6744.33	0.064	0.022	C III	6744.38	V3	3s' 3P*	3p' 3D	5	7
6747.04	0.040	0.013	[Cr IV]	6747.50		3d3 4F	3d3 2G	6	8
6755.90	0.009	0.003	[Fe IV]	6756.62		3d5 4G	3d5 2I	12	12
	*	*	He I	6755.80		3s 3S	20p 3P*	3	*
6761.56	0.020	0.007	[Fe IV]	6762.15		3d5 4G	3d5 3I	10	12
	*	*	C III	6762.17	V3	3s' 3P*	3p' 3D	5	5
6765.54	0.002	0.001	O V	6764.58	V12	3p' 3P	3d' 3D*	1	3
6769.57	0.003	0.001	He I	6769.55		3s 3S	19p 3P*	3	*
6780.13	0.101	0.034	C II	6779.93	V14	3s' 4P*	3p' 4D	4	6
	*	*	C II	6780.60	V14	3s' 4P*	3p' 4D	2	4
6783.79	0.012	0.004	C II	6783.90	V14	3s' 4P*	3p' 4D	6	8
6787.16	0.025	0.008	C II	6787.22	V14	3s' 4P*	3p' 4D	2	2
	*	*	He I	6785.73		3s 3S	18p 3P*	3	*
6791.62	0.036	0.012	C II	6791.47	V14	3s' 4P*	3p' 4D	4	4
	*	*	[Ni II]	6791.48		4s 4F	4s 4P	6	2
6795.08	0.245	0.081	[K IV]	6795.00	F1	3p4 3P	3p4 1D	3	5
6800.56	0.029	0.009	C II	6800.68	V14	3s' 4P*	3p' 4D	6	6
6804.84	0.011	0.004	He I	6804.90		3s 3S	17p 3P*	3	*
6812.39	0.004	0.001	C II	6812.29	V14	3s' 4P*	3p' 4D	6	4
6821.48	0.007	0.002	Ne II	6821.39		4f 1[4]*	6g 2[4]	*	*
6827.01	0.135	0.044	[Kr III]	6826.90		4p4 3P	4p4 1D	5	5
	*	*	C I	6828.12	V21	3p 1P	4d 1D*	3	5

Table 2. continued.

λ_{obs}	$F(\lambda)$	$I(\lambda)$	Ion	λ_{lab}	Mult	Lower Term	Upper Term	g_1^a	g_2^a
6829.16	0.063	0.021	O VI	6826.97			Raman line		
6840.35	0.003	0.001	Fe II	6840.98		4D sp6F*	4p2 6D	6	4
6845.99	0.006	0.002	O II	6846.81	V45	3d 4F	4p 4D*	8	8
6850.25	0.081	0.026	[Co III]	6849.20		3d7 2H	3d7 2F	12	8
*	*		[Mn VI]	6852.00		2d2 3F	2d2 1D	7	5
6856.09	0.011	0.004	He I	6855.96		3s 3S	15p 3P*	3	*
6863.43	0.004	0.001	C III	6862.71	V19	3p' 3D	3d' 3D*	5	5
6891.04	1.339	0.423	He II	6890.88	5.12	5g+ 2G	12h+ 2H*	50	*
6933.65	0.037	0.011	[Fe II]	6933.66		4s 4D	4s 4F	6	8
6945.79	0.028	0.009	N I	6945.18	V55	3p 4P*	5s 4P	6	6
6959.20	0.032	0.010	Fe II	6959.32	V63	b2G	z4F*	10	8
6975.91	0.014	0.004	N II	6975.64		3d 3P*	4p 3P	5	3
6981.63	0.028:	0.009	N I	6982.03	V55	3p 4P*	5s 4P	4	2
6989.80	0.045	0.014	He I	6989.40	3.12	3s 3S	12p 3P*	3	*
6996.89	0.033	0.010	[Fe IV]	6997.10		3d5 4G	3d5 2D	6	4
7002.24	0.099	0.039	O I	7002.17		3p 3P	4d 3D*	5	3
*	*		O I	7002.20		3p 3P	4d 3D*	5	5
*	*		O I	7002.23		3p 3P	4d 3D*	5	7
*	*		O I	7002.25		3p 3P	4d 3D*	1	3
7005.97	10.230	3.085	[Ar V]	7005.67		3p2 3P	3p2 1D	5	5
7021.58	0.022	0.007	?	*				*	*
7031.85	0.041	0.012	O IV	7032.36	V12.01	4s 2S	4p 2P*	2	4
7036.01	0.013:	0.004	[Fe IV]	7036.30		3p5 4P	3p5 2D	4	6
7047.43	0.054	0.016	[Fe II]	7047.43		4s 4D	4s 4F	2	4
7054.08	0.085	0.025	O IV	7053.62	V12.01	4s 2S	4p 2P*	2	2
7065.45	22.560	6.655	He I	7065.25	V10	2p 3P*	3s 3S	9	3
7088.36	0.010:	0.003	O VI	7083.97			Raman line		
7099.58	0.034	0.010	[Pb II]	7099.80		5p 2P	6p 2P	2	4
7103.11	0.029	0.009	[Ni II]	7102.66		4s 2F	4s 2P	6	4
*	*		N IV	7103.28	V4	3p 3P*	3d 3D	1	3
7112.86	0.066	0.019	C II	7112.48	V20	3p' 4D	3d' 4F*	2	4
*	*		[Cr IV]	7110.50		3d3 4F	3d3 4P	4	2
*	*		C I	7111.48	V26	3p 3D	4d 3F*	3	5
*	*		C I	7113.18	V26	3p 3D	4d 3F*	7	9
*	*		Si II	7113.42		5p 2P*	7s 2S	2	2
7115.83	0.050	0.015	C II	7115.63	V20	3p' 4D	3d' 4F*	6	8
7119.87	0.020	0.006	C II	7119.90	V20	3p' 4D	3d' 4F*	12	14
7136.02	74.610	21.393	[Ar III]	7135.80	F1	3p4 3P	3p4 1D	5	5
7155.23	0.276	0.078	[Fe II]	7155.16		3d7 4F	3d7 2G	10	10
7160.79	0.093	0.026	He I	7160.56	3.10	3s 3S	10p 3P*	3	9
7165.18	0.030	0.009	?	*				*	*
7170.86	1.648	0.465	[Ar IV]	7170.62	F2	3p3 2D*	3p3 2P*	4	4
7177.77	1.688	0.476	He II	7177.50	5.11	5g+ 2G	11h+ 2H*	50	*
7183.03	0.058	0.016	[Fe IV]	7183.99		3d5 4D	3d5 4F	8	8
7189.44	0.102	0.029	[Fe IV]	7190.72		3d5 4D	3d5 4F	6	6
*	*		N II	7188.20	V52	3d 3P*	4p 3D	5	5
7196.06	0.075	0.021	[Cr IV]	7196.70		3d3 2D2	3d3 2F	6	6
7203.08	0.024	0.007	?	*				*	*
7208.17	0.018	0.005	C I	7208.86		3p 1S	6d 3P*	1	3
7213.42	0.068	0.019	C III	7212.29	V39	5p 3P*	6d 3D	3	*
*	*		N II	7214.71	V52	3d 3P*	4p 3D	8	8
7220.04	0.070	0.019	[Cs III]	7219.70		4p5 2P	5p5 2P	4	2
*	*		[Fe IV]	7222.80		3d5 4D	3p5 4F	8	10
7231.34	0.391	0.108	C II	7231.12	V3	3p 2P*	3d 2D	2	4
7237.52	2.062	0.567	C II	7236.42	V3	3p 2P*	3d 2D	4	6

Table 2. continued.

λ_{obs}	$F(\lambda)$	$I(\lambda)$	Ion	λ_{lab}	Mult	Lower Term	Upper Term	g_1^a	g_2^a
	*	*	C II	7237.17	V3	3p 2P*	3d 2D	4	4
	*	*	[Ar IV]	7237.26	F2	3p3 2D*	3p3 2P*	6	4
7242.44	0.022	0.006	N II	7241.78	V52	3d 3P*	4p 3D	3	3
7251.23	0.034:	0.009	C IV	7251.79		7p 2P*	9s 2S	4	2
7254.88	0.141	0.039	O I	7254.53	V20	3p 3P	5s 3S*	1	3
	*	*	N II	7256.53	V52	3d 3P*	4p 3D	1	3
7263.14	1.410	0.384	[Ar IV]	7262.76	F2	3p3 2D*	3p3 2P*	4	2
7267.98	0.064	0.018	O II	7267.63		3d 4P	4p 4S*	4	4
7270.97	0.043	0.012	?	*				*	*
7274.64	0.020	0.005	C I	7274.61		3p 1S	7s 3P*	1	3
7281.52	2.565	0.695	He I	7281.35	V45	2p 1p*	3s 1S	3	1
	*	*	[I II]	7282.90		5p4 3P	5p4 1D	5	5
7289.01	0.044	0.012	Ne II	7288.71		4p 2S*	3d' 2D	2	4
7292.99	0.078	0.021	O II	7292.96		3d 4D	4p 4P*	6	6
7297.84	0.195	0.052	He I	7298.04		3s 3S	9p 3P*	3	9
7301.34	0.062	0.017	[Fe II]	7301.56		4s 4D	4p 4F*	6	6
7306.91	0.116	0.031	O III	7307.04	V24.03	4s 3P*	4p 3P	3	5
7320.00	66.740	17.854	[O II]	7318.92	F2	2p3 2D*	2p3 2P*	6	2
	*	*	[O II]	7319.99	F2	2p3 2D*	2p3 2P*	6	4
7330.39	55.200	14.674	[O II]	7329.67	F2	2p3 2D*	2p3 2P*	4	2
	*	*	[O II]	7330.73	F2	2p3 2D*	2p3 2P*	4	4
	*	*	[Ar IV]	7331.40		3p3 2D*	3p3 2P*	6	2
	*	*	[Fe II]	7330.22		3d7 2P	3d7 2F	4	8
7377.88	0.132	0.035	[Ni II]	7377.83		3d9 2D	4s 2F	6	8
	*	*	[Zr VII]	7379.70		5p4 3P	5p4 3P	5	3
7385.55	0.008:	0.002	[Br III]	7385.10		4d3 2D	4d3 2P	4	4
7388.17	0.074	0.019	[Fe II]	7388.18		3d7 4F	3d7 2G	6	8
7412.53	0.018	0.005	[Ni II]	7411.61		3d9 2D	3s 2F	4	6
	*	*	[Cr IV]	7410.90		3d3 2H	3d3 2F	10	6
7442.40	0.009	0.002	N I	7442.90		3s 4P	3p 4S*	4	4
7452.60	0.087	0.022	[Fe II]	7452.60		3d7 4F	3d7 2G	8	10
7455.52	0.024	0.006	O III	7455.35	V24.03	4s 3P*	4p 3P	5	5
7463.30	0.005	0.001	Si III	7462.65		4d 3D	5p 3P*	8	6
7468.35	0.021	0.005	N I	7468.31		3s 4P	3p 4S*	6	4
7473.67	0.015	0.004	O I	7473.24	V55	3s'' 3P*	3p''3D	5	5
	*	*	C I	7473.30	V29.03	3p 3S	4d 3P*	3	1
7487.02	0.031	0.008	C III	7486.52	V41	5d 3D	6f 3F*	*	*
7500.01	0.102	0.026	He I	7499.85	3.8	3s 3S	8p 3P*	3	9
7507.89	0.014	0.003	N I	7507.61	V100	3p 2D*	5s 2P	4	4
7510.28	0.012	0.003	N II	7509.24		3d 3P*	4p 1P	5	3
	*	*	C II	7508.90	V16.08	2p3 2P*	3p' 2P	2	4
7515.14	0.017	0.004	O III	7515.99	V24.03	4s 3P*	4p 3P	5	3
7519.83	0.008	0.002	C II	7519.89	V16.08	2p3 2P*	3p' 2P	2	2
7530.67	1.848	0.457	[Cl IV]	7530.54		3p2 3P	3p2 1D	3	5
7535.13	0.056	0.014	[Xe IV]	7535.40		5p3 4S	5p3 2D	4	4
7561.44	0.007	0.001	Fe II	7561.42		3P 4p4P*	5D 5d6P	4	6
7574.42	0.012	0.003	Fe II	7574.00		e4H	3H 5p4H*	10	10
	*	*	Fe II	7574.90		u2D*	3F 4d4G	4	6
7578.46	0.047	0.011	C III	7578.16	V35	3d' 3F*	5g 3G	5	7
7582.27	0.046	0.011	N IV	7582.40	V22	6g 3G	7h 3H*	*	*
7592.89	3.084	0.746	He II	7592.74	5.10	5g+ 2G	10h+ 2H*	50	*
	*	*	C III	7592.28	V35	3d' 3F*	5g 3G	7	9
	*	*	O V	7592.00	V29	7h3,1H*	8i3,1I	*	*
	*	*	[Se II]	7592.00		4p3 4S	4p3 2D	4	4
7611.58	0.057	0.014	O V	7610.90	V30	7i3,1I	8k3,1K*	*	*

Table 2. continued.

λ_{obs}	$F(\lambda)$	$I(\lambda)$	Ion	λ_{lab}	Mult	Lower Term	Upper Term	g_1^a	g_2^a
7614.09	0.080	0.019	C III	7612.65	V35	3d' 3F*	5g 3G	9	11
	*	*	[Ni II]	7612.72		4s 4F	4s 2D	4	4
	*	*	[Fe II]	7613.12		4s 4D	4s 4P	4	4
7618.04	0.937	0.225	N V	7618.46	V13	7g+ 2G	8h+ 2H*	*	*
7672.78	0.187	0.044	?	*				*	*
7675.56	0.226	0.053	[Fe II]	7675.30		4s 6D	3d7 4P	4	2
7679.68	0.155:	0.036	He I	7679.52	3.16	3s 1S	16p 1P*	1	3
7686.06	0.151:	0.035	[Fe II]	7686.94		4s 6D	3d7 4P	6	4
	*	*	N III	7686.83	V24	5d 2D	6f 2F*	6	8
7691.63	0.067:	0.016	Mg I	7691.55	V29	3d 1D	7f 1F*	5	7
	*	*	Mg I	7691.55		3d 1D	7f 3F*	10	12
7703.10	0.179	0.042	N IV	7702.96	V23	6h 3H*	7i 3I	*	*
7706.84	0.095	0.022	C IV	7706.50		6d 2D	7f 2F*	10	14
7712.60	0.291	0.068	O IV	7713.30	V21	6h 2H*	7i 2I	12	12
7725.79	1.098	0.254	C IV	7726.20	v8.01	6h 2H*	7i+ 2I	*	*
7735.33	0.160	0.037	C IV	7735.71		8g 2G	11f 2F*	18	14
7750.82	20.280	4.648	[Ar III]	7751.06		3p4 3P	3p4 1D	3	5
	*	*	He I	7757.67	3.14	3s 1S	14p 1P*	1	3
7771.85	0.019	0.003	C III	7771.76	V26	3p' 3S	3d' 3P*	3	1
	*	*	O I	7771.94	V1	3s 5S*	3p 5P	5	7
7774.03	0.016	0.002	O I	7774.17	V1	3s 5S*	3p 5P	5	5
7815.82	0.185	0.042	He I	7816.03	3.7	3s 3S	7p 3P*	9	11
7833.10	0.017	0.004	O III	7832.48	V26.06	4p 3S	4d 3P*	3	3
7837.36	0.017	0.004	C I	7837.10	V32	3p 3P	4d 3P*	3	1
7848.22	0.016	0.004	O III	7848.03	V26.03	4p 3D	4d 3D*	3	3
7860.23	0.097	0.021	C I	7860.89	V32	3p 3P	4d 3P*	5	5
7875.54	0.463	0.102	[P II]	7875.99		3p2 1D	3p2 1S	5	1
	*	*	C IV	7875.50		10g 2G	19h 2H*	*	*
	*	*	Mg II	7877.05	V8	4p 2P*	4d 2D	2	4
7883.00	0.064	0.014	[Cr V]	7884.40		3d2 3F	3d2 1D	7	5
7889.58	0.031	0.007	[Ni III]	7889.90		3d8 3F	3d8 1D	7	5
7896.78	0.031	0.007	Mg II	7896.37	V8	4p 2P*	4d 2D	8	10
	*	*	N II	7897.62	V61.10	4p 1P	5s 1P*	3	3
7905.80	0.016	0.003	N II	7906.08		3d 1P*	4p 3D	3	5
7910.75	0.012	0.002	Ne II	7910.25		4p 4D*	5s 2P	4	2
7913.29	0.030	0.006	Fe II	7912.68		w6P*	3H 4d2F	6	6
7918.51	0.010	0.002	N I	7918.44		3p 2P*	4d 4D	2	4
7925.24	0.019	0.004	[Fe IV]	7925.00		3d5 4D	3d5 2F2	8	8
7930.69	0.007	0.001	Mg I	7930.79	V42	3d 3D	10f 3F*	*	*
7936.17	0.018	0.003	O IV	7936.22		3d 2P*	3s 2P	4	2
7939.39	0.006	0.001	O I	7939.51	V35	3s' 3D*	3p' 3F	7	5
7944.26	0.017	0.003	O I	7943.15	V35	3s' 3D*	3p' 3F	7	7
7947.88	0.016	0.003	C IV	7947.38		6d 2D	7p 2P*	6	4
	*	*	C IV	7948.14		6d 2D	7p 2P*	4	2
	*	*	O I	7947.55	V35	3s' 3D*	3p' 3F	7	9
7952.38	0.031	0.007	O I	7952.16	V35	3s' 3D*	3p' 3F	3	5
7972.88	0.014	0.002	He I	7971.67	3.11	3s 1S	11p 1P*	1	3
7981.86	0.006	0.001	O I	7981.94	V19	3p 3P	3s' 3D*	3	3
7985.56	0.033	0.007	O I	7986.98	V19	3p 3P	3s' 3D*	3	5
7992.95	0.010	0.002	C I	7992.53	V88	2p3 3P*	6f 1[3]	3	5
	*	*	C I	7993.42	V88	2p3 3P*	6f 1[3]	5	*
7995.28	0.007	0.001	O I	7995.07	V19	3p 3P	3s' 3D*	5	7
7999.25	0.016	0.003	[Cr II]	8000.08		3d5 6S	4s 6D	6	10
8015.78	0.032	0.007	C I	8015.00	V31	3p 3P	4d 3D*	3	5
	*	*	He I	8015.99	3.20	3p 3P*	20d 3D	9	*

Table 2. continued.

λ_{obs}	$F(\lambda)$	$I(\lambda)$	Ion	λ_{lab}	Mult	Lower Term	Upper Term	g_1^a	g_2^a
8018.59	0.063	0.013	C I	8018.56	V31	3p 3P	4d 3D*	1	3
*	*		N III	8019.09	V26	5f 2F*	6g 2G	16	18
8020.75	0.018	0.004	C III	8021.14	V44	5d 1D	6f 1F*	5	7
8024.92	0.014	0.003	[Fe IV]	8024.10		3d5 4D	3d5 2F2	6	8
8030.71	0.024	0.005	C II	8028.86	V27.02	3p'4P	3d' 4P*	2	2
*	*		C I	8028.18	V31	3p 3P	4d 3D*	5	5
8035.63	0.028	0.006	He I	8035.10	3.19	3p 3P*	19d 3D	9	*
8045.40	5.029	1.049	[Cl IV]	8045.63		3p2 3P	3p2 1D	5	5
*	*		C II	8048.32	V27.02	3p'4P	3d' 4P*	4	4
*	*		[Te II]	8049.60		5p3 4S	5p3 2D	4	4
8057.25	0.032	0.006	He I	8057.59	3.18	3p 3P*	18d 3D	8	*
8061.73	0.008	0.001	C II	8062.12	V27.02	3p'4P	3d' 4P*	4	6
*	*		C II	8062.78	V27.02	3p'4P	3d' 4P*	6	4
8075.96	0.005	0.001	C II	8076.64	V27.02	3p'4P	3d' 4P*	6	6
8083.44	0.034	0.007	He I	8084.33	3.17	3p 3P*	17d 3D	8	*
8087.68	0.029	0.006	Fe II	8087.28		3F 4p2F*	3F 4d2D	6	6
*	*		O V	8088.00		4s 3P*	4p 3D	5	5
8093.33	0.032	0.007	He I	8093.31	3.17	3p 3P*	17s 3S	9	9
8102.27	0.036	0.007	Si III	8102.86	V37	5g 3G	6h 3,1H*	*	*
8110.35	0.016	0.003	Fe II	8110.22		4P sp4P*	3F 4d4P	4	4
8116.02	0.061	0.012	He I	8116.30	3.16	3p 3P*	16d 3D	9	*
8127.18	0.043	0.009	O III	8127.50		5f G[5]	6g H[6]*	11	*
*	*		[Cr II]	8125.30		3d5 6S	4s 6D	6	8
8131.33	0.012	0.003	O VI	8131.80		8p 2P*	9s 2S	6	2
8137.79	0.095	0.019	[Fe V]	8137.20		3d4 3H	3d4 1I	11	13
8144.33	0.058	0.012	Fe II	8144.08		e4D	3F 4p4D*	4	2
8150.79	0.090	0.018	N I	8150.66	V125	3p 2P*	5s 2P	2	2
8155.82	0.088	0.017	He I	8155.78	3.15	3p 3P*	15d 3D	9	*
8159.22	0.108	0.021	N IV	8159.60		6p 1P	7S 1S	3	1
8163.36	0.018:	0.003	N V	8163.42		7p 2P*	8s 2S	4	2
8166.52	0.149:	0.029	O III	8168.00		5f G[5]	6g H[6]*	9	*
*	*		N I	8166.23	V139	3s' 2D	5p 2D*	6	6
*	*		N I	8166.51	V139	3s' 2D	5p 2D*	4	6
8172.94	0.291:	0.057	O III	8172.10	V24.04	4s 1P*	4p 1D	3	5
8180.17	0.042:	0.008	?	*				*	*
8184.17	0.138	0.028	N I	8184.87	V2	3s 4P	3p 4P*	4	6
8189.29	0.059	0.012	N I	8188.02	V2	3s 4P	3p 4P*	2	4
*	*		C III	8189.00		5g' 3H*	6h' 3I	*	*
8190.79	0.060	0.012	Si III	8190.43	V31	5f 3F*	6g 1G	7	9
*	*		Si III	8191.43	V30	5f 3F*	6g 3G	5	7
8196.24	1.448	0.289	C III	8196.48	V43	5g 3,1G	6h 3,1H*	*	*
8203.21	0.145	0.029	He I	8203.90	3.14	3p 3P*	14d 3D	8	*
8207.01	0.081	0.016	?	*				*	*
8210.84	0.069	0.014	N I	8210.72		3s 4P	3p 4P*	4	4
*	*		[Cs VI]	8210.60		4p4 3P	5p4 3P	5	3
8215.15	0.179	0.036	N I	8216.30	V2	3s 4P	3p 4P*	6	6
*	*		Ne II	8214.57		3d 4D	4p 4D*	4	6
8219.58	0.062	0.012	?	*				*	*
8222.54	0.078	0.015	N I	8223.13	V2	3s 4P	3p 4P*	4	2
8229.76	0.044	0.008	[Cr II]	8229.67		3d5 6S	4s 6D	6	6
8236.46	5.503	1.084	He II	8236.77	5.9	5g+ 2G	9h+ 2H*	50	*
8241.62	0.109	0.022	N I	8242.39	V2	3s 4P	3p 4P*	6	4
8244.67	0.105	0.021	O III	8244.10		5g G[5]*	6h H[6]	*	*
8249.79	0.040	0.008	H I	8249.90	P40	3d+ 2D	40f+ 2F*	18	*
8252.07	0.032	0.006	H I	8252.40	P39	3d+ 2D	39f+ 2F*	18	*

Table 2. continued.

λ_{obs}	$F(\lambda)$	$I(\lambda)$	Ion	λ_{lab}	Mult	Lower Term	Upper Term	g_1^a	g_2^a
	*	*	O III	8250.80		5g F[4]*	6h G[5]	*	*
8254.73	0.079	0.015	H I	8255.02	P38	3d+ 2D	38f+ 2F*	18	*
8257.58	0.111	0.022	H I	8257.86	P37	3d+ 2D	37f+ 2F*	18	*
8261.13	0.306	0.060	H I	8260.94	P36	3d+ 2D	36f+ 2F*	18	*
8264.30	0.389	0.076	H I	8264.29	P35	3d+ 2D	35f+ 2F*	18	*
	*	*	He I	8265.71	3.9	3s 1S	9p 1P*	1	3
8267.78	0.427	0.083	H I	8267.94	P34	3d+ 2D	34f+ 2F*	18	*
	*	*	O III	8268.80		5g H[6]*	6h I[7]	*	*
8271.48	0.372	0.073	H I	8271.93	P33	3d+ 2D	33f+ 2F*	18	*
8275.97	0.356	0.069	H I	8276.31	P32	3d+ 2D	32f+ 2F*	18	*
8280.72	0.412	0.080	H I	8281.12	P31	3d+ 2D	31f+ 2F*	18	*
8286.01	0.517	0.101	H I	8286.43	P30	3d+ 2D	30f+ 2F*	18	*
8291.89	0.547	0.106	H I	8292.31	P29	3d+ 2D	29f+ 2F*	18	*
8298.44	0.657	0.127	H I	8298.84	P28	3d+ 2D	28f+ 2F*	18	*
8305.90	0.691	0.134	H I	8305.90	P27	3d+ 2D	27f+ 2F*	18	*
	*	*	N III	8307.55	V5.01	3s' 2P*	3p' 2P	2	4
8313.68	0.863	0.166	H I	8314.26	P26	3d+ 2D	26f+ 2F*	18	*
8319.35	0.062	0.012	He II	8319.91	6.50	6s+ 2S	50p+ 2P*	72	*
8323.07	0.865	0.166	H I	8323.43	P25	3d+ 2D	25f+ 2F*	18	*
8330.02	0.096	0.018	He II	8330.26	6.48	6s+ 2S	48p+ 2P*	72	*
8333.39	1.017	0.195	H I	8333.78	P24	3d+ 2D	24f+ 2F*	18	*
	*	*	C III	8332.99	V12.01	4d 3D	3d' 3F*	7	9
8341.51	0.211	0.040	He I	8342.37	V68	3s 3S	6p 3P*	3	9
	*	*	C III	8341.59	V12.01	4d 3D	3d' 3F*	5	7
8345.10	1.073	0.205	H I	8345.55	P23	3d+ 2D	23f+ 2F*	18	*
	*	*	C III	8347.94	V12.01	4d 3D	3d' 3F*	3	5
	*	*	N III	8344.86	V5.01	3s' 2P*	3p' 2P	2	2
8358.62	1.158	0.220	H I	8359.01	P22	3d+ 2D	22f+ 2F*	18	*
	*	*	C III	8358.72	V12.01	4d 3D	3d' 3F*	5	5
8361.38	0.403	0.077	He I	8361.71		3s 3S	6p 3P*	3	1
8370.37	0.046	0.009	He II	8370.93	6.42	6s+ 2S	42p+ 2P*	72	*
8374.15	1.198	0.227	H I	8374.48	P21	3d+ 2D	21f+ 2F*	18	*
	*	*	C III	8375.04	V12.01	4d 3D	3d' 3F*	7	5
8378.96	0.058	0.011	He I	8378.77	3.20	3d 1D	20p 1P*	5	3
8386.45	0.139	0.026	N III	8386.48	V5.01	3s' 2P*	3p' 2P	4	4
8392.04	1.431	0.270	H I	8392.40	P20	3d+ 2D	20f+ 2F*	18	*
8398.63	0.236	0.044	He II	8398.90	6.39	6s+ 2S	39p+ 2P*	72	*
8405.63	0.046	0.009	Ne II	8405.62		4p 2S*	5s 2P	2	2
8409.52	0.044	0.008	He II	8409.80	6.38	6s+ 2S	38p+ 2P*	72	*
8413.46	1.537	0.288	H I	8413.32	P19	3d+ 2D	19f+ 2F*	18	*
8422.08	0.137	0.026	He I	8421.80	3.18	3d 3D	18p 3p*	15	*
	*	*	He II	8421.55	6.37	6s+ 2S	37p+ 2P*	72	*
8433.95	0.395	0.074	[Cl III]	8433.70		3p3 2D*	3p3 2P*	4	4
	*	*	He II	8434.38	6.36	6s+ 2S	36p+ 2P*	72	*
8438.10	1.765	0.328	H I	8438.00	P18	3d+ 2D	18f+ 2F*	18	*
8446.58	1.535	0.285	O I	8446.36	V4	3s 3S*	3p 3P	3	5
	*	*	He II	8448.39	6.35	6s+ 2S	35p+ 2P*	72	*
8451.66	0.073	0.014	He I	8451.10	3.17	3d 3D	17p 3p*	15	*
8459.19	0.012	0.002	Ne II	8459.86		3d' 2S	4p' 2P*	2	2
8463.71	0.067	0.012	He II	8463.70	6.34	6s+ 2S	34p+ 2P*	72	*
8467.41	2.041	0.376	H I	8467.26	P17	3d+ 2D	17f+ 2F*	18	*
8480.94	0.395	0.073	[Cl III]	8480.85		3p3 2D*	3p3 2P*	6	4
	*	*	He II	8480.67	6.33	6s+ 2S	33p+ 2P*	72	*
8486.37	0.062	0.011	He I	8486.16	3.16	3d 3D	16d 3p*	15	*
8488.93	0.026	0.005	He I	8488.62	3.16	3d 3D	16p 3p*	15	*

Table 2. continued.

λ_{obs}	$F(\lambda)$	$I(\lambda)$	Ion	λ_{lab}	Mult	Lower Term	Upper Term	g_1^a	g_2^a
8499.93	0.397	0.073	[Ni III]	8499.60		3d8 3F	3d8 1D	5	5
	*	*	He II	8498.90	6.32	6s+ 2S	32p+ 2P*	72	*
8502.63	2.825	0.516	H I	8502.49	P16	3d+ 2D	16f+ 2F*	18	*
	*	*	[Cl III]	8502.00		3p3 2D*	3p3 2P*	4	2
8519.40	0.103	0.019	He II	8519.40	6.31	6s+ 2S	31p+ 2P*	72	*
8529.17	0.092	0.017	He I	8529.05	3.15	3d 3D	15f 3F*	15	*
8531.76	0.028	0.005	He I	8531.40	3.15	3d 3D	15p 3F*	15	
8541.92	0.102	0.018	He II	8541.80	6.30	6s+ 2S	30p+ 2P*	72	*
8545.55	3.044	0.551	H I	8545.38	P15	3d+ 2D	15f+ 2F*	18	*
	*	*	[Cl III]	8549.00		3p3 2D*	3p3 2P*	6	2
8567.15	0.138	0.025	He II	8566.99	6.29	6s+ 2S	29p+ 2P*	72	*
	*	*	N I	8567.74	V8	3s 2P	3p 2P*	2	4
8578.85	1.809	0.324	[Cl II]	8578.70		3p4 3P	3p4 1D	5	5
8582.52	0.253	0.045	He I	8582.54	3.10	3p 3P*	10d 3D	9	9
8594.88	0.154	0.027	He II	8594.91	6.28	6s+ 2S	28p+ 2P*	72	*
	*	*	N I	8594.00	V8	3s 2P	3p 2P*	2	2
8598.55	4.016	0.715	H I	8598.39	P14	3d+ 2D	14f+ 2F*	18	*
8608.34	0.017	0.003	He I	8608.36	3.15	3p 1P*	15d 1D	3	5
8616.95	0.347	0.061	[Fe II]	8616.95		4s 4H	4s 2I	14	14
8626.43	0.142	0.025	He II	8626.10	6.27	6s+ 2S	27p+ 2P*	72	*
8633.28	0.020	0.003	He I	8632.82	3.10	3p 3P*	10s 3S	9	9
8648.49	0.119	0.021	He I	8648.10	3.13	3d 3D	13f 3F*	15	*
8651.22	0.047	0.008	He I	8651.70	3.13	3d 3D	13d 3F*	15	*
8661.95	0.293	0.051	He II	8661.40	6.26	6s+ 2S	26p+ 2P*	72	*
8665.15	5.134	0.897	H I	8665.02	P13	3d+ 2D	13f+ 2F*	18	*
	*	*	C III	8665.22	V45	5f 3F*	6g 3G	9	11
8680.35	0.035	0.006	N I	8680.28	V1	3s 4P	3p 4D*	6	8
8683.41	0.032	0.006	N I	8683.40	V1	3s 4P	3p 4D*	4	6
8685.95	0.026	0.005	N I	8686.15	V1	3s 4P	3p 4D*	2	4
8701.75	0.201	0.035	He II	8701.30	6.25	6s+ 2S	25p+ 2P*	72	*
	*	*	N I	8703.25	V1	3s 4P	3p 4D*	2	2
8705.86	0.047	0.008	O II	8705.81		4d 4F	5f F2*	8	6
8711.79	0.024	0.004	N I	8711.70	V1	3s 4P	3p 4D*	4	4
8719.41	0.006	0.001	N I	8718.83	V1	3s 4P	3p 4D*	6	6
8721.72	0.007	0.001	Ne II	8721.89		3d 4P	4p 2D*	4	4
8727.25	1.473	0.253	[C I]	8727.13		2p2 1D	2p2 1S	5	1
	*	*	[Fe III]	8728.84		3d6 3P	3d6 3D	5	7
	*	*	N I	8728.89	V1	3s 4P	3p 4D*	4	2
	*	*	[Fe VII]	8729.90		3d2 1D	3d2 1G	5	9
	*	*	He I	8729.95	3.13	3p 1P*	13d 1D	3	5
8733.60	0.172	0.030	He I	8733.30	3.12	3d 3D	12f 3F*	15	*
8736.31	0.070	0.012	He I	8735.90	3.12	3d 3D	12d 3F*	15	*
8740.53	0.038	0.007	He I	8740.04	3.12	3d 3D	12p 3F*	15	*
8747.19	0.292	0.050	He II	8747.00	6.24	6s+ 2S	24p+ 2P*	72	*
	*	*	N I	8747.37	V1	3s 4P	4d 4D*	6	4
8750.65	5.631	0.962	H I	8750.48	P12	3d+ 2D	12f+ 2F*	18	*
8776.86	0.144	0.024	He I	8776.60	3.9	3p 3P*	9d 3D	1	3
8789.18	0.008	0.001	O II	8788.83		4d 4F	5f G4*	6	8
8794.87	0.090	0.015	C II	8793.80	V28.01	3p' 2D	3d' 2F*	6	8
8799.22	0.304	0.051	C II	8799.10	V28.01	3p' 2D	3d' 2F*	4	6
	*	*	He II	8798.90	6.23	6s+ 2S	23p+ 2P*	72	*
	*	*	[P I]	8799.61		3p3 4S*	3p3 2D*	4	4
8806.93	0.037	0.006	Mg I	8806.76	V7	3p 1P*	3d 1D	3	5
8816.76	0.018	0.003	He I	8816.50	3.12	3p 1P*	12d 1D	3	5
8829.90	0.063	0.011	[S III]	8829.40		3p2 3P	3p2 1D	1	5

Table 2. continued.

λ_{obs}	$F(\lambda)$	$I(\lambda)$	Ion	λ_{lab}	Mult	Lower Term	Upper Term	g_1^a	g_2^a
	*	*	He I	8830.61	3.12	3p 1P*	12s 1S	3	1
8845.54	0.285	0.048	He I	8845.20	3.11	3d 3D	11f 3F*	15	*
	*	*	He I	8846.46	3.11	3d 1D	11p 1P*	5	3
	*	*	[Ba V]	8845.64		5p4 3P	5p4 3P	5	1
8849.00	0.148	0.025	He I	8849.00	3.9	3p 3P*	9s 3S	9	9
8854.31	0.051	0.009	He I	8854.19	3.11	3d 3D	11p 3P*	15	*
	*	*	[Se III]	8854.20		4p2 3P	4p2 1D	3	5
8858.99	0.427	0.071	He II	8859.25	6.22	6s+ 2S	22p+ 2P*	72	*
8862.92	7.753	1.288	H I	8862.79	P11	3d+ 2D	1f+ 2F*	18	*
8873.40	0.075	0.012	C I	8873.39	V49	3p 1D	5s 1P*	5	3
8892.05	0.194	0.032	[Fe II]	8891.91		3d7 4F	3d7 4P	8	4
8899.05	0.041	0.007	C I	8899.31		3d 1D*	8p 1D	5	5
	*	*	Ne II	8899.33		4p 2P*	3d' 2P	2	4
8914.91	0.044	0.007	He I	8914.83	3.7	3s 1S	7p 1P*	1	3
8929.31	0.429	0.070	N V	8930.43		9g 2G	11f 2F*	18	14
	*	*	He II	8929.21	6.21	6s+ 2S	21p+ 2P*	72	*
8968.78	0.109	0.018	Ne I	8968.53		4s 2[2]*	6p 2[1]	5	3
8973.66	0.071:	0.011	Fe II	8973.95		4D sp6D*	5D 5d4D	8	6
	*	*	Fe II	8974.52		w4G*	5D 5d4D	6	6
8978.02	0.160	0.026	?	*				*	*
8982.74	0.147	0.024	N II	8983.28	V65.03a	4d 1D*	5f 1[3]	5	7
8985.13	0.160	0.026	?	*				*	*
8989.72	0.144	0.023	Mg I	8989.03		4p 3P*	8s 3S	1	3
8997.28	0.550	0.089	He I	8997.04	3.10	3d 3D	10f 3F*	15	*
9002.18	0.078	0.013	Fe II	9002.37		4f 4[5]*	5D 6d6D	10	10
9005.57	0.077	0.012	O II	9005.43		4p 2D*	4s' 2D	6	4
9011.30	0.525	0.084	He II	9011.20	6.20	6s+ 2S	20p+ 2P*	72	*
	*	*	[Rb IV]	9008.75		4p4 3P	4p4 1D	3	5
	*	*	He I	9009.28	3.10	3d 3D	10p 3P*	3	1
9015.04	12.500	2.000	H I	9015.00	P10	3d+ 2D	10f+ 2F*	18	*
9033.93	0.006	0.001	[Fe II]	9033.50		3d7 4F	3d7 4P	6	2
9052.12	0.072	0.012	[Fe II]	9051.95		3d7 4F	3d7 4P	8	6
9069.19	- ^b	-	[S III]	9069.19		3p2 3P	3p2 1D	3	5
9095.36	0.390	0.061	C I	9095.47		3d 3D*	9p 3D	5	7
9103.21	0.185	0.029	?	*				*	*
9109.01	0.681	0.107	He II	9108.50	6.19	6s+ 2S	19p+ 2P*	72	*
9123.78	0.895	0.140	[Cl II]	9123.60		3p4 3P	3p4 1D	3	5
9133.32	0.213:	0.033	[Fe II]	9133.62		3d7 2G	4s 2F	8	8

^a For a feature blended with a few lines from the same multiplet, this is a sum of statistical weights.^b Saturated even if in short exposures.

Table 4. UV line fluxes.

Wavelength (Å)	Ion	$F(\lambda)^a$	$I(\lambda)$ [$I(\text{H}\beta) = 100$]
1240	N V	0.15	35.94
1335	C II	0.09	10.56
1400	O IV]+Si IV	0.60	49.54
1485	N IV]	0.65	42.28
1548	C IV	12.5	695.97
1551	C IV	7.77	430.00
1573	C III+[Ne V]	0.21	11.10
1602	[Ne IV]	0.27	13.80
1640	He II	4.40	211.23
1663	O III]	0.74	34.51
1750	N III]	0.60	27.06
1883	[Si III]	0.04	2.29
1892	Si III]	0.05	3.00
1906	[C III]	4.40	280.75
1908	C III]	7.00	446.49
2324	[O III]+CII]	1.90	185.00
2422	[Ne IV]	1.20	54.14
2425	[Ne IV]	0.45	19.96
2470	[O II]	0.76	25.73
2512	He II	0.25	6.65
2732	He II	0.56	6.68
2783	[Mg V]	0.92	9.53
2796	Mg II	1.04	10.46
2804	Mg II	1.68	16.56
2830	He I	0.16	1.48
2929	[Mg V]	0.45	3.39
3024	O III	0.87	5.53
3046	O III	1.33	8.19
3134	O III	9.71	52.30
3203	He II	3.05	14.95

^a $10^{-12} \text{ erg cm}^{-2} \text{ s}^{-1}$.